Feinberg Graduate School
Weizmann Institute of Science

Thesis for the degree
Doctor of Philosophy

Molecular Monolayers for Hybrid n-Si / organic Inversion Layer Solar Cells

Rotem Har-Lavan

Prof. David Cahen

August 2011

Submitted to the scientific Council of the
Weizmann Institute of Science
Rehovot, Israel

Abstract

In this thesis I am interested in the way(s) by which self-assembled monolayers (SAMs) control the surface energetics and passivation of the oxide-free Si surface, and of semiconductor surfaces in general. The Metal-Insulator-Semiconductor (MIS) structure, suggested for cheap yet efficient solar cells, demands high quality, homogeneous passivation over macroscopic areas. Placing a molecular SAM between the semiconductor absorber and the metal top electrode, helps us to probe the basic physics of those structures, as well as the qualities of SAMs as interfacial layers, and define some of their limitations as well. One of the key features of a good MIS cell is that the semiconductor (near)surface is inverted, i.e., effectively is of different doping type than the bulk of the material, due to sufficiently strong band bending.

According to our current understanding the interfacial layer in MIS and other inversion layer solar cells has 4 different roles:

1. passivation of surface states by satisfying the surface atom's dangling bonds,
2. preventing direct metal-semiconductor chemical interaction,
3. introducing a surface dipole that can increase the initial potential difference between the metal and semiconductor,
4. as a medium for fixed charges (that will affect the interface energetics).

Among these, the first two are necessary conditions and have to be fulfilled for the cell's V_{OC} to exceed that of its metal-semiconductor parallel, while the last two are optional and can increase even further the inversion induced by the metal, i.e., by the difference between the metal and semiconductor work functions.

I used self-assembled monolayers of alkyl chains, bound to oxide-free n-Si through Si-O-C bonds to satisfy the surface bonds of the Si. The second of the necessary requirements was met by using a semi-transparent Au film that was chemically bound to the terminal thiol group of the monolayer, with a 10 carbon alkyl chain as buffer between metal and semiconductor. Indeed the 480 mV V_{OC}, measured under illumination for this bottom-up constructed cell, is higher than for any n-Si/Au junction before.

The hydroquinone-methanol treatment to Si(100) was earlier shown to be the best chemical passivation for Si surfaces. Obviously, the surface bonds in this molecular treatment are well taken care of, but our measurements also demonstrate an impressively large negative surface dipole introduced by the monolayer, effectively reducing the electron affinity of the Si by as much as 500 meV. We combined this molecular treatment with a Hg top electrode, which is chemically inert to Si to fulfill the first three of the above requirements. Indeed, with the aid of the surface dipole the junction was pushed into strong inversion , despite the rather small work function of the Hg. Using a primary alcohol with alkyl chains of different lengths, rather than just methanol enabled me to tune the magnitude of the dipole while preserving the excellent surface passivation. In contact with Hg, the junctions followed the Schottky-Mott model for metal-semiconductor contact almost ideally in a way never reported before for Si-based junctions.

One chapter of this work is also dedicated to the chemical mechanism, not analyzed before, by which the hydroquinone-methanol bind to the Si surface and passivate it so efficiently.

For large area solar cells, the Hg top electrode was replaced by a conducting polymer - PEDOT:PSS. The polymer was chosen because it can be deposited in a gentle manner by spin-coating, so as not to damage the molecular surface passivation, and for its high work function, so as to induce inversion in the Si. As it is a degenerate p-type semiconductor, the polymer should also block majority

carrier electrons from the Si from moving into the top electrode, thus forcing the junction to rely on minority carrier transport alone - a favorable property for photovoltaics (reduces probability for recombination). The n-Si/PEDOT:PSS junction was measured with and without molecular monolayer and found s to be strongly-inverted for substrates of moderate doping only, different to our expectations based on the electrostatics prior to junction formation. I suggest that the polymer solution reacts with the surface to dramatically alter its surface dipole, but maintain its passivation, and propose routes by which one can overcome this drawback.

תקציר

עניינה של המובאת בזאת בדרכים שבהן חד-שכבות (monolayers) מבצעות פאסיבציה חשמלית ושולטות באנרגטיקה של פני-שטח של סיליקון, ומוליכים למחצה אחרים, ללא תחמוצת. מבנה מתכת-מבודד-מוליך למחצה (ממ"מ), שהוצע לפני שנים כחלופה זולה אך יעילה לתאי השמש המקובלים מסוג p-n, דורש פאסיבציה איכותית ועל-פני משטחים גדולים. שימוש בחד-שכבות מולקולריות בין המוליך למחצה (מל"מ) שבולע את האור ובין האלקטרודה המתכתית נותן בידינו אפשרות לבחון את הפיסיקה הבסיסית של מבנים אלו, וכן את התכונות של חד-השכבות בתור שכבת ביניים, כמו גם להכיר את מגבלותיהן. אחד היסודות לפעולה מוצלחת של מבנה ממ"מ כתא-שמש הוא כיפוף פסי-אנרגיה המושרה על שכבת המל"מ הקרובה לממשק עם המבודד שגורם בפועל להיפוך הסימום (type inversion) ביחס לעומק המל"מ.

על-פי הבנתנו העדכנית לשכבת הביניים 4 תפקידים בתא-שמש במבנה ממ"מ ודומיו:

א) פאסיבציה חשמלית של מצבי פני-שטח באמצעות קשירה כימית של אטומי השטח של המל"מ,

ב) בידוד המל"מ מן המתכת על-מנת למנוע תגובה כימית ביניהם,

ג) תוספת של דיפול פני שטח שיוכל להגדיל את הפרשי הפוטנציאלים בין המל"מ למתכת,

ד) מצע מארח למטענים כלואים שביכולתם לשנות את האנרגטיקה של הממשק.

שני התפקידים הראשונים שהוזכרו הכרחיים על-מנת שהתא מסוג ממ"מ יפיק מתח מעגל-פתוח V_{OC} גבוה משל מקבילו ללא המבודד, בעוד שני התפקידים האחרים הינם אופציונאליים, וביכולתם להגדיל עוד יותר את הבדלי פונקציות העבודה בין המל"מ למתכת , ובאמצעות כך את הפוך הסימום המושרה על המל"מ.

על-מנת לקשור כימית את אטומי השטח של הסיליקון, השתמשתי בחד-שכבות של שרשראות פחממניות, שנקשרות למשטח (ללא תחמוצת) דרך קשרי Si-C או קשרי Si-O-C. את הדרישה ההכרחית השנייה יישבתי תוך שימוש בשכבה שקופה-למחצה של זהב, קשורה כימית לראש הגופריתי של חד-השכבה ומופרדת מהמל"מ בשכבה בעובי עשרה פחמנים. אכן תאים אלו, שנבנו מלמטה-למעלה (bottom-up), השיגו תחת הארה מתח מעגל-הפתוח של $480\,mV$ – גבוה יותר מכל צומת זהב/סיליקון בעבר.

טיפול פני-שטח בתמיסת מתאנול והידרו-כינון (HQ-MeOH), הוא ככל הידוע הפאסיבציה הכימית היציבה, הטובה ביותר עבור סיליקון. הטיפול מצליח, ככל הנראה, למלא יפה את הקשרים הכימיים של אטומי פני השטח של הסיליקון. בנוסף הראו המדידות שלנו כי השכבה תורמת גם דיפול פני-שטח שלילי גדול למדי, המוריד בפועל את

האפיניות החשמלית עד $500\,meV$. שילוב של טיפול פני השטח המדובר עם מגע עליון של כספית נוזלית – שאינה מגיבה כימית עם סיליקון – עונה לשלושת הדרישות הראשונות ברשימה. בעזרת דיפול השטח אכן עובר הסיליקון היפוך סימום חזק, וזאת, למרות פונקציית העבודה ההתחלתית הנמוכה של הכספית. כמו כן הראתי שניתן לכייל את גודלו של דיפול פני-השטח תוך שמירה על איכות הפאסיבציה, על-ידי שימוש באלכוהולים בעלי אורך שונה כממסים בטיפול – במקום מתאנול. הצמתים שנוצרו במגע חשמלי עם כספית, לאחר טיפולים אלו, עקבו אחרי מודל שוטקי-מוט (Schottky-Mott) בצורה כמעט-אידאלית, דבר שמעולם לא דווח עבור צמתי סיליקון.

פרק אחד בעבודה מוקדש למנגנון הכימי, שעדיין לא פוענח, שבאמצעותו נקשרים ההידרו-כינון והמתאנול לסיליקון ומבצעים פאסיבציה יעילה כל-כך של פני-השטח.

על-מנת ליצור תאי שמש בשטח מקרוסקופי, החלפתי את הכספית בפולימר מוליך מסוג PEDOT:PSS. הפולימר נבחר בשל פונקציית העבודה הגבוהה שלו (המתאימה להשרות היפוך-סימום על הסיליקון), ובשל השיטה הרכה שבה הוא מונח שיש בה כדי לשמר את השכבה המולקלרית. בהיותו מל״מ מנוון מסוג P אמור הפולימר לחסום את נושאי מטען הרוב (אלקטרונים) הבאים מן הסיליקון וכך לכפות על ההתקן להסתמך על נושאי מטען המיעוט – תכונה מבוקשת עבור תאי-שמש – כיוון שבכך פוחתת ההסתברות לרקומבינציה.

צמתי הסיליקון/פולימר נמדדו עם החד-שכבה המולקלרית ובלעדיה ובניגוד לציפיות שבוססו על המדידות האלקטרו-סטאטיות לפני יצירת הצומת, נמצא שרק עבור דוגמאות בעלות רמת סימום התחלתי נמוך ובינוני אכן מתקיים היפוך-הסימום החזק המבוקש. העלתי השערה שהפולימר מגיב עם פני השטח בצורה שמשנה משמעותית את הדיפול אך משמרת את הפאסיבציה, ועל כן הצעתי דרכים בעזרתם, אני סבור, ניתן להתגבר על קושי זה.

Table of Contents

Chapter 1 General Introduction....10

Chapter 2 Background – Inversion layer solar cells....16

2.1 Preface....17
2.2 The Schottky-Mott model and formation of inversion layer....18
2.3 Metal-Insulator-Semiconductor (MIS) solar cells....22
2.4 4 roles of the ultra-thin insulating layer in inversion layer solar cells....27
2.4.1 Surface state passivation....27
2.4.1.1 The origin of surface states....27
2.4.1.2 Probing for surface state....31
2.4.1.3 Surface state passivation....31
2.4.2 Chemical passivation – preventing direct metal–semiconductor reaction....35
2.4.3 Accommodation of fixed (trapped) charges – field effect passivation....37
2.4.4 Additional interface dipole....40
2.5 MIS Inversion Layer (MIS-IL) solar cell....42
2.6 Practical limitations of MIS-IL solar cell....45
2.7 Degenerate-Semiconductor – Insulator – Semiconductor (SIS) solar cells....49
2.8 Recent publications....53
2.9 Summary and future prospects....54
2.10 References....56

Chapter 3 All covalently bonded solar cell: n-Si-O-C11-S-Au....66

3.1 Introduction....67
3.2 Results and discussion....68
3.3 Summary....72
3.4 References....73

Chapter 4 Ambient organic molecular passivation of Si yields near-ideal, Schottky-Mott limited, junctions....76

4.1 Introduction....77
4.2 Results....80
4.2.1 Surface / interface dipole control over Si/Hg Schottky barrier height....80
4.2.2 HQ-methanol treatment – the case of strong inversion....84
4.2.2.1 Surface dipole....84
4.2.2.2 Current-voltage characteristics....85
4.2.2.3 PV measurement....88
4.3 Discussion....89
4.4 Summary....91
4.5 Methods....92
4.6 References....93

Chapter 5 Hydroquinone–methanol reaction with H-terminated Si surface bridging reaction mechanism and electrostatics 97

5.1 Introduction....97
5.2 Surface characterization (XPS, ATR-FTIR) 99
5.3 Evolution of the surface dipole using CPD-SPV measurements....103
5.4 Discussion....108
5.5 Summary and further investigations. 111
5.6 References....112

Chapter 6 Hybrid, chemically passivated n-Si / PEDOT:PSS Semiconductor–Insulator-Semiconductor solar cell....114

6.1 Introduction....115
6.2 Experimental....117
6.3 Results....119
6.4 Summary....123
6.5 References....124

Chapter 7 Inherent limitation of PEDOT:PSS as top contact in hybrid SIS solar cell.....126

7.1 Introduction.....127
7.2 Results.....127
7.3 Discussion 131
7.4 References.....134

Chapter 8 General Discussion and Future Prospects.....135

8.1 Surface control by SAMs on oxide-free semiconductor.....136
8.2 An experimental window to fundamental semiconductor physics.....137
8.3 The HQ-MeOH surface reaction with Si(100).....137
8.4 Inversion layer solar cells.....138
8.5 SAMs in inversion layer solar cells.....139
8.6 Hybrid n-Si / PEDOT:PSS inversion layer solar cell.....140
8.7 References.....141

List of abbreviations

SAM – self-assembled monolayer

SCR - space charge region

SBH - Schottky barrier height

SS - surface state

CNL - charge Neutrality Level

FL - Fermi level

XPS – X-ray photoemission spectroscopy

FTIR – Fourier transform infrared spectroscopy

ATR – attenuated total reflection

CPD – contact potential difference

HQ – hydroquinone

MeOH – methanol

MS - metal-semiconductor

MIS – metal-insulator-semiconductor

MIS-IL metal-insulator-semiconductor inversion layer

SIS – semiconductor-insulator-semiconductor

PEDOT:PSS - poly(3,4-ethylenedioxythiophene) poly(styrenesulfonate)

MIGS - metal induced gap states

ALD - atomic-layer-deposition

PECVD - plasma enhanced chemical vapor deposition

TCO - transparent conductive oxide

ITO - Indium-tin-oxide

CIGS - $CuIn_xGa_{(1-x)}Se_2$

IP - ionization potential

TLM - transfer line method

IDIS - induced density of interface states

Chapter 1

General Introduction

Self-assembled monolayers (SAMs) were introduced 3 decades ago, and are popular research tools in various disciplines since. Nowadays, organic monolayers can be bound to many different surface topographies, not only planar ones, on metals, on semiconductors and on dielectrics. The field of molecular electronics – exploring the electronic properties of organic molecules – can generally be divided into the approach to electrically probe a single molecule, as illustrated in the left of Fig. 1-1, and that, which targets molecular monolayers instead, usually in a planar macroscopic structure, as illustrated in the right of Fig. 1-1 . In the latter transport across thousands of molecules is averaged out in a single measurement, and it will be the choice if the interest is in 2D ensemble effects, such as cooperative insulating capabilities or the surface layer (rather than a point) dipole, are to be monitored.

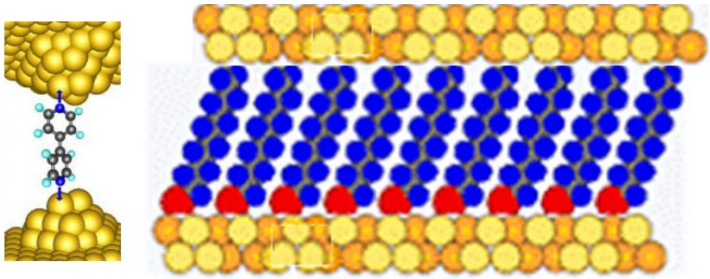

Fig. 1-1: Exploring the electronic properties of organic molecules, either in a single molecule junction (left), or in macroscopic junction, using self-assembled monolayers (right).

Binding SAMs to the surface of a semiconductor, e.g. Si, for molecular electronics, in which case the semiconductor also functions as one of the measurement electrodes, not only brings the researchers closer to realistic electronic devices, but also opens up a window to different physical phenomena that cannot be observed when only metal electrodes are used. For example, the surface dipole, introduced by the monolayer, will have a large impact on the J-V behavior of a metal-molecule-semiconductor junction, compared to its effect on a metal-molecule-metal junction.

The field on molecular monolayers on Silicon can also be divided to two major sub groups which are monolayers on native grown SiO_X and monolayers on oxide-free Silicon. While monolayers on

oxide have shown unique mechanical and structural properties, in terms of electrical properties they suffer from many problems. The native oxide, which is usually of thickness comparable to, or even thicker than the probed monolayer and morphologically irregular, tend to screen the molecular properties and to buffer the intimate molecules-semiconductor interactions that can be highly informative. As for oxide-free monolayers, in the last decade several methods were demonstrated to chemically bind an alkyl monolayer directly to an oxide-free Si surface through Si-C or Si-O-C bonds. In contrast to what is the case for binding to the native-oxide, with SAMs directly bound to the semiconductor the surface is abrupt, well-defined, and for good quality surface preparation and monolayers, homogeneous, a fact that enables measurements of the electrical properties of the monolayer with very high reproducibility. If the self-assembly mechanism produces dense binding of the molecules to the surface in a way that saturates most of the chemical dangling bonds – the SAM can also serve as an excellent electrical passivation layer, as will be thoroughly explained throughout this thesis. These properties of SAMs on the oxide-free semiconductor surface in turn, enable researchers to probe the bulk semiconductor with only minimal surface intervention. This ability to fine-tune surface properties of semiconductors makes the oxide-free monolayers very appealing in the field of photovoltaics.

Photovoltaics is the art and science of interfaces. For most types of cells, it is the absorption of photons in the base semiconductor (sometimes called absorber) that generates electron-hole pairs in it. Nevertheless, unless efficiently separated from each other, those charge carriers would recombine and not be able to drive an external load. The separation of electrons from holes is carried out or completed at the interfaces of the solar cell, and it is the point with the poorest performance in the interfaces of the active layers that dictates the properties of the entire interface and sometimes of the entire device. In addition, photovoltaics is deals with macro-, instead of micro-electronics , i.e., devices are fabricated

intentionally to be large in area. This last aspect makes solar cells to be among the most demanding applications in terms of surfaces and interfaces.

Going back to the self-assembly process, one of its big advantages is that large areas or volumes can be covered, if only the proper conditions are met. If indeed molecular monolayers on oxide-free semiconductors can provide us with high level of control over surface potential and passivation, that makes those systems attractive for photovoltaics.

Among the various types of solar cells, the metal-insulator-semiconductor (MIS) structure is conceptually one of the simplest ones. Compared to p-n junction solar cells made of a p-type semiconductor that forms a junction with an n-type semiconductor, in an MIS structure there is only one type of semiconductor with its back and top metal contacts. While the back contact is a regular ohmic one, it is the top contact that requires the ultimate surface passivation in order to a utilize its electrostatic potential to separate holes from electrons efficiently. Traditionally, high quality passivation was accomplished using an ultra-thin oxide layer that was grown between the semiconductor and the top metallic contact and, hence, the MIS acronym. The exact role of the interfacial layer, apart from that it passivated the surface, remained vague, though, through those years.

All the works gathered in this thesis deal with the electric behavior of SAMs at the interface between a semiconductor and a metal or conducting polymer. I used the system's photovoltaic characteristic as a probe to the SAM and its control over the interface. *I took this approach not only to realize if, and under which conditions SAMs can be used in an MIS solar cell, but also to understand the MIS concept in general and the role of the interfacial layer in those structures, in particular.*

Outline of this thesis

This thesis integrates the field of molecular electronics with the inversion layer solar cell. The latter was last reviewed more than 30 years ago, and seemed to lack some fundamental understanding of interface behavior, of the type that has been gained more recently in the area of molecular electronics and in studies on other types of photovoltaic cells.

In **chapter 2** I give a rather broad review of the family of inversion layer solar cells – MIS, SIS, MIS-IL and hybrid organic-inorganic inversion layer solar cells. The focal point of this review is the chemical and electrostatic role of the interfacial layer in those cells in view of recent findings and understanding of surface and interface behavior.

In **chapter 3** I demonstrate an MIS solar cell, fabricated using bottom-up techniques, and with an insulating layer that is a molecular monolayer, covalently bound to both semiconductor and the metal.

In **chapter 4** I use the hydroquinone-alcohol treatment, that was suggested to passivate the surface of oxide-free Si (on the basis of bulk life-time measurements) better than any other chemical treatment, on n-Si. I demonstrate near-ideal metal-semiconductor behavior with a Hg electrode. This effect is rather dramatic for Si, the most important electronic material, that was thought to be inherently Fermi-level pinned.

Chapter 5 is dedicated to the hydroquinone-metahnol (HQ-MeOH) reaction. The surface composition immediately after treatment is explored using XPS and FTIR, the reaction is studied using dipole and passivation measurements and a mechanism is suggested

A hybrid organic-inorganic SIS solar cell configuration is presented in **Chapter 6**. The upper electrode here is the degenerate p-type composite polymer PEDOT:PSS, and the semiconductor

interface is H-terminated for passivation. PEDOT:PSS, compared to evaporated metal, can and is softly deposited using spin-coating, a fact that is important in order to retain the high level of surface passivation at the interface.

In **Chapter 7** I compare n-Si(100) / PEDOT:PSS solar cells fabricated with H-termination and with an HQ-MeOH molecular monolayer. Surprisingly, none of the obvious differences in surface potential between those routes before PEDOT:PSS deposition, is expressed in the eventual solar cell performances. I attribute this phenomenon to a surface reaction that likely occurs upon contact with PEDOT:PSS, changing the surface dipole, but leaving no dangling bonds.

To sum this thesis up, a general discussion and future directions for inversion layer solar cells in general, and particularly with molecular monolayers are brought in **chapter 8**.

Chapter 2

Background – Inversion layer solar cells

Abstract. The context of my entire work is a family of solar cells based on inversion layer induced onto the semiconductor absorber by a metal, by a dielectric material hosting fixed charges, or by another semiconductor. In this chapter I review the MIS, SIS and MIS-IL solar cells that was last reviewed in 1978. In the family of inversion layer solar cells interfaces play a crucial role, even more dramatic than in other forms of solid state photovoltaics. A close attention is given to the fourfold role of the ultra-thin insulating / interfacial layer that is introduced between the semiconductor absorber and the upper electrode. Our current understanding relies also on recent findings in the field of molecular electronics and especially from organic monolayers self-assembled onto oxide-free semiconductor surfaces. 5 decades of on and off research on inversion layer solar cells is revised according to our new look on interfaces and interfacial layers.

This Chapter is to be published as an invited review in *Journal of physical chemistry letters*.

2.1 Preface

This review of inversion layer solar cells addresses a growing family of different photovoltaic structures based on **inorganic absorbers**, which share a common mechanism for charge separation. Inversion layer solar cells are constructed essentially by one type of semiconductor, which is type inverted close to its interface with an adjacent layer by means of electrostatics only, as explained below, to form a *de facto* p-n homojunction and allow efficient electron-hole separation. This approach to photovoltaics eliminates the high energy diffusion process steps as used in a conventional p-n homojunction (e.g., Si cells) or, for heterojunctions, the need to pair different p-type and n-type semiconductors that match for an efficient photovoltaic dance, as is the case for 2nd generation cells based on CdTe or Cu(In.Ga)Se_2,CIGS (but see below). The family of inversion layer solar cells, here reviewed, is made up of Metal-Insulator-Semiconductor (MIS), MIS Inversion layer (MIS-IL), Semiconductor-Insulator-Semiconductor (SIS), and hybrid organic/inorganic inversion layer solar cells.

Inversion layer solar cells hold a promise for high conversion efficiencies of the inorganic absorbers, as laboratory efficiencies of 16% for ITO/SiO_2/p-Si SIS[1] and 18.5% for MIS-IL[2] were demonstrated, with relatively cheap, low-energy fabrication processes that might lead to overall cost efficiency and grid parity. Looking in the future, the fact that only a single semiconductor is needed for these kinds of solar cells opens up the possibility to explore absorber materials that are different than commonly used ones.

Although the physics of inversion layer formation is well understood, in practiceexperiments led the field and theory lagged behind, similar to what happened with several other solar cell types (polycrystalline CdTe- and CIGS-based cells) in terms of their chemistry and physics. Specifically, the purpose of using an ultra-thin insulating layer in MIS cells remained unclear over 4 decades of research, and its properties were usually analyzed in retrospect, in view of the solar cell's performance.

In this manner SiO_2, with various deposition techniques, was used as a buffer layer in different metal – semiconductor (both n-type and p-type) configurations because of it was know and available, rather than because of its preferable properties.

Semiconductor surface chemistry for molecular electronics with semiconductors is providing a fresh view of what were thought to be well-known aspects of solid state electronics and an inversion layer was created in Si, by using a sub-nm molecular monolayer as buffer layer in the Hg / n-Si system.[3] Atop of that, new experimental techniques, that were not available two decades ago, allow one to monitor the electrostatic properties of the material used, before, during and after junction formation, and to better understand the different role of each of the layers and their interplay. Thus, the purpose of this introduction, aside from reviewing the field of interest and place the current work into perspective, is to shed some light on the electrostatic considerations that should be included for materials selection for inversion layer solar cells. This review should also assist in the future design of new materials to meet the requirements of inversion layer solar cells.

2.2 The Schottky-Mott model and formation of inversion layer

Ideally, according to the Schottky-Mott model,[4] if an n-type semiconductor is brought into intimate contact with a high-work function metal, electrons will be depleted from the semiconductor, with electrons flowing from the semiconductor, where the electron electrochemical potential is higher, to the metal where they have a lower electrochemical potential. This flow is thought to leave positively charged atomic sites in the region close to the metal/semiconductor interface, eventually forming a built-in potential equal to the difference between initial Fermi levels or electrochemical potentials. Fig. 2-1**.** illustrates the ideal metal/semiconductor junction formation for an n-type semiconductor and a high work-function metal, before and after electronic contact formation. In the model, the energy

barrier for electrons to cross from the metal into the semiconductor, also called the Schottky barrier, will be

$$\Phi_{Bn} = \Phi_m - X_{SC} \tag{1}$$

where X_{SC} is the semiconductor electron affinity, and Φ_m is the metal work function. The same principles hold for a p-type semiconductor and a low work function metal, with holes as the majority charge carriers rather than electrons.

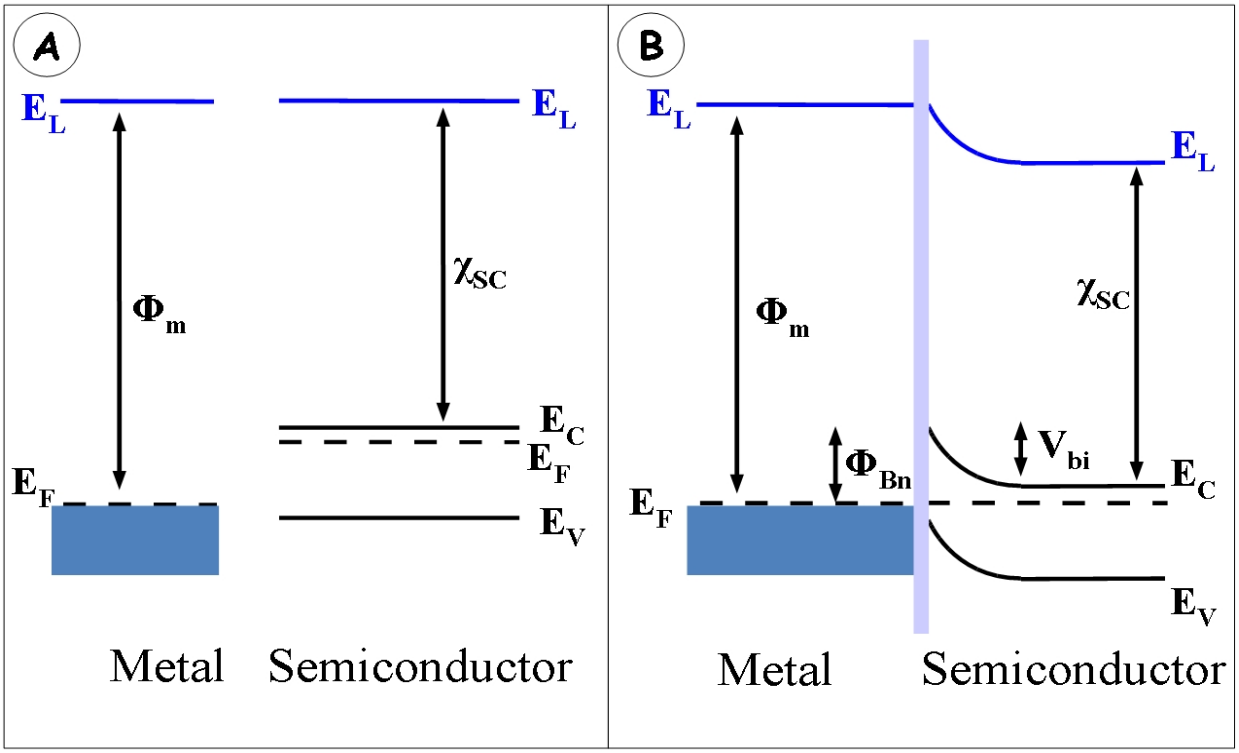

Fig. 2-1: Formation of metal/semiconductor junction according to the Schottky-Mott model. A) When separated the n-type semiconductor has an electron affinity X_{SC}, which is lower than the metal work function Φ_m. B) When brought into intimate contact electrons are depleted from the high-potential semiconductor moving to the lower-potential metal. This flow is ought to leave positively charged atomic sites in the region close to the interface, eventually forming a potential barrier Φ_{Bn} equal to the difference between initial Fermi levels.

For n-type semiconductor, if the number of electrons depleted from the region adjacent to the junction - the space charge region (SCR) – is greater than the number of positive charges left behind, the semiconductor can be said to be type-inverted.

In the extreme case, where the potential difference between semiconductor electron affinity and the metal work function is large enough, the SCR might be depleted **fully** of its doped electrons – the "strong inversion threshold". For potential difference larger than this any additional potential difference will be compensated by migration of mobile minority carriers (holes) from the bulk into the SCR, rather than further depletion of electrons. The semiconductor is now considered to be under strong inversion with mobile minority carriers from the bulk forming the majority of mobile carriers next to the semiconductor's interface. The junction can now be thought of as a *de facto* n-p junction, formed without high temperature diffusion process steps.

In terms of charge separation for photovoltaic applications, the holes, which are now majority carriers in the inversion layer, have a relatively long life time, allowing them to diffuse freely to the metal before recombining. Electrons are photogenerated in a region with a large electric field, which provides the driving force to remove then from the interface into the bulk semiconductor to the back contact. Charge separation in the semiconductor inversion layer is illustrated in Fig. 2-2.

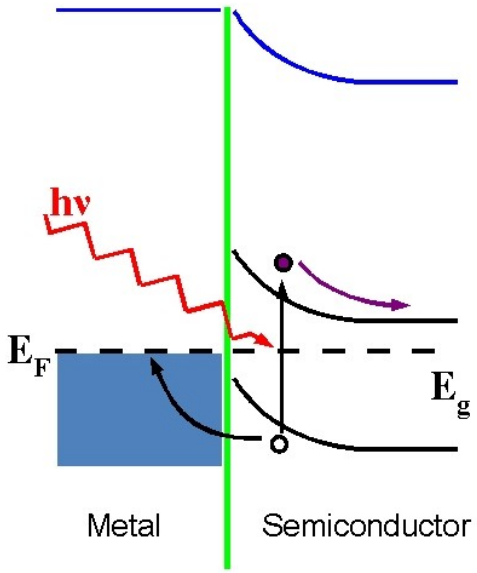

Fig. 2-2: Charge separation due to inversion layer, formed next to the semiconductor / metal interface. Photo-generated electrons experience a large energy barrier, preventing them from getting to the metal layer. Because holes are majority carriers in the inversion layer, they can diffuse to the metal before recombining.

A lot of experiments were carried out in the 1960's to examine the validity of the Schottky-Mott model , by measuring / deducing from measurements the Schottky barrier height (SBH) of junctions of metals of different work function on semiconductors. It was shown that metal/semiconductor junctions, based on wide bandgap, mostly ionic semiconductors such as GaS, ZnS, ZnO, SnO_2 etc. followed the Schottky-Mott model almost ideally. Si-, GaAs- and Ge-based junctions, though, seemed to obey the empirical "2/3 rule" i.e., yield a SBH equal to 1/3 of the bandgap for p-type substrates and 2/3 the bandgap for n-type substrates, almost independent of the metal used (Fig. 2-5). This behavior, already suggested by Bardeen in 1947, is known as Fermi level pinning and is caused by surface states with electronic energy levels within the semiconductor forbidden gap.5 Of course, a Fermi-level-pinned semiconductor cannot be drawn into strong inversion and transport across junctions with semiconductor Fermi level pinning will be dominated by majority carriers. For photovoltaic

applications such majority carrier-dominated device is less suitable, because photo-generated minority carriers will have a short life-time and are likely to recombine on their way to the metal electrode.

We note in passing that both of the 2nd generation, CdTe and the Cu(In.Ca)Se2 solar cells inversion plays a role, although in ways that are different from those considered here. In the case of the latter also the hardly studied single crystal analog is likely to be inverted, although the situation is more like that of a normal p/n junction in that the reason is Cu-depletion from the surface, which leads to a n-type skin on top of the p-material. The type conversion occurs also in the polycrystalline material, because in the solar cell the material 's grain boundaries are well-passivated, leaving only a minor conduction band discontinuity, while there is a significant valence band one, sufficient to type-convert the material.[6]

For CdTe the situation is somewhat different as here it is the very strong band bending at the grain boundaries that type converts those boundaries, creating local p/n junctions.[7] In both cases these junctions are in addition to the normal p/n junction formed most commonly with CdS.

2.3 Metal-Insulator-Semiconductor (MIS) solar cells

The MIS solar cell is an evolution of the Schottky barrier solar cell and is, as its name indicates, composed of basically 3 layers:

1. A moderately doped Semiconductor with ohmic back contact
2. An ultra-thin Insulating layer, usually a 2-3 nm thick oxide.
3. A semi-transparent Metal layer or a grid metal electrode.

Historically, the MIS structure was first introduced in photovoltaics in the early 1970's as a route to use semiconductors, different from Si, especially GaAs, as absorbers for solar cells and with the hope of

achieving higher conversion efficiencies than with the Si p-n junctions of that time (~12%).[8] It was found that an ultra-thin oxide layer, grown on the surface of the semiconductor, prior to metal deposition, can, in some cases, increase the junction's SBH and, thus, the voltage that can be obtained from the solar cell. In other words, the interfacial oxide layer was shown to unpin the semiconductor Fermi level, thus allowing more efficient use of the difference between the metal and semiconductor work functions.

Two seminal papers by Shewchun and Green in 1974 refocused attention on Si by showing experimentally that, with Al as top electrode and a 1-3 nm thick interfacial oxide layer, p-Si can be drawn into strong inversion, to dramatically increase the V_{OC} while retaining high photo-generated currents.[9] With the addition of numerical simulations, those papers laid the foundation and defined the terminology of minority carrier-dominated MIS solar cells.[10]

Numerical and analytical examinations of the MIS structure identified how the characteristics of a diode (and solar cell), dominated by minority-carrier transport, differ from one that is majority carrier-dominated.[10] [11] [12] [13] [14] Postulating that the presence of an insulating layer is crucial it was possible to solve the continuity equations for certain electrostatic conditions, and, thus, simulate the current-voltage behavior for each of the cases for a given insulator width. Results of such numerical calculations, following (later work of) Tarr et al.[12] are shown in Fig. 2-3. The dark current of a minority carrier junction is independent of insulator width for reverse and low forward biases, because it is minority carrier diffusion from/to the interface that limits the current. In a majority carrier-dominated junction, though,it is majority carrier tunneling through the insulator, which depends on the insulator width, that limits the current.

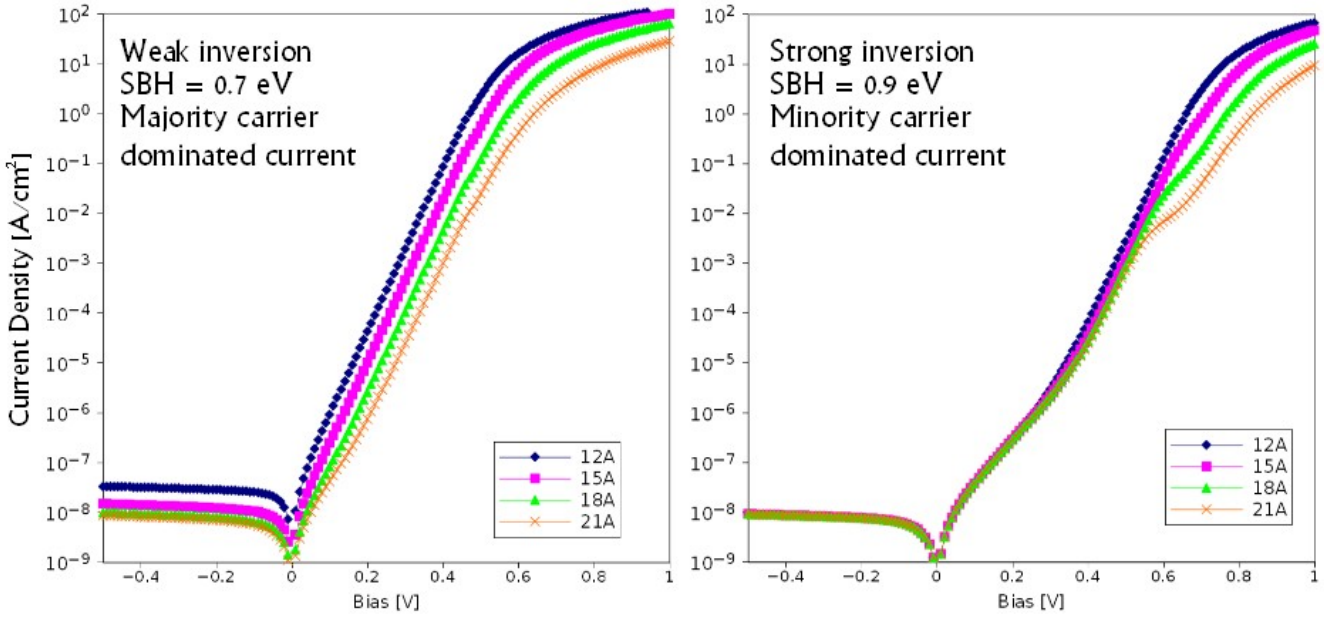

Fig. 2-3: Numerical calculations of current through ultra-thin MIS junctions. In a majority carrier-dominated junction (left), it is tunneling of majority carriers through the insulator that limits the current and, therefore, the current depends on insulator thickness. The dark current of a minority carrier junction (right) is independent of insulator thickness at reverse and low forward biases, because the process that limits the current is minority carrier diffusion from/to the interface.

When the junction is illuminated and operates as a solar cell minority carriers have to tunnel from the semiconductor through the insulator and into the metal, and majority carriers have to diffuse to the back contact. Any majority carrier current to the metal will be counted as loss and thus should be reduced to minimum. The major difference between minority and majority carrier-dominated junctions is illustrated in Fig. 2-4 taken from [15]. For majority carrier-dominated junctions, it is the insulator that suppresses undesired majority currents, but its thickness should also be a delicate compromise to allow minimal-loss minority carrier transport. Those opposing requirements cannot be fully met at the same time, but can be fine-tuned to their singular optima. In minority carrier-dominated junctions, though, it is the potential barrier within the SCR that prevents majority carriers from approaching the metal. In that case there is a relatively broad range of insulator widths that allow high open-circuit voltage and high general conversion efficiency. Interestingly, for minority carrier-dominated junctions, **the optimal**

insulator thickness seems to be infinitesimal – the best MIS insulator is the one that only affects the electrostatics without any tunnel barrier.

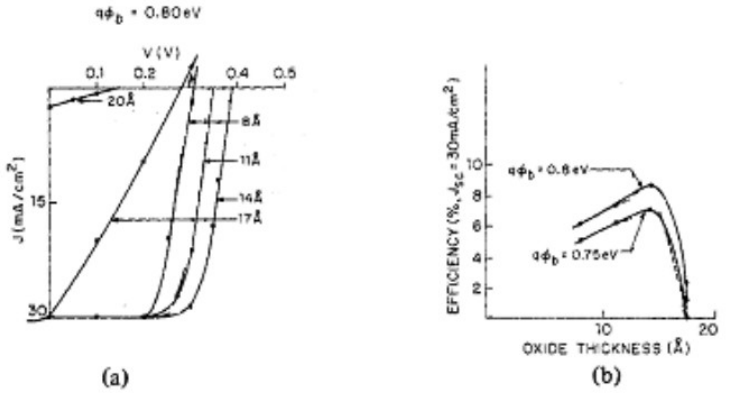

Theoretical results on MIS majority-carrier devices. (a) Illuminated *I–V* curve and (b) efficiency versus oxide thickness.

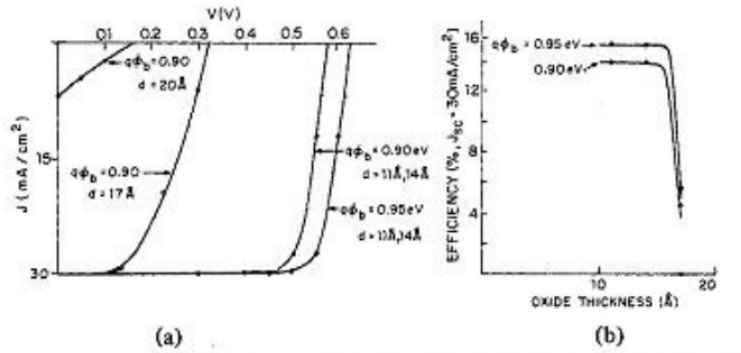

Theoretical results on MIS minority-carrier devices. (a) Illuminated *I–V* curve and (b) efficiency versus oxide thickness.

Fig. 2-4: Comparison of simulated solar cell performance of majority and minority carrier-dominated junctions. After Ng & Card 1980. For a majority carrier-dominated junction (top) there is a delicate compromise with singular optima between the need to suppress majority carriers tunneling to the metal and minimal loss of the desired minority carrier current. For minority-carrier dominated junctions (bottom) a broader range of insulator widths is permitted, and the optimal thickness is infinitesimal, because majority carriers cannot reach the interface because they are stopped by the energy barrier within the SCR.

Those important works have showed the advantages of minority carrier-dominated devices over majority carrier-dominated ones for photovoltaic applications. Unfortunately, the analyses avoided the important questions regarding MIS, such as what is the electrostatic contribution of the insulating layer in making an MIS structure a minority carrier-dominated one.

Fonash was the first to suggest the different possible roles that the insulating layer might be playing in making the MIS structure advantageous over its MS parallel.[16] Pulfrey in his review from 1978 [17] reduced the rather long list of Fonash to the three most probable contributions of the insulating layer to the junction's electrostatics:

1. surface state passivation,
2. buffer layer - preventing direct metal–semiconductor reaction,
3. accommodation of fixed charges

He then surveyed the different MIS works that were available at the time and checked in how far they fit his assumptions about the insulating layer. Ng and Card in their review distinguished the behavior of majority and minority carrier-dominated solar cells, especially with respect to their PV performances with different insulator widths.15 Generally speaking, no **metal** was shown to form minority-carrier dominated MIS with Si but Al (with p-Si).

One more role of the insulator that was overlooked over decades of MIS research is the additional interface dipole that can be introduced by the interfacial layer. This dipole can be as large as 0.5 eV in magnitude, and can completely change the junction electrostatics as was pointed out by Yaffe et al.[3]

In this review I will follow the methodology, used by Pulfrey[17] to examine the role of the insulating layer in an MIS solar cell and its derivatives, from a 40 years perspective. First , I will briefly explain the four different contributions of the interfacial layer to the junction electrostatics and the way that they should affect the solar cell, based on the junction. Then I will bring experimental evidence of work that uses one or more of those properties. After having established understanding of MIS and SIS solar cells, I will present our own contributions to the field, using molecular monolayer as an interfacial

layer, and an organic conducting polymer as the top-electrode. Finally, I will discuss how our research can be taken further, and suggest other directions within the field.

2.4 4 roles of the ultra-thin insulating layer in inversion layer solar cells.

2.4.1 Surface state passivation

2.4.1.1 The origin of surface states

The concept of surface states was first suggested by Bardeen to account for the discrepancy between the Schottky-Mott model for metal-semiconductor contacts and experimental measurements, carried out mainly, at that time, on Si and Ge.[5] Bardeen realized that the presence of electronic states on the surface, energetically within the semiconductor forbidden gap, will dramatically alter the metal-semiconductor electrostatics, and the eventual junction characteristics. Furthermore, he argued, that for surface state densities, $N_{SS}>10^{13}cm^{-2}eV^{-1}$ the semiconductor Fermi level will align according to the surface state occupation, with or without metal and regardless of the kind of metal used. This situation is known as Fermi level pinning.

With growing use of metal/semiconductor junctions and of research on semiconductors in general and on Si, in particular, the terms Fermi level pinning and surface states are commonly used and became synonyms for ill-behaved MS contacts. The origin of those states was mostly unclear, and this became an area of vast research in the second half of the last century. The explanations for surface states can be divided roughly into two schools:

1. Physical (internal) origin
2. Chemical (external) origin

The band structure of semiconductors is an outcome of the periodic nature of the crystal lattice. According to the **physical origin school**, the abrupt termination or alteration of this periodicity at the

surface can lead to the appearance of new localized allowed states inside or outside the bulk energy bands of the semiconductor. If these states are within the bands, they are called surface resonances and the carriers in them will easily delocalize, because of overlap with the bands. If the states are outside the bands, inside the gap, they are called surface states and it is these that play a major role in many aspects of semiconductor devices. The reasons are that they function as preferred recombination sites and that they can lead to Fermi level pinning as already mentioned. Usually within the terminology of this school, surface states are divided into acceptor- and donor-like states ,which can be either occupied or unoccupied, depending on their position relative to the Fermi level, with states below the Fermi level occupied by electrons. An acceptor-like surface state is negative if filled and a donor-like surface state is positive if unoccupied. The Charge Neutrality Level (CNL) is defined as the energy at which the density of acceptor-like state below it equal that of the donor-like states above it i.e., the net surface charge is zero. Initially, because the SBH was mostly independent of the metal used, it was believed that the SS position and distribution are solely a semiconductor properties and can be calculated *a priori*.

Kurtin, McGill and Mead pointed out the difference between the strong pinning reported for covalent semiconductors and the weak pinning for many ionic compound semiconductors. They have used the parameter of interface behavior S, as seen in Fig. 2-5, to express how much the experimental system is pinned and deviates from the ideal Schottky-Mott model (S=1 ideal system, S--> 0 strongly pinned system). S is defined as:

$$S = \frac{d\,\Phi_{Bn}}{d\,(\Phi_m - X_{SC})} \qquad (2)$$

They suggested that deviations from the Schottky-Mott model is related to how much the band structure is perturbed by the lattice termination. The more covalent the crystal is, they claimed, the

larger the perturbation is.[18] We note that for Si, which is the most covalent semiconductor, a wet etching process either in dilute HF solution or in NH_4F leads to hydride-terminated Si surface.[19] This crystal termination is known to yield excellent electrical passivation, i.e., low surface state density, as measured by surface photovoltage,[20] and photo-conductance decay life-time measurement,[21] even though this is probably the most abrupt stable lattice termination for Si that is possible.

A more advanced model from the same school, and one that is still widely accepted these days, is that of Metal-Induced Gap States (MIGS), first suggested by Heine.[22] According to that model, if a metal is brought into electronic contact with a semiconductor, each of the continuum of states in the metal decays exponentially into the semiconductor. That decay induces new gap states in the semiconductor within a few angstroms from its interface with the metal, making that region *de facto* metallic. Even a density as low as 0.02 states / atom / eV suffices to firmly pin the semiconductor Fermi level.[23]

The same phenomenon, measured as surface states or Fermi level pinning, can be approached from a very different perspective which I call the "**chemical origin**". Sakurai et al. [24] started from a perfect Si-SiO_2 interface, with no intrinsic surface states, and calculated the perturbation in energy caused by different kinds of vacancies or crystal dislocations. According to their model, a Si dangling bond produces a trap state at midgap energy, whereas an O-vacancy or Si-Si weak bond, and Si-O weak bond will produce states higher and lower than mid bandgap respectively. Termination on the crystal with hydrides, hydroxides, and halogen atoms will only produce states within the valence or conduction bands.

Freeouf suggested that the metal work function in the Schottky-Mott model should be revised to accommodate different interface phases or microstructures, which are formed through the metallization process. The effective work function at the interface is more of a weighted average of local work

functions, and in the case of compound semiconductors is mainly affected by the work function of the anion material.[25] Referring to the difference between wide and narrow bandgap pinning properties, Brillson suggested that stronger Fermi level pinning has to do with the higher reactivity of covalent semiconductors, than of their ionic counterparts, towards the deposited metals.[26]

In particular Si forms metal-silicides with practically every metal apart from Hg, Tl, Pb, and Bi, with very low ΔH_f and was shown recently to form Au-silicide already upon room-temperature sputtering of Au on Si(100).[27] Metal-silicides were shown to form rectifying majority-carrier dominated junctions with n-Si with the SBH ranging from 0.5 to 0.87 eV[28] as can be seen in Fig. 2-6 - similar to the values obtained for direct metal-Si contacts.

Tung addressed the effect of direct chemical interaction between metal and semiconductor on the resulting SBH in a different way. The polarizable metal-semiconductor chemical bonds, he argued, act to screen the metal work function from the semiconductor, effectively reducing the SBH to the experimentally found levels.[29] The fact that different surface morphologies of the same semiconductors produced different SBHs with the same metal was attributed by Tung to the fact that the SBH is usually measured over a very large area, thus averaging the surface inhomogeneities.[30]

The fact that Hg is one of the only metals that is not miscible and does not react with Si was used by Wittmer and Freeouf to demonstrate near ideal Schottky-Mott behavior with H-terminated p-Si,[24] thus further weakening the MIGS model. If indeed surface states are formed inherently from the decay of the electron wavefunction in the metal, into the semiconductor, the tail of the Hg wavefunction should have affected the Si in the same manner through the Angstrom-thick hydride layer, as was the case for other metals, but it did not. The same principle was recently demonstrated by us with a sub-nm molecular monolayer separating Hg and n-Si, producing near-ideal Schottky barriers (see chapter 4)

In summary, notwithstanding their wide acceptance and common use, experimental results obtained over the pat two decades, have called into question models that ascribe Fermi level pinning (especially for Si, Ge and GaAs) solely to surface states of physical origin.

2.4.1.2 Probing for surface state

When looking for surface states and measure their distribution it is important to note that there are actually two types of states, regardless of whether they are of physical or chemical origin. On the bare surface of the semiconductor before metal deposition, we can look for s**urface states** that are the product of lattice termination / dangling bonds. The same is true for the discontinuation of Bloch functions on the semiconductor/oxide borderline or for oxide inhomogeneities, if measurements are carried out in ambient atmosphere. If such states are charged then they lead to band bending, which is relatively easy to probe using either photoemission spectroscopy[31] or techniques that measure the surface photovoltage.[32] [20] Gap states are also preferred recombination sites. Thus, measurements of minority carrier lifetime, via, e.g., microwave photoconductivity, or time-resolved photoluminescence, can serve as an indirect indicator for surface state density.[33]

On the other hand, there are **interface states,** which form only if the semiconductor and metal are brought into intimate contact, either by MIGS or by metal-semiconductor interactions. These are harder to probe and usually can only be deduced *ad hoc* from the diode's current-voltage and capacitance-voltage measurements.

2.4.1.3 Surface state passivation

In view of current understanding that surface states and Fermi level pinning are electrostatic manifestations of either a semiconductor surface that has dangling chemical bonds, vacancies etc., or of metal-semiconductor interactions, the task of surface state elimination seems better defined than ever.

Here I will discuss the goal of making a defect-free interfacial layer, while the prevention of direct metal-semiconductor interaction will be discussed in the next section.

Most inorganic materials, including semiconductors, tend to react with air to grow native oxides, immediately after cleaving or etching, so as to minimize their surface energy. Such oxides are mostly poorly defined and inhomogeneous with lots of defects and vacancies> As a result it is a poor passivation layer. For a compound semiconductor further inhomogeneity and irreproducibility is the outcome of the fact that oxides of different valencies can mutually exist within the naturally occurring oxide layer. Thus, to passivate the surface of a semiconductor one cannot rely on the native oxide layer, but should, rather, replace it with a better defined layer with controlled chemical binding to the surface atoms of the semiconductor.

For Si a thermally grown oxide, either dry (grown in O_2 atmosphere) or wet (H_2O atmosphere) can be optimized to yield a surface with a very low density of surface states.[34] Heating the Si wafer to 500 -1000 ºC results in a high oxygen diffusion rate that helps to fully saturate the surface Si atoms and to reach the well-defined, stable SiO_2 stoichiometry. The thermally grown oxide is also dense enough to prevent later metal contamination from reaching the surface. Indeed, most successful MIS structures, surveyed by Pulfrey, had thermally grown oxide as their interfacial layer.17 In some cases, to be later discussed in the section dealing with SIS structure, a freshly grown native oxide was used, rather than a thermally grown one. It is worth noting, though, that if the deposition of the top layer requires elevated temperatures in a non-inert atmosphere, as is the case for the ITO spray-pyrolysis technique,[35] this step is likely to saturate the oxide and make it similar to a thermally grown one.

Another dielectric, used in the photovoltaic industry for passivation of Si surfaces and that was shown to produce very low recombination velocities, is Si_3N_4, deposited by plasma enhanced chemical vapor deposition (PECVD).[36] This treatment, as the more recently introduced Al_2O_3 passivation by

means of atomic layer deposition (ALD),[37] actually consists of a thin SiO_2 buffer layer that saturates the Si bonds, between the Si and the main dielectric film. The high density of fixed charges in the dielectric layer repels minority-carriers from the interface and thus reduces recombination velocity as will be thoroughly discussed in section 2.4.3 of this review.

Various types of thin insulators that were physically deposited on the semiconductor absorber to construct an MIS structure, but without chemically addressing the surface bonds, did not manage to unpin the surface Fermi level. That was the case, for example, for Bi_2O_3 evaporated on n-GaAs[38] and Langmuir Blodgett films of an anthracene derivative, deposited on n-CdTe[39] . Both show majority carrier-controlled current-voltage characteristics.

In the last decade organic molecules that self-assemble into a monolayer onto a semiconductor surface, were explored in molecular electronics research. The main attractive feature of self-assembled monolayers for surface passivation stems from the fact that their deposition is normally under much milder conditions than those needed for growing a thermal oxide, with temperatures varying from room-temperature to 250ºC. In practice, only monolayers on oxide-free Si were probed for their passivation properties. These can be self-assembled via either Si-C or Si-O-C chemical bonds by way of different adsorption techniques.[40] Molecular monolayers are, by definition, thin layers – usually 1-2 nm, as required for MIS. As can be seen in Table 1 below, some of them yield excellent passivation.

Self-assembly procedure	Molecules used	Minority-carrier life time τ_{eff}	Surface recombination velocity	Substrate	Ref.
Molecular vapor in UHV	9,10-phenanthrenequinone	122 μs	130 cm/s	reconstructed 2x1 n-Si(100)	Avasthi[41]
Thermal alkylation	1-10-decene-carboxilic acid	130 μs	120 cm/s	FZ n-Si(100)	Sieval[42]
Two step chlorination alkylation	methyl	230 μs	44 cm/s	FZ n-Si(111) >4000 Ω.cm	Nemanick[43]
Iodine assisted	I2 + methanol	700μs	~10 cm/s	FZ p-Si(100) 5 Ω.cm	Takato[44]
Quinhydrone – assisted	Quinhydrone + methanol	4.5 ms	4.2 cm/s	FZ p-Si(100) 150 Ω.cm	Takato[45]

Table 1: properties of Si surfaces passivated by self assembled monolayer of different deposition techniques.

For an organic monolayer to passivate the surface of a semiconductor it needs, as was discussed before, interact directly with its surface atoms. For that reason, some commonly used families of organic monolayers, which bind to the naturally occurring oxide rather than to the semiconductor itself, **will not be useful** as interfacial layer in an MIS structure. Such is the case for of silanes to SiO_2 on Si,[46] for thiols and phosphonates commonly self-assembled on the native oxide of GaAs, and for carboxylic acids adsorbed on II-VI chalcogenides and III-V's.[47] 48 In the case of oxide semiconductors, such as ZnO or TiO_2, the above-mentioned families might provide acceptable surface state passivation, though this remains still to be demonstrated

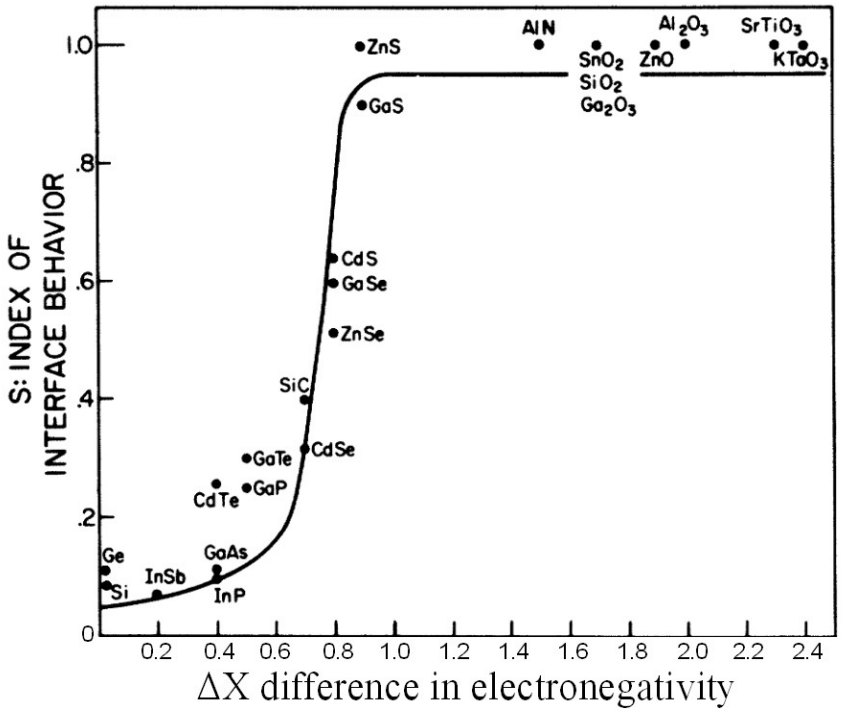

Fig. 2-5: The index of the interface behavior, S, as a function of the crystal ionicity, after Kurtin, McGill, and Mead 1969. Ionic semiconductors, such as GaS and ZnO follow almost perfectly the Schottky-Mott model with S>0.9, while covalent semiconductors such as Si, Ge, and GaAs exhibit S → 0, a high level of Fermi level pinning and barrier heights almost independent of metal work function.

2.4.2 Chemical passivation – preventing direct metal–semiconductor reaction.

As noted above, Fermi level pinning will prevent reaching strong inversion conditions within the semiconductor's SCR. Therefore, it is crucial to prevent surface state creation by direct metal-semiconductor interactions. With Hg as the top electrode on n-Si, modified by an alkoxy monolayer, we could demonstrate strong inversion conditions, yielding corresponding photovoltaic performance of V_{OC}=560 mV and 80% fill factor.[49]

Nevertheless, this requirement is not easily achieved with commonly used metals, especially if the buffer layer ought to be < 3 nm thick. Even if a very mild metal deposition technique is used, metal atoms may electromigrate through all or part of the interfacial layer, due to the built-in electric field.

Such process can cause localized interactions, which will electrically act as hot-spots, because the SBH there will be lower than in the surroundings. In such situation relatively high majority carrier currents can flow, which will effectively dominate junction behavior.

For a SiO_2 interfacial layer on Si, strong inversion conditions were reported for Al, Ti, and Cr, whereas Au, Pt, and Ni only produced majority carrier-controlled devices.[17] [15] Another case that was reported to yield a minority carrier solar cell with a SiO_2 interfacial layer is the ITO/SiO_2/n-Si SIS structure that will be discussed later. It seems that thin SiO_2 can only serve as a buffer layer for metals which are easily oxidized, because then spurious metal atoms will probably react first with the SiO_2 to form an additional insulating interfacial phase, rather than reaching the Si surface to react with it. In the case of compound oxide semiconductor contacts, such as NiO_2, MoO_3, ZnO and ITO, one can expect that with careful deposition strong inversion can be reached with a SiO_2 buffer layer, because electro-migration is less probable.

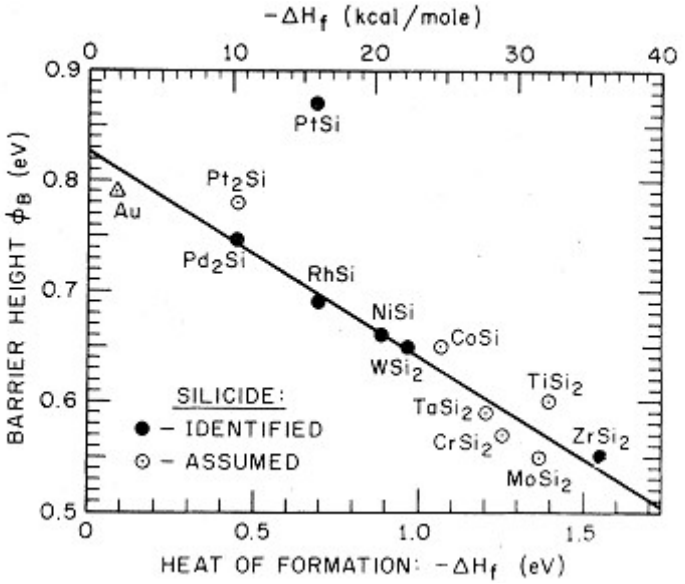

Fig. 2-6: Schottky barrier height of transition metal silicides with n-Si vs. their heat of formation. From Andrews & Phillips 1975.

Self-assembled monolayers can be prepared to be dense and homogeneous over large areas, but even then grain boundaries within the monolayer seem to be inevitable and are likely to act as point defects, if followed by metal evaporation (including indirect evaporation) or sputtering.[50] [51] [52] A molecular monolayer with an exposed reactive chemical end group might block penetration and migration of metal atoms, if soft deposition techniques such as nano-transfer printing[53] are used. A spin-coated conducting polymer[54] or transparent conductive oxide (TCO) deposited by ALD might be used for that purpose.

2.4.3 Accommodation of fixed (trapped) charges – field effect passivation

In the early days of semiconductor research surface states were usually categorized as fast and slow surface states according to their average lifetime. The fast surface states were said to interact strongly with the semiconductor's space charge region, due to their loci on the immediate surface, which allowed for rapid charge injection. The slow surface state are those buried within the native oxide layer with weaker interaction with the semiconductor, which leads to a longer lifetime.[55] With the improvement in surface characterization and control of surface parameters, slow surface states were realized to be trapped charges in the oxide, i.e., they are a property of the dielectric layer rather than of the semiconductor itself.

The fixed charges in a dielectric film stem from deviation from the stated stoichiometry i.e., from defects or vacancies. For each type of vacancies the energy can be calculated *a priori,* especially whether the specific vacancy introduces positive or negative charge into the film. Another source of charges in the dielectric film can be foreign ions, trapped in the insulating matrix during film deposition. This source explains how the type and density of charges can vary from one deposition technique to the other and, of course, between one dielectric and another. In the case of crystalline

dielectrics, the grain boundaries can also introduce states within the bandgap, but these will not be discussed here.

For the fixed charges to be advantageous for inversion layer solar cells no trap state can be present in the immediate interface with the semiconductor, as was explained above. In other words slow surface states are only beneficial for our application in the absence of any fast surface-states. This been said, the charges, trapped in the matrix, are far enough from the interface to prevent their diffusion to the semiconductor substrate. Their absolute charge, thus, has to be cancelled out by charges of the opposite type gathered either next to the semiconductor's interface with the dielectric, or at the outer insulator/air surface or by both. Positive charges trapped in the insulating layer on a p-type semiconductor, should, following that logic, drive minority carriers, electrons, in the semiconductor to its interface with the dielectric and, thus, assist its inversion. The same logic holds for negative charges on an n-type semiconductor.

The commonly used insulating film in MIS solar cells and in microelectronics in general is thermally grown SiO_2 on Si. This oxide is known to host positive charges ,which stem from oxygen vacancies.[56] It seems, though, that with the present experimentally available control over oxidation parameters, the density of those vacancies has diminished, because their effect is not as pronounced now as it was in the early days of MIS solar cells, when the oxide was definitely positively charged and reaching strong inversion was possible only in p-Si for that reason.17

Another common insulating film in the photovoltaic industry is Si_3N_4, usually used for passivation and as anti-reflective coating. Si_3N_4 is grown by plasma-enhanced chemical vapor deposition (PECVD).[36] It is known to host a high density of positive charges, probably introduced by the plasma. If grown on n-type material, its positive charge repels the minority carriers away from the interface and thus reduces surface recombination rates. This type of passivation, which resembles the

high doping used in back surface field solar cells, is called field-effect passivation. Recently, atomic-layer-deposited (ALD) Al_2O_3 was introduced in photovoltaics as back field passivation for p-Si. Excellent passivation was reached due to the high quality of the film along with the high density of negative charges in it, which was measured (using corona) to be $Q_{SS} > 10^{13} cm^{-2}$.[37] As in the case of Si_3N_4 plasma-assisted deposition led to higher fixed charges and thus yielded better passivation properties.57 One should note that for both of those passivation techniques an ultra-thin layer of SiO_2 buffers between the Si and the charged dielectric and provides the surface state passivation that is required to enjoy the additional benefits of the electric field that is due to the charged dielectric. Both of those insulating films are usually too thick to be used as an interfacial layer in MIS or SIS structures but can be very useful (and Si_3N_4 indeed was) when an MIS-IL structure is considered as will be explained below.

Another strategy to get a high density of fixed charges is to trap positive or negative ions in the dielectric layer. This step is usually done after basic surface state passivation has been achieved and in that manner those ions are prevented from getting to the sensitive semiconductor interface. For Si_3N_4, Hezel and colleagues introduced Cs^+ ions by dipping the sample prior to PECVD deposition (after a 1.3 nm thermal oxide formed) in an alcohol solution of CsCl.[58] Kobayashi et al. suggested the crown-ether cyanide treatment for the n-Si/ SiO_2 / ITO SIS structure to increase the V_{OC} of the solar cell.[59] The authors claim that the CN^- ions bind directly to the Si atoms to decrease the surface state density, does not seem likely, because the treatment is carried out after a thermal oxide was grown for 15 min at 650ºC.[60] Instead, we suggest that with the elevated temperature needed for later ITO deposition, the CN^- ions diffuse into the oxide and contribute to the inversion of the SCR by electrostatic interaction.

2.4.4 Additional interface dipole

An aspect that was generally overlooked in research on MIS / SIS structures is the way the insulating layer affects the work function of the semiconductor by introduction of an interfacial dipole. An external surface dipole Δ_S on a semiconductor (especially one that occurs over a layer thin enough to tunnel through) lowers or increases the local vacuum level at the interface, depending on the direction of the dipole. Such a dipole, as illustrated in Fig. 2-7, changes the energy needed to extract an electron from the semiconductor into the vacuum level and, thus, can be thought of as altering the electron affinity, the ionization potential and the work function of the semiconductor ($X_{SC} \rightarrow X_{eff}$ etc.). When the semiconductor with its interfacial layer is brought into intimate contact with a metal or a second semiconductor, it is the difference between the effective work functions (or electrochemical potentials) of the two that is the driving force for charge carrier migration from the semiconductor to the metal or vice versa, and the creation of a SCR within the semiconductor.

Lately, in the field of molecular electronics, it was repeatedly demonstrated that changing the surface dipole and X_{eff} of a semiconductor and then forming a junction with a single metal indeed changes the eventual barrier height in the same manner as that obtained by using metals of different work functions on a semiconductor of a single type.[61] [62] [63] In that case the Schottky-Mott model is slightly revised to yield the following expression for the barrier height (for n-type):

$$\Phi_{Bn} = \Phi_m - X_{eff} \tag{3}$$

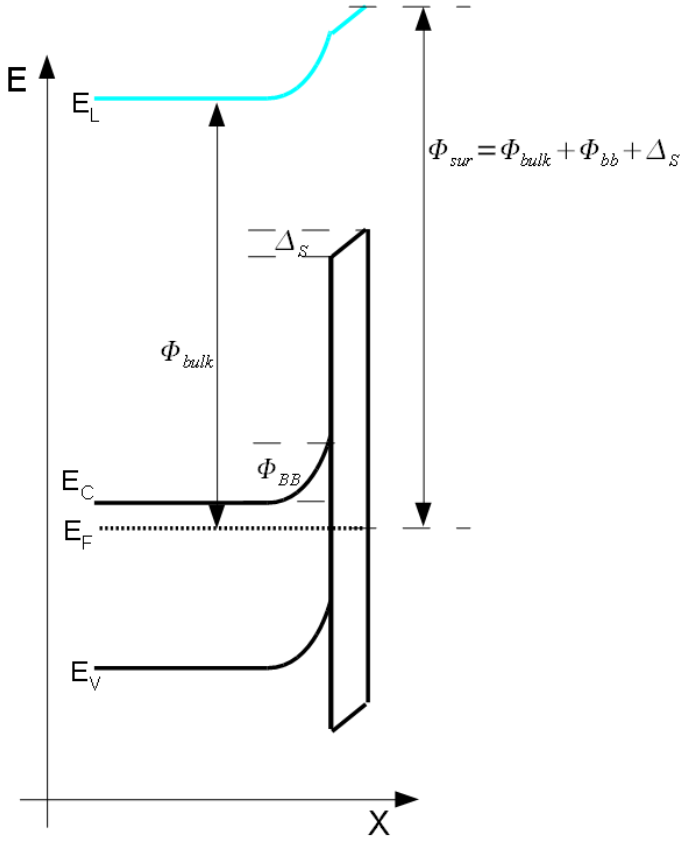

Fig. 2-7: Schematic illustration of how the work function, measured at the surface of a semiconductor, is determined by the work function of the clean surface, the band bending, due to the space charge, and the surface dipole.

Our work with hydroquinone-alcohol monolayers on oxide-free n-Si, chapter 4, shows that with high quality surface passivation the barrier height can be varied tremendously in that way with a near ideal (Schottky-Mott) correlation between the measured X_{eff} before junction formation and the Φ_{Bn} obtained after junction formation.

The surface dipole is an interplay between the terminating atomic layer of the semiconductor, the interfacial layer, and the vacuum, and thus cannot be easily predicted. Experimental measurement of surface dipoles, on the other hand, got a lot of attention recently, due to the emergence of organic electronics, and the importance of energy band alignment in that field.[64] For an ultra-thin layer, the surface dipole can be extracted by comparing the work function, measured after layer deposition, to the

known bulk semiconductor work function, and knowing the band bending in the SCR as illustrated in Fig. 2-7 below. Ultraviolet photoemission spectroscopy (UPS) is a common way to probe the surface work function, while data collected by X-ray photoemission spectroscopy (XPS) can be analyzed to produce band bending information.[31] [65] Another method to measure the (relative) work function, which can be used in ambient environment, is to determine the contact potential difference (CPD) by vibrating Kelvin probe . The complimentary photo-saturation surface photovoltage (SPV) measurement, carried out in the same experimental setup, can be used to assess the semiconductor's band bending, and, thus, to extract the dipole contribution to the work function of the modified surface.[66]

2.5 MIS Inversion Layer (MIS-IL) solar cell

The metal in the MIS structure is aimed to invert the SCR of the semiconductor absorber, and to efficiently collect the photo-generated minority carriers. However, for photovoltaic action to occur light has to pass through the metallic window, and the reflection and absorption losses due to the metal, posed a major problem for this direction in photovoltaics.

A different way to invert the underlying semiconductor, and to avoid reflection losses from the metallic top-electrode, was suggested by Salter.[67] If a dielectric layer, containing fixed charges of a single type (as was discussed in the previous section), is to be deposited on the semiconductor surface, with an ultra-thin insulating buffer between them, charges of the same polarity will be repelled from the semiconductor/buffer interface, while those of the opposite polarity will be attracted to it. If for example, a dielectric, containing trapped positive charges, will be deposited onto p-Si, majority holes will be repelled or depleted from the SCR of the Si, while minority carrier electrons will be attracted into it ,thus inverting its type to make *de facto* N^+-Si (capitals N, P are commonly used for highly doped semiconductors, compared to n, p used for low / moderately doped ones). In order to fully deplete the

SCR of a semiconductor of its majority charge carriers the dielectric is required to host a fixed charge of density $Q_{SS} > Q_{inv}$ where:

$$Q_{inv} = q \cdot N \cdot X_d = \sqrt{(2 q \epsilon_s \epsilon_0 N \Phi_S)} \tag{4}$$

where q is the elementary charge, N is the initial doping density, X_d is the SCR width, ϵ_s, ϵ_0 are the vacuum and the semiconductor's relative permittivity respectively and Φ_S , the built-in potential needed for strong inversion can be calculated:

$$\Phi_S = 2 \Phi_{Fn,Fp} = 2 \cdot \frac{kT}{q} \ln \frac{N}{n_i} \tag{5}$$

where k is the Boltzmann constant, T is the temperature, and n_i is the intrinsic carrier density.

Fig. 2-8 below shows the density of fixed charges required to fully invert the SCR of Si of various doping densities.

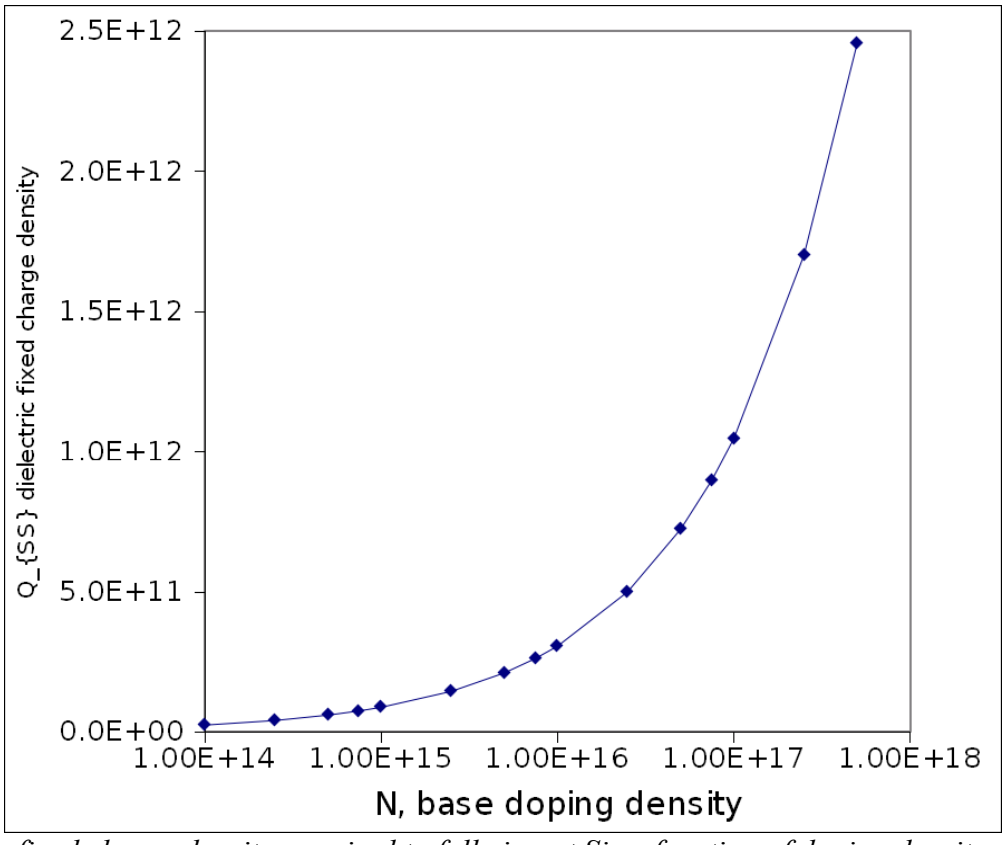

Fig. 2-8: The fixed charge density, required to fully invert Si as function of doping density.

Due to the strong inversion within the SCR the minority carriers will be able to diffuse rather freely in that layer to get to a thin metal grid that needs to shade no more than 10% of the solar cell's active area, as can be seen in Fig. 2-9**.** In this approach, later named MIS-IL for inversion layer, a n-P+ or p-N+ junction can be formed without high energy diffusion process steps. If well-designed this dielectric can also serve as anti-reflective-coating (ARC) to dramatically reduce the reflections from the high refractive index semiconductor surface.

Indeed, thermally grown SiO_2 was shown to be positively charged – to induce **certain** level of band bending even without an upper metal contact. First MIS-IL solar cells were presented using thermally grown SiO_2 both as the ultra-thin interfacial layer and the inversion-inducing dielectric, with reasonable inversion layer conduction.[67] [68] [69] [70] In retrospect it seems that this fact also worked in favor of p-Si -based MIS solar cells to enable their strong inversion with Al. An MIS cell, based on n-Si, though, was bound to be dominated by majority carriers, regardless of the work function of the metal, used as top contact.[15] The density of positive charges in the thermal oxide sufficed to invert the Si/SiO_2 interface but sheet resistance within the inversion layer remained rather high, and a dense mesh of metallic fingers was required to collect the photo-generated current with minimal losses.[70]

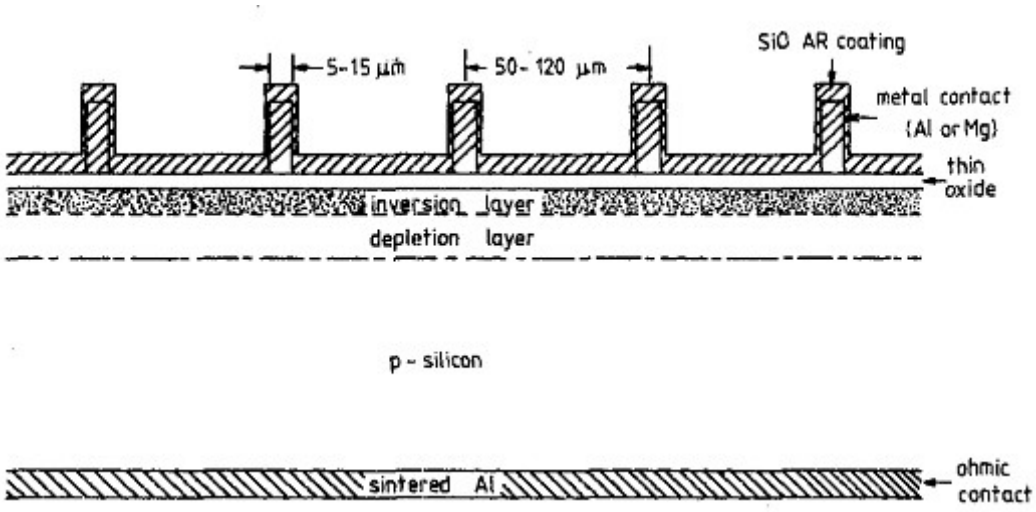

Fig. 2-9: Schematic cross section of an MIS-IL solar cell. A thin dielectric film containing fixed positive charges, deposited on a p-Si absorber, induces inversion within the SCR of the Si - allowing minority carriers, electrons, to diffuse freely to the metal grid finger. From Godfrey et al. 1980

A big advance was made with the introduction of plasma enhanced CVD Si_3N_4 dielectric films.71 Since the beginning of 1980's Si_3N_4, that was later measured to host 2-3*10^{12} cm^{-2} positive charges, became the leading dielectric for MIS-IL solar cells, based on p-Si.72 On top of the higher density of fixed charges, compared to the thermally-grown oxide, Si_3N_4 is deposited at temperatures ranging from 250ºC to 400ºC, lower than those needed to grow SiOx, thus allowing cheaper fabrication. As noted earlier introducing Cs^+ ions into the nitride layer enhances its charge capacity and this led to 18.5% conversion efficiency,[2] improved to 19.5% with textured surface to minimize reflection losses, as shown in Fig. 2-10, .[73]

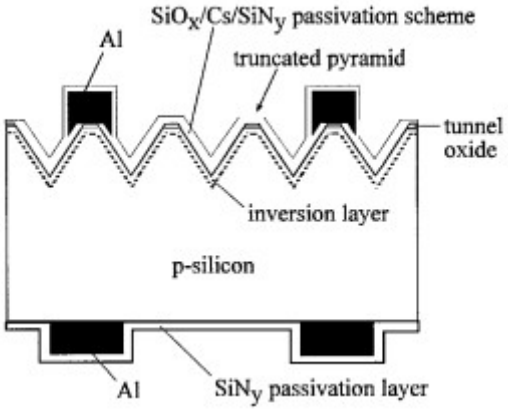

Fig. 2-10: Texturized MIS-IL solar cell on p-Si with Cs-doped Si_3N_4 as inversion-inducing dielectric and ARC.

2.6 Practical limitations of MIS-IL solar cell

The transition to the MIS-IL structure solved one of the big problems of the MIS structure – the loss that stems from reflection and absorption of the top metallic contact. Nevertheless, current collection had now to rely on the limited lateral conduction within the inversion layer to the collection grid fingers. A simplified calculation of that general limitation will be given here, while a more detailed numerical analysis for a p-Si MIS-IL structure with plasma enhanced Si_3N_4 was carried out by

Kuhlman et al.[74] The sheet resistance of the inversion layer (R_{sh} in Ω/□) can be roughly calculated using:[67]

$$R_{sh}=\frac{1}{Q_{min}\cdot\mu_{min,inv}} \tag{6}$$

where $\mu_{min,inv}$ is the mobility of minority carriers within the inversion layer, a mobility that is lower than the bulk mobility value. For a Si inversion layer the electron and hole mobilities were measured to be 500 and 200 $cm^2/V\cdot s$ respectively.[75] Q_{min} is the density of minority carriers, attracted from the bulk to the interface (in $C\cdot cm^{-2}$). For a thick enough (>100 nm) dielectric:

$$Q_{min}=Q_{SS}-Q_{inv} \tag{7}$$

Fig. 2-11 below plots the calculated series resistance of the inversion layer for p-Si inverted by a Si_3N_4 layer with $2.3\cdot10^{12}$ cm^{-2} positive charges,[72] and for n-Si inverted by Al_2O_3 with $1.2\cdot10^{13}$ cm^{-2} negative charges.[37] Although the hole mobility is inferior to the electron mobility both in the bulk and in an inversion layer, Al_2O_3 deposited with plasma assisted ALD hosts 5 times the charges of Si_3N_4 thus inducing stronger inversion and lower sheet resistance of the inversion layer. Recently, Sidhu et al. measured the higher value of R_{sh}=16kΩ/□ for an inversion layer, induced by ALD (no plasma) Al_2O_3 on n-Si 1 Ωcm, using a modified transfer line method (TLM).[76] We attribute this result to the lower charge density in the dielectric, due to non-optimal deposition properties.

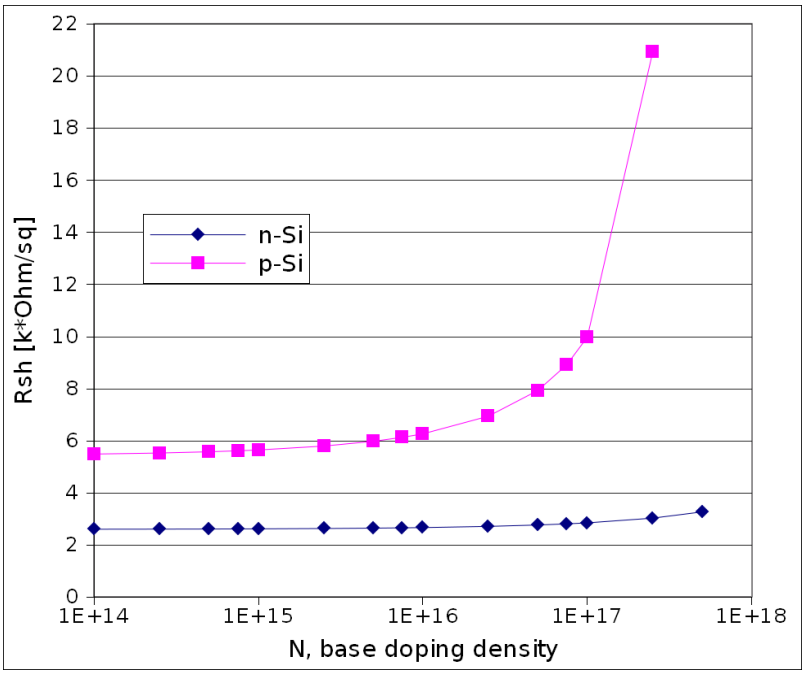

Fig. 2-11: Calculated inversion layer series resistance vs. base doping density. For n-Si, Al_2O_3 with 1.2 10^{13} cm^{-3} fixed negative charges was used, while the p-Si case was calculated using Si_3N_4 with 2.3 0^{12} cm^{-3} fixed positive charges.

With high values of sheet resistance the current collection fingers of the MIS-IL ought to be rather dense, compared to what is the case for conventional p-n junction solar cells. Using SiO_2 and Si_3N_4, all the prototypes published, used photolithographically defined 5 µm – 30 µm wide fingers, spaced 100 µm – 300 µm apart. However, while the MIS and MIS-IL solar cells were originally suggested as a cheap alternatives with comparable conversion efficiencies to the conventional p-n junction solar cells, using photolithography, instead of screen printing to realize metal grid contacts, is not a practical proposition (but possibly, in the future ink-jet printing may replace photolithography). In Fig. 2-12 the inversion layer contribution to the solar cell's series resistance in a double busbar configuration is calculated, following Meier et al[77] for different grid line spacing (2b):

$$R_S = 1/3\, b^2 R_{sh} \tag{8}$$

If a burden of 1 Ω cm^2 is set as a threshold, the grid spacing for p-Si $N_A=5\cdot10^{16}$ cm^{-3} with plasma enhanced Si_3N_4 should be <300 µm. Taking into account that the finest line width using state of the art screen printing techniques is ~50 µm – this will result in intolerable ~20% shading. The situation is somehow improved if n-Si $N_D=5\cdot10^{16}$ cm^{-3} with plasma-assisted Al_2O_3 is to be used, since 600 µm spacing will still meet this threshold, which will imply ~10% area shadowing.

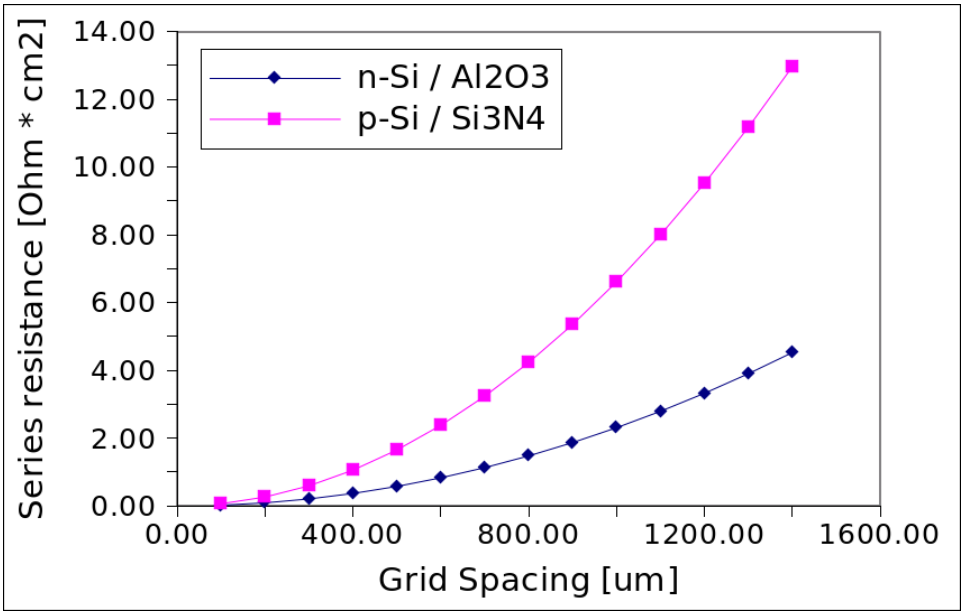

Fig. 2-12: Inversion layer contribution to the cell's series resistance with N= $5\cdot10^{16}$ cm^{-3} as a function of grid spacing.

Martín et al. suggested that MIS-IL solar cells should be fabricated with their inversion layer at the back, as can be seen in Fig. 2-13 below.[78] In the back inversion layer emitter (BILE) configuration that they advocate, shadowing losses are minimized because the dense grid needed to compensate for the high sheet resistance of the inversion layer is at the solar cell's back side, and light has only to pass through the sparse grid of what is in common cells the ohmic "back" contact. Moreover, with the inversion layer at the back Al can be used to invert the p-Si and positively charged Si_3N_4 with its mild charge density need not be relied on. According to their calculations, total conversion efficiency can be improved from 18.5% to 19.5% in that manner.

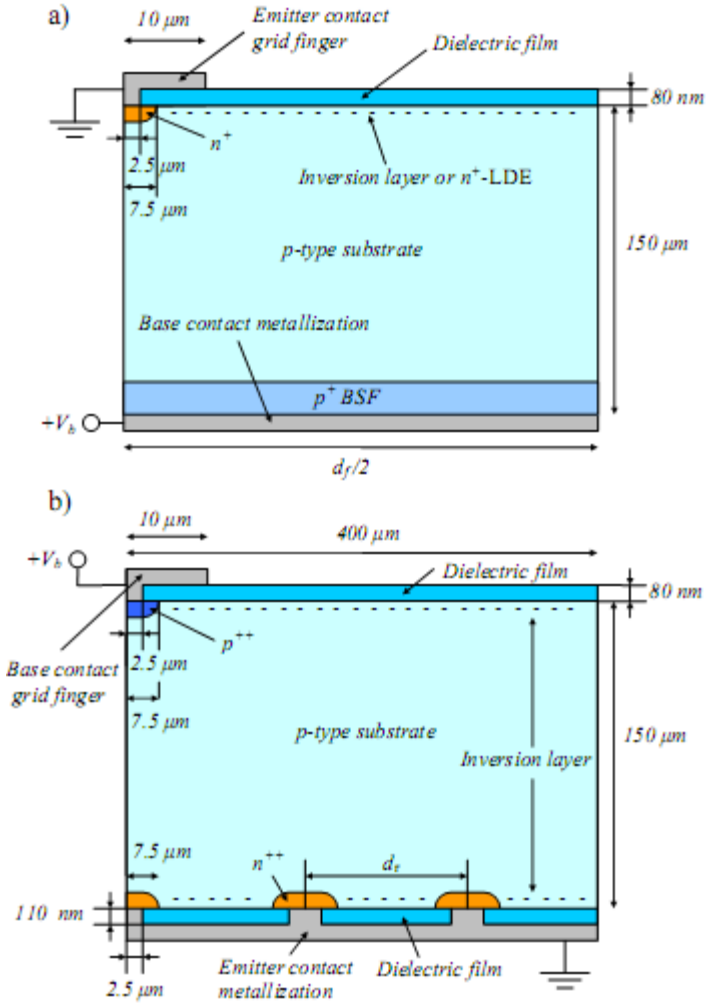

Fig. 2-13: Suggested configuration for MIS-IL solar cell. Top) regular front inversion layer emitter (FILE) cell - dense grid lines imply higher shadowing of the active area. Bottom) Suggested back inversion layer emitter (BILE) - sparse front grid allows up to 1% improvement in conversion efficiency.

2.7 Degenerate-Semiconductor – Insulator – Semiconductor (SIS) solar cells

A unique branch of the MIS solar cells family is that of degenerate Semiconductor – Insulator – Semiconductor (SIS) solar cells. In SIS cells that emerged in the late 1970's, a degenerate wide band gap semiconductor, which is transparent in the visible and has a low resistivity, is used instead of the metal top-electrode of the MIS structure. Ideally by doing so, one can avoid the reflectance losses that have to do with the thin metal contact layer, or the shading losses of the metallic grid current collector.

The vast majority of the work in the field used Tin-doped Indium Oxide (ITO) as the upper electrode. ITO is a solid solution of In_2O_3 and SbO_2 (usually 10% Sn_2O_3 by weight). Electrically, it is a degenerate n-type semiconductor with a wide bandgap 4.2 eV>E_G>3.6 eV, which is tunable with deposition properties.[79] The work function of clean ITO is $\Phi_{ITO} \approx 4.7eV$, but different oxygen concentrations might reduce that value to 4.3 eV.[80] Already in the late 1970's Si SIS solar cells with ITO as their top semiconducting window were fabricated with some degree of success and double digit efficiencies were reached for both p-Si[81] and n-Si[82] This is somewhat surprising if only the work function of the ITO is taken into account, because it definitely cannot invert both doping types simultaneously. Jain et al. tried to explain that by postulating either positive or negative fixed charges within the insulating layer, depending on the deposition process used.[83] They too admit it to be an *ad hoc* explanation because, at the time, there was no way to measure that property. Shewchun et al., on the other hand, explained the duality by the variabilty of ITO's work function,[84] again without substantial evidence.

Looking at the band structure of those SIS solar cells points to the fact that we are actually talking about two types of SIS cells, rather than one, as can be seen in Fig. 2-14 below. Sen and Srivastava gave the efficiency calculation for n-type ITO on top of n-Si absorber, shown in Fig. 2-14 **a)**.[85] In this N+-n structure the SCR of the Si, close to the Si-insulator interface, should be inverted by the work function of the ITO in order for the junction to be minority carrier-dominated. In that regard the N+-n SIS solar cell is exactly like its MIS parallel with the obvious advantage of a transparent "metal". This approach to photovoltaics was continued throughout the 1990's and 2000's mainly by Vasu and Subrahmanyam,[86] and by Nakato and colleagues, using electron beam evaporation and spray-deposition methods to deposit the ITO.[87] [88] Kobayashi and others went forward to examine the influence of cyanide treatment done on the Si prior to the SiO_2 deposition on the ITO-SiO_2-n-Si SIS

solar cell performance.89 One should note that some of the later works deposit ITO on freshly etched Si with no intentional interfacial layer.[88] We contend that with elevated substrate temperatures needed for spray-pyrolysis in oxygen-containing atmosphere, some Si oxide is formed at the interface of Si and ITO.

This field has regained some interest in the last couple of years with the steep rise of oil prices, due to the potentially relatively low fabrication costs of the cells.[90]

Similar in structure but physically different is the SIS solar cell, made from ITO on p-Si, as illustrated in Fig. 2-14 **b).** Shewchun and colleagues dealt with this structure both numerically and experimentally and pointed out that the majority carrier transport from the absorber to the upper electrode is not suppressed by the energy barrier alone, as in an MIS cell, but also by the lack of allowed states in the wide band gap of the top semiconductor.[91] [1] This diagnosis should have been emphasized further to state that the degenerate N+ ITO-p-Si is inherently a minority carrier device, just like CdS-CdTe heterojunction for example, regardless of the depletion state of the space charge region. The insulating layer along with the inversion of the space charge region acts to eliminate the otherwise probable recombination at the interface between the valence band of the Si and the ITO's conduction band. Of course the case in which a P+ window is used on top of an n-type absorber is, for all practical purposes, equivalent.

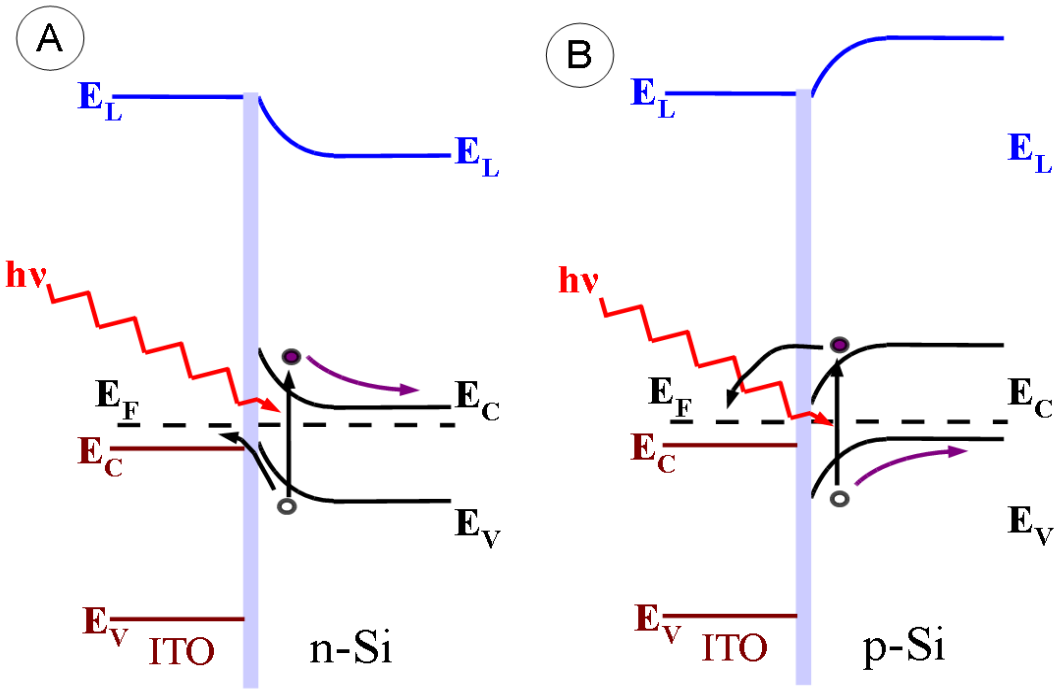

Fig. 2-14: Ideal band alignment for ITO / Si SIS solar cells. a) with n-Si absorber the the junction is physically the same as an MIS structure – strong inversion of the Si SCR induced by the difference in work functions repels majority carriers from the interface inwards, thus making the junction minority carrier-dominated. b) The device is inherently minority carrier-dominated due to the absence of available states in the band gap of the ITO for the majority carriers (holes) from the Si to tunnel to. The space charge and the insulating layer act further to eliminate recombination between the Si valence band and the ITO conduction band or via interface states in the Si gap.

This inherent difference between N+-n and N+-p types of SIS was generally overlooked, and the fact that the two share the same acronym might serve as an indication for that. In practice, even though the difference between the ionization potential (IP) of the p-Si and the work function of the ITO could never account for strong inversion, even when the SiO_2 interface dipole is taken into account, those cells exhibits the ideal V_{OC} for almost every doping level that was used. Their main loss mechanism as noted by Shewchun et al. is a low short-circuit current J_{SC}[92] that stems, probably, from interface state-

assisted recombination. With an n-Si absorber, on the other hand, most of the papers report close to the ideal J_{SC} – either 33-36 mA/cm^2 at AM1.5 or 40 mA/cm^2 at AM0 illumination conditions.

2.8 Recent publications

Recent years have seen a revival, judging by the number of publications , in the use of MS and MIS configurations for photovoltaics. This late bloom is motivated by the growing interest in renewable energy solutions in general, but also has to do with a desire to apply some of the products of the immense nanotechnology research effort, such as carbon nanotubes,[93] graphene,[94] and other potential substitutes for ITO. The relatively simple fabrication of MS / MIS structures make them ideal candidates for technology demonstration purposes. In terms of interface passivation, if Si is wet etched just prior to electrode deposition, the hydrogen termination temporarily passivates the Si / electrode interface. In the case of porous electrodes it will then oxidize uncontrollably, but a continuous or amorphous film electrode might retard this process. Indeed, a high V_{OC} was demonstrated in some cases, probably because the upper electrodes tested in that way, are casted or transferred from solution and did not react spontaneously with the underlying Si. Nevertheless, unless interface issues were explicitly negotiated – which is true for a small minority of the publications - there is no reason to believe that those devices where anything but unstable, or not very reproducible.

Using improved interface control learned from the field of molecular electronics, Maldonado et al. Used a two step chlorination-alkylation process to passivate the surface of n-Si by methyl termination. A semi-transparent Au top electrode was realized by spray coating of organically capped Au nanoparticles from solution, followed by soft sintering under oxide-free environment.[95] A different bottom-up approach was taken by us to realize a similar n-Si/ alkyl monolayer / Au junction, where the monolayer bound the Si surface was initially terminated with a thiol group. Au NP's were then attached to the thiols, and those served then as seeds for electroless deposition of semi-transparent Au, again

from solution.[96] For both cases the V_{OC} measured, 560 mV for $N_D=3\cdot10^{16}$ cm^{-3}, and 480 mV for $N_D=1$-$2\cdot10^{15}$ cm^{-3}, respectively is higher than ever reported for n-Si/Au junctions,[17] which indicates that the Si surface was well passivated by the molecular monolayer and that no direct Au-Si interaction occurred.

The H-termination of the Si surface after wet etch in HF or NH4F solutions is known to provide a very good chemical passivation, but hydroxylation and oxidation that follow are less controllable and result in a layer of poor quality and high density of surface states. We have shown that if an amorphous conducting polymer is spin-coated immediately onto the freshly etched Si, the surface does not seem to get pinned even over a period of weeks . If an P+-n SIS structure is formed, using a degenerate p-type polymer, such as PEDOT:PSS, onto n-Si, a maximal VOC is measured even if the SCR within the Si is not strongly inverted.[97] Sushobahn et al. demonstrated a similar design, but with only 10 nm thick P3HT buffer layer between the Si and the PEDOT:PSS, which might further improve the inversion properties of the Si.[98]

2.9 Summary and future prospects

More than 3 decades have passed since the last review of MIS solar cell was conducted and publishd by Pulfrey.[17] Since then the family of inversion layer solar cells was expanded to include the SIS the MIS-IL and lately the hybrid organic / inorganic inversion layer solar cells. The four-fold role of the interfacial layer that remained somehow vague through those decades was re-emphasized:

1. to passivate surface states – to provide defect free interface while satisfying surface dangling bonds.
2. to prevent direct metal-semiconductor interactions
3. to accommodate fixed charges
4. to provide additional surface dipole

and ass of these can be achieved using an interfacial layer from just a few to 20 Å thick.

The field of molecular electronics has taught us techniques by which better control over surfaces and dipole can be obtained, using a self-assembled organic monolayer directly bound to the semiconductor. In principle, such self-assembly can be used for a large area solar cell, with moderate means adequate for mass production. To this end, Si surfaces have seen most of the research with different binding and fabrication strategies available. Other semiconductors were less explored even though some work was done for GaAs,[99] Ge[100] and SiC.[101]

With a molecular monolayer as the interfacial layer, the material of the upper window, either conducting or dielectric, should be softly deposited to preserve the monolayer's advantageous properties. ALD is suggested to be such a soft deposition method, relevant for Al_2O_3 on n-type materials, which from simple calculation was shown to be the only dielectric that is charged enough to fit for a low-cost MIS-IL configuration. ALD can also be used for different TCO (NiO_2, MoO_3) that will not react as easily with the semiconductor absorber, in SIS configurations, as metals and thus will ease the interfacial layer demands.

Conducting polymers are also interesting for SIS structure. These are usually deposited from solution and are not likely to react with the semiconductor, either. On the other hand, the availability of commercially reproducible material besides PEDOT:PSS is limited, and the stability of those materials in ambient atmosphere, under illumination, and heat is yet to be proven.

2.10 References

1. Shewchun, J., Burk, D. & Spitzer, M.B. MIS and SIS solar cells. *IEEE Transactions on Electron Devices* **27**, 705–716 (1980).
2. Metz, A., Meyer, R., Kuhlmann, B., Grauvogl, M. & Hezel, R. 18.5% efficient first-generation MIS inversion-layer silicon solar cells. *Proc. 26th Photovoltaic Specialists Conference,* 31-34 (IEEE, 1997).
3. Yaffe, O. et al. Molecular Electronics at Metal/Semiconductor Junctions. Si Inversion by Sub-Nanometer Molecular Films. *Nano Lett.* **9**, 2390-2394 (2009).
4. Mott, N.F. & Gurney, R.W. *Electronic Processes in Ionic Crystals*. (Oxford University Press: 1948).
5. Bardeen, J. Surface States and Rectification at a Metal Semi-Conductor Contact. *Phys. Rev.* **71**, 717 (1947).
6. Azulay, D. et al. Current routes in polycrystalline CuInSe2 and Cu(In,Ga)Se2 films. *Solar Energy Materials and Solar Cells* **91**, 85-90 (2007).
7. Visoly-Fisher, I., Cohen, S.R., Gartsman, K., Ruzin, A. & Cahen, D. Understanding the Beneficial Role of Grain Boundaries in Polycrystalline Solar Cells from Single-Grain-Boundary Scanning Probe Microscopy. *Advanced Functional Materials* **16**, 649-660 (2006).
8. Stirn, R.J. & YEH, Y.C.M. Solar and laser energy conversion with Schottky barrier solar cells. *Proc. 10th Photovoltaic Specialists Conference,* 15–24 (IEEE, 1974).
9. Shewchun, J., Green, M.A. & King, F.D. Minority-carrier MIS tunnel-diodes and their application to electron-voltaic and photo-voltaic energy-conversion .2. Experiment. *Solid State Electron.* **17**, 563-572 (1974).

10. Green, M.A., King, F.D. & Shewchun, J. minority-carrier MIS tunnel-diodes and their application to electron-voltaic and photo-voltaic energy-conversion .1. Theory. *Solid State Electron.* **17**, 551-561 (1974).
11. Shewchun, J., Singh, R. & Green, M.A. Theory of metal-insulator-semiconductor solar cells. *J. Appl. Phys.* **48**, 765 (1977).
12. Tarr, N.G., Pulfrey, D.L. & Camporese, D.S. An analytic model for the MIS tunnel junction. *IEEE T. Electron. Dev.* **30**, 1760-1770 (1983).
13. El-Sayeda, M.A.-G. & Abdel-Rady, S. Effect of interface states on conversion efficiency of non-uniformly doped MIS solar cell. *Desalination* **209**, 15-22 (2007).
14. Card, H.C. & Yang, E.S. MIS-Schottky theory under conditions of optical carrier generation in solar cells. *Appl. Phys. Lett.* **29**, 51 (1976).
15. Ng, K.K. & Card, H.C. A comparison of majority- and minority-carrier silicon MIS solar cells. *IEEE T. Electron. Dev.,* **27**, 716-724 (1980).
16. Fonash, S.J. The role of the interfacial layer in metal−semiconductor solar cells. *J. Appl. Phys.* **46**, 1286 (1975).
17. Pulfrey, D.L. MIS solar cells: A review. *IEEE T. Electron. Dev.* **25**, 1308–1317 (1978).
18. Kurtin, S., McGill, T.C. & Mead, C.A. Fundamental Transition in the electronic Nature of Solids. *Phys. Rev. Lett.* **22**, 1433 (1969).
19. Higashi, G.S., Chabal, Y.J., Trucks, G.W. & Raghavachari, K. Ideal hydrogen termination of the Si (111) surface. *Appl. Phys. Lett.* **56**, 656 (1990).
20. Angermann & H. Angermann Characterization of wet-chemically treated silicon interfaces by surface photovoltage measurements. *Analytical and Bioanalytical Chemistry* **374**, 676-680 (2002).
21. Nammori, T., Okamoto, K., Nunoi, T. & Hayashi, Y. Minority Carrier Lifetime Measurement in HF Solution to Evaluate Si Substrates for Solar Cells. *Jpn. J. Appl. Phys.* **29**, L166-L168 (1990).

22. Heine, V. Theory of Surface States. *Phys. Rev.* **138**, A1689 (1965).

23. Tersoff, J. Recent models of Schottky barrier formation. *J. Vac. Sci. Technol. B* **3**, 1157 (1985).

24. Sakurai, T. Theory of continuously distributed trap states at Si-SiO2 interfaces. *J. Appl. Phys.* **52**, 2889 (1981).

25. Freeouf, J.L. & Woodall, J.M. Schottky barriers: An effective work function model. (1981).

26. Brillson, L.J. Transition in Schottky Barrier Formation with Chemical Reactivity. *Phys. Rev. Lett.* **40**, 260 (1978).

27. Chang, J.F., Young, T.F., Yang, Y.L., Ueng, H.Y. & Chang, T.C. Silicide formation of Au thin films on (1 0 0) Si during annealing. *Materials Chemistry and Physics* **83**, 199-203 (2004).

28. Andrews, J.M. & Phillips, J.C. Chemical Bonding and Structure of Metal-Semiconductor Interfaces. *Phys. Rev. Lett.* **35**, 56 (1975).

29. Tung, R.T. Chemical Bonding and Fermi Level Pinning at Metal-Semiconductor Interfaces. *Phys. Rev. Lett.* **84**, 6078 (2000).

30. Tung, R.T. Recent advances in Schottky barrier concepts. *Materials Science and Engineering: R: Reports* **35**, 1-138 (2001).

31. Hunger, R. et al. Chemical and electronic characterization of methyl-terminated Si(111) surfaces by high-resolution synchrotron photoelectron spectroscopy. *Phys. Rev. B* **72**, 045317 (2005).

32. Yamagishi, H. Fermi Level Stabilization and Surface States at the Interfaces of Si(111) Surfaces and Insulating Layers. *J. Phys. Soc. Jpn.* **25**, 766-773 (1968).

33. Sanders, A. & Kunst, M. Characterization of silicon wafers by transient microwave photoconductivity measurements. *Solid-State Electronics* **34**, 1007-1015 (1991).

34. Stephens, A.W., Aberle, A.G. & Green, M.A. Surface recombination velocity measurements at the silicon–silicon dioxide interface by microwave-detected photoconductance decay. *J. Appl. Phys.* **76**, 363 (1994).

35. García, F.J., Muci, J. & Tomar, M.S. Preparation of (thin film SnO2)/(textured n-Si) solar cells by spray pyrolysis. *Thin Solid Films* **97**, 47-51 (1982).

36. Lauinger, T., Schmidt, J., Aberle, A.G. & Hezel, R. Record low surface recombination velocities on 1 Ωcm p-silicon using remote plasma silicon nitride passivation. *Appl. Phys. Lett.* **68**, 1232 (1996).

37. Hoex, B., Gielis, J.J.H., van de Sanden, M.C.M. & Kessels, W.M.M. On the c-Si surface passivation mechanism by the negative-charge-dielectric Al_2O_3. *J. Appl. Phys.* **104**, 113703–113707 (2008).

38. Wang, E.Y. & Pandelisev, K.A. The effect of chemical surface treatments on non-native (Bi2O3) GaAs metal-insulator-semiconductor solar cells. (1981).

39. Roberts, G.G., Petty, M.C. & Dharmadasa, I.M. Photovoltaic properties of cadmium-telluride/langmuir-film solar cells. *Solid-State and Electron Devices, IEE Proceedings I* **128**, 197-201 (1981).

40. Buriak, J.M. Organometallic chemistry on silicon surfaces: formation of functional monolayers bound through Si-C bonds. *Chem. Commun.* 1051-1060 (1999).

41. Avasthi, S. et al. Silicon surface passivation by an organic overlayer of 9,10-phenanthrenequinone. *Appl. Phys. Lett.* **96**, 222109 (2010).

42. Sieval, A.B. et al. Silicon Surface Passivation by Organic Monolayers: Minority Charge Carrier Lifetime Measurements and Kelvin Probe Investigations. *J. Phys. Chem. B* **107**, 6846-6852 (2003).

43. Nemanick, E.J., Hurley, P.T., Brunschwig, B.S. & Lewis, N.S. Chemical and Electrical Passivation of Silicon (111) Surfaces through Functionalization with Sterically Hindered Alkyl Groups. *J. Phys. Chem. B* **110**, 14800-14808 (2006).

44. Takato, H., Sakata, I. & Shimokawa, R. Surface passivation of silicon substrates using quinhydrone/methanol treatment. *Proc. 3rd photovoltaic Energy Conversion,* **2**, 1108-1111 Vol.2 (IEEE, 2003).

45. Takato, H., Sakata, I. & Shimokawa, R. Quinhydrone/methanol treatment for the measurement of carrier lifetime in silicon substrates. *Jpn. J. Appl. Phys. 2* **41**, L870-L872 (2002).

46. Sagiv, J. Organized monolayers by adsorption. 1. Formation and structure of oleophobic mixed monolayers on solid surfaces. *J. Am. Chem. Soc.* **102**, 92-98 (1980).

47. Cohen, R. et al. Controlling electronic properties of CdTe by adsorption of dicarboxylic acid derivatives: Relating molecular parameters to band bending and electron affinity changes. *Advanced Materials* **9**, 746–749 (1997).

48. Vilan, A., Shanzer, A. & Cahen, D. Molecular control over Au/GaAs diodes. *Nature* **404**, 166-8 (2000).

49. Har-Lavan, R., Ron, I., Thieblemont, F. & Cahen, D. Hybrid photovoltaic junctions: metal/molecular organic insulator/semiconductor MOIS solar cells. *Photonics for Solar Energy Systems II* **7002**, 70020M-10 (2008).

50. Jung, D.R., Czanderna, A.W. & Herdt, G.C. Interactions and penetration at metal/self-assembled organic monolayer interfaces. *Journal of Vacuum Science & Technology A: Vacuum, Surfaces, and Films* **14**, 1779-1787 (1996).

51. Stewart, D.R. et al. Molecule-Independent Electrical Switching in Pt/Organic Monolayer/Ti Devices. *Nano Letters* **4**, 133-136 (2004).

52. Shpaisman, H. et al. Electronic Contact Deposition onto Organic Molecular Monolayers: Can We Detect Metal Penetration? *Advanced Functional Materials* **20**, 2181-2188 (2010).

53. Loo, Y.-L., Willett, R.L., Baldwin, K.W. & Rogers, J.A. Additive, nanoscale patterning of metal films with a stamp and a surface chemistry mediated transfer process: Applications in plastic electronics. *Appl. Phys. Lett.* **81**, 562 (2002).

54. Akkerman, H.B., Blom, P.W.M., De Leeuw, D.M. & De Boer, B. Towards molecular electronics with large-area molecular junctions. *Nature* **441**, 69–72 (2006).

55. Many, A., Goldstein, Y. & Grover, N.B. *Semiconductor surfaces*. (North-Holland Amsterdam: 1965).

56. Deal, B.E., Sklar, M., Grove, A.S. & Snow, E.H. Characteristics of the Surface-State Charge (Qss) of Thermally Oxidized Silicon. *J. Electrochem. Soc.* **114**, 266 (1967).

57. Dingemans, G., Seguin, R., Engelhart, P., Sanden, M.C.M. van de & Kessels, W.M.M. Silicon surface passivation by ultrathin Al_2O_3 films synthesized by thermal and plasma atomic layer deposition. *physica status solidi (RRL) - Rapid Research Letters* **4**, 10-12 (2010).

58. Bauch, W., Jäger, K. & Hezel, R. Effect of Cs contamination on the interface state density of MNOS capacitors. *Applied Surface Science* **39**, 356-363 (1989).

59. Kobayashi, H., Asano, A., Takahashi, M., Yoneda, K. & Todokoro, Y. Decrease in gap states at ultrathin SiO_2/Si interfaces by crown-ether cyanide treatment. *Appl. Phys. Lett.* **77**, 4392 (2000).

60. This claim was probably true for their early works in which cyanide treatment was performed on freshly etched H-terminated n-Si, e.g. 1.Kobayashi, H., Tachibana, S., Yamanaka, K., Nakato, Y. & Yoneda, K. Improvement of ⟨indium-tin-oxide/silicon oxide/n-Si⟩ junction solar cell characteristics by cyanide treatment. J. Appl. Phys. 81, 7630 (1997). and [89].

61. Vilan, A. & Cahen, D. How organic molecules can control electronic devices. *Trends Biotechnol* **20**, 22-9 (2002).

62. Salomon, A., Berkovich, D. & Cahen, D. Molecular modification of an ionic semiconductor–metal interface: ZnO/molecule/Au diodes. *Appl. Phys. Lett.* **82**, 1051 (2003).

63. Goh, C., Scully, S.R. & McGehee, M.D. Effects of molecular interface modification in hybrid organic-inorganic photovoltaic cells. *J. Appl. Phys.* **101**, 114503-12 (2007).

64. Kera, S. et al. Impact of an interface dipole layer on molecular level alignment at an organic-conductor interface studied by ultraviolet photoemission spectroscopy. *Phys. Rev. B* **70**, 085304 (2004).

65. The UPS / XPS combination is convenient since both techniques are carried out in ultra-high vacuum chamber and both can use synchrotron as the source of photons.

66. Kronik L. & Shapira Y. Surface photovoltage phenomena: theory, experiment, and applications. *Surf. Sci. rep.* **37**, 1-206 (1999).

67. Salter, G.C. & Thomas, R.E. Silicon solar cells using natural inversion layers found in thermally-oxidized p-silicon. *Solid-State Electronics* **20**, 95-104 (1977).

68. Godfrey, R.B. & Green, M.A. A 15% efficient silicon MIS solar cell. *Appl. Phys. Lett.* **33**, 637 (1978).

69. Godfrey, R.B. & Green, M.A. 655 mV open-circuit voltage, 17.6% efficient silicon MIS solar cells. *Appl. Phys. Lett.* **34**, 790 (1979).

70. Godfrey, R.B. & Green, M.A. High-efficiency silicon minMIS solar cells—Design and experimental results. *IEEE T.Electron. Dev.* **27**, 737-745 (1980).

71. Hezel, R. Silicon nitride for the improvement of silicon inversion layer solar cells. *Solid-State Electronics* **24**, 863-868 (1981).

72. Dauwe, S., Schmidt, J., Metz, A. & Hezel, R. Fixed charge density in silicon nitride films on crystalline silicon surfaces under illumination. *Proc. 29th photovoltaic Specialists Conference,*162-165 (IEEE, 2002)

73. Hezel, R. Recent progress in MIS solar cells. *Prog. Photovolt: Res. Appl.* **5**, 109-120 (1997).

74. Kuhlmann, B., Aberle, A.G., Hezel, R. & Heiser, G. Simulation and optimization of metal-insulator-semiconductorinversion-layer silicon solar cells. *IEEE T. Electron. Dev.* **47**, 2167-2178 (2000).

75. Takagi, S., Toriumi, A., Iwase, M. & Tango, H. On the universality of inversion layer mobility in Si MOSFET's:Part I-effects of substrate impurity concentration. *IEEE T. Electron. Dev.* **41**, 2357-2362 (1994).

76. Sidhu, R., Bennett, M., Zahler, J. & Carlson, D. Direct Measurement of Induced Inversion Layer Sheet Resistance by Transmission Line Method. *Proc. 37th photovoltaic Specialists Conference,* TBP (IEEE, 2011).

77. Meier, D.L. et al. Determining Components of Series Resistance from Measurements on a Finished Cell. P*roc. 4th Photovoltaic Energy Conversion* **2**, 1315-1318 (IEEE, 2006).

78. Martín García, I., Lövblom, R., Alcubilla González, R. & others High-efficiency solar cells based on inversion layer emitters. *Proc. 24th European Photovoltaic Solar Energy Conference,* 1985-1991 (2009).

79. Kim, H., Horwitz, J.S., Piqué, A., Gilmore, C.M. & Chrisey, D.B. Electrical and optical properties of indium tin oxide thin films grown by pulsed laser deposition. *Appl. Phys.A* **69**, S447-S450 (1999).

80. Sugiyama, K., Ishii, H., Ouchi, Y. & Seki, K. Dependence of indium–tin–oxide work function on surface cleaning method as studied by ultraviolet and x-ray photoemission spectroscopies. *J. Appl. Phys.* **87**, 295 (2000).

81. DuBow, J.B., Burk, D.E. & Sites, J.R. Efficient photovoltaic heterojunctions of indium tin oxides on silicon. *Appl. Phys. Lett.* **29**, 494 (1976).

82. Feng, T., Ghosh, A.K. & Fishman, C. Efficient electron-beam-deposited ITO/n-Si solar cells. *J. Appl. Phys.* **50**, 4972 (1979).

83. Jain, V.K., Purohit, R.K. & Sharma, B.L. Efficiency calculations of various heterostructure solar cells with n/indium tin oxide/ as the top wide band gap semiconductor. *Solar Cells* **6**, 335-342 (1982).

84. Shewchun, J. et al. The operation of the semiconductor-insulator-semiconductor solar cell: Experiment. *J. Appl. Phys.* **50**, 2832 (1979).

85. Sen, K. & Srivastava, R.S. SIS Solar Cell Theory and Calculations. *phys. stat. sol. (a)* **69**, 413-418

(1982).

86. Vasu, V. & Subrahmanyam, A. Photovoltaic properties of indium tin oxide (ITO)/silicon junctions prepared by spray pyrolysis-dependence on oxidation time. *Semiconductor Science Technology* **7**, 320-323 (1992).
87. Kobayashi, H., Ishida, T., Nakato, Y. & Mori, H. Mechanism of carrier transport through a silicon-oxide layer for ⟨indium-tin-oxide/silicon-oxide/silicon⟩ solar cells. *J. Appl. Phys.* **78**, 3931 (1995).
88. Ishida, T., Kouno, H., Kobayashi, H. & Nakato, Y. Dependence of Photovoltages of Spray-Deposited Indium Tin Oxide/Silicon Oxide/Silicon Junction Solar Cells on Spray Solvents. *J. Electrochem. Soc.* **141**, 1357-1361 (1994).
89. Kobayashi, H. et al. Studies on interface states at ultrathin SiO_2/Si(100) interfaces by means of x-ray photoelectron spectroscopy under biases and their passivation by cyanide treatment. *J. Appl. Phys.* **83**, 2098 (1998).
90. Malik, O., De la Hidalga-W, F.J., Zúñiga-I, C. & Ruiz-T, G. Efficient ITO-Si solar cells and power modules fabricated with a low temperature technology: Results and perspectives. *Journal of Non-Crystalline Solids* **354**, 2472-2477 (2008).
91. Shewchun, J., Dubow, J., Myszkowski, A. & Singh, R. The operation of the semiconductor-insulator-semiconductor (SIS) solar cell: Theory. *J. Appl. Phys.* **49**, 855 (1978).
92. Shewchun, J., Burk, D., Singh, R., Spitzer, M. & Dubow, J. The semiconductor-insulator-semiconductor (indium tin oxide on silicon) solar cell: Characteristics and loss mechanisms. *J. Appl. Phys.* **50**, 6524 (1979).
93. Wei, J. et al. Double-Walled Carbon Nanotube Solar Cells. *Nano Letters* **7**, 2317-2321 (2007).
94. Li, X. et al. Graphene-On-Silicon Schottky Junction Solar Cells. *Advanced Materials* **22**, 2743-2748 (2010).
95. Maldonado, S., Knapp, D. & Lewis, N.S. Near-Ideal Photodiodes from Sintered Gold Nanoparticle

Films on Methyl-Terminated Si(111) Surfaces. *J. Am. Chem. Soc.* **130**, 3300-3301 (2008).

96. Har-Lavan, R., Ron, I., Thieblemont, F. & Cahen, D. Toward metal-organic insulator-semiconductor solar cells, based on molecular monolayer self-assembly on n-Si. *Appl. Phys. Lett.* **94**, 043308-3 (2009).
97. Har-Lavan, R., Joshi, P., Yaffe, O., Levine, I. & Cahen, D. Hybrid Chemically Passivated n-Si / PEDOT:PSS Semiconductor-Insulator-Semiconductor Solar Cell. *Proc. 37th photovoltaic Specialists Conference,* TBP, (IEEE, 2011).
98. Avasthi, S. & Sturm, J.C. Charge Separation And Minority Carrier Injection In P3HT-Silicon Heterojunction Solar Cells. *Proc. 37th photovoltaic Specialists Conference,* TBP, (IEEE, 2011).
99. Sheen, C.W. & Shi, J.X. A new class of organized self-assembled monolayers: alkane thiols on GaAs (100). *J. Am. Chem. Soc* **114**, 1514 (1992).
100. Sharp, I.D., Schoell, S.J., Hoeb, M., Brandt, M.S. & Stutzmann, M. Electronic properties of self-assembled alkyl monolayers on Ge surfaces. *Appl. Phys. Lett.* **92**, 223306 (2008).
101. Rosso, M., Giesbers, M., Arafat, A., Schroën, K. & Zuilhof, H. Covalently Attached Organic Monolayers on SiC and Si_XN_4 Surfaces: Formation Using UV Light at Room Temperature. *Langmuir* **25**, 2172-2180 (2009).

Chapter 3

All covalently bonded solar cell

n-Si-O-C_{11}-S-Au

Abstract. In this preliminary work, Alkyl chain molecules on oxide-free n-Si were used to test the concept of hybrid Metal-Organic Insulator-Semiconductor (MOIS) solar cells, and the use of self-assembled monolayer as insulating layer in such cells. Test structures were made by binding alkyl chain molecules via Si-O-C bonds to oxide-free n-Si surfaces, using self-assembly. With thiol groups at the terminals away from the Si, binding of Au nanoparticles, followed by electroless Au plating yields semi-transparent top contacts. First cells give, under 25 mW/cm^2 white light illumination, open-circuit voltage (Voc) = 0.48 V and 0.58 Fill Factor (FF). Because with Sulfur termination the molecules have a dipole that limits inversion of the Si, we also used methyl-terminated monolayers. Even though then we can work, at this point, only with a Hg top contact, without chemical bond to the molecules, we get, using only radiation (~AM 1.5) collected around the contact, the expected higher Voc = 0.54 V, and respectable 0.8 FF, justifying further MOIS cell development.

This Chapter is published as:
'Toward metal-organic insulator-semiconductor solar cells, based on molecular monolayer self-assembly on n-Si' Har-Lavan, R.; Ron, I.; Thieblemont, F.; Cahen D. *Apllied Physics Letters*, **2009**, 94, 043308

3.1 Introduction

Metal-Insulator-Semiconductor (MIS) junctions present a conceptually simple approach to photovoltaics. They attracted much interest in the past, because of their potential for cheap solar cell production.[1] [2] In principle, in this structure the close proximity of the photovoltaic (PV) junction to the cell's illuminated side should allow better solar radiation collection, especially of short wavelengths, than in standard p-n junction solar cells. Best, single crystal Si-based, MIS cells achieved conversion efficiencies of up to 21%, approaching the best of their p-n junction analogs.[3]

The role of the interfacial layer in the MIS cell was studied theoretically, both analytically [4] [5] [6] and numerically.[7] [8] These studies claim that the insulating layer can almost fully passivate the semiconductor surface. In that case the semiconductor's equilibrium band bending is dominated primarily by the difference between the (n-type) semiconductor electron affinity and the metal work-function, following the Schottky-Mott model. Then, with the appropriate semiconductor-metal combination (n-semiconductor / high work function metal; p-semiconductor / low work function metal) the semiconductor interface will be strongly depleted or even inverted. In the latter case a p-n homojunction forms underneath the insulating layer. The current-voltage characteristics of a cell with such depletion / inversion conditions will be:

- *in reverse and moderate forward bias:* the diode dark current is limited by thermionic emission of majority carriers over the potential barrier (depletion), or by minority carrier generation and recombination rates (inversion). In both cases forward current increases exponentially with applied bias with a slight difference in the pre-exponential factor between them, a situation we will refer to as “semiconductor-limited”;

- *at higher forward bias:* the current rises exponentially with bias until it equals the rate at which minority carriers are supplied by tunneling from the metal. Beyond that, the diode becomes ”tunneling-limited”.

The current under illumination is, ideally, a superposition of the photo- and dark currents. This is true if the insulator is thin enough that the uncompensated photocurrent can flow without the diode entering the tunneling-limited regime. Various analyses [6] [8] [9] show that this notion is valid up to a 1.5 – 2 nm insulator thickness, depending on the energy barrier height within the semiconductor. With thicker insulators the FF drops rapidly, although the open-circuit voltage (V_{oc}) decreases only slightly.

Recently, it was shown that high quality, nm-thick monolayers of insulating organic molecules can be formed controllably on semiconductors.[10] [11] [12] With this development it should be possible to make Metal - Organic Insulator - Semiconductor (MOIS) solar cells. Then, the variety of organic molecules that can be formed on oxide-free, H-terminated Si should enable exploration and optimization of the role(s) of the insulator's physical and electronic properties for optimization in (inorganic) MIS photovoltaics. A possible advantage of MOIS cells themselves could be milder preparation conditions with concomitant lower fabrication costs, than those of all-inorganic cells. Self-assembly of organic monolayers can be done at relatively low temperatures (< 230 ºC), and metallic top electrodes can be deposited non-destructively by various methods,[13] including bottom-up techniques, such as growing and ripening of nano-particles.[14]

3.2 Results and discussion

To test the MOIS solar cell approach we set out to prepare an all solid-state covalently bound structure, by adsorbing a well-characterized thiol-terminated alkoxy monolayer onto n-Si via Si-O-C bonds.[15] Samples were prepared by treating single side polished 1-10 Ohm-cm n-Si (100) with a solution of $HOC_{11}H_{22}SH$. The samples were then characterized by ellipsometry, water contact angle,

FT-IR and XPS to verify monolayer quality and that the surface is free of measurable oxide, as explained elsewhere.[11] A continuous but porous, semi-transparent Au film is then grown on the thiol terminated monolayer in a two-step process. First Au nano-particles (NPs), 3-5 nm in diameter, are bound to the monolayer from a toluene suspension.[16] The NPs serve to seed the top electrode for electro-less deposition. This, all-covalently-bound approach, leads to a structure with well-defined insulator thickness (as compared to, e.g., ref.[17] where PV behavior of methyl-passivated n-Si, contacted by spray-coating Au nano-particles *and subsequent sintering*, is shown).

To make the NP monolayer into a useful solar cell top contact requires transforming the NP layer into an electrically continuous metal film with low sheet resistance, as transparent as possible to that part of the solar spectrum that can be absorbed by the absorber. Using slow electro-less plating [18] for 5 min, while monitoring film growth, gave a continuous film with 50-60% overall transparency over the 300-1000 nm wavelength range.

Fig. 3-1 shows current-voltage characteristics of a 2x2 mm n-Si-O-C_{11}-S-Au structure, fabricated as described above, under ~25 mW/cm^2 illumination. The open-circuit voltage, Voc, was 480 mV, higher than reported for plain n-Si-Au or even n-Si-SiO_2-Au cells[19] and the fill factor, FF, was 58%. Results at 25 mW/cm^2 instead of a higher illumination intensity are shown, because increasing the intensity slightly increased the V_{OC} but decreased the fill factor dramatically (see supplemental material). This behavior can indicate, as discussed above, that the uncompensated photocurrents approach the currents of the tunneling-limited regime.

The transition point between semiconductor- and tunneling-limited current regimes is easily found from temperature dependent I-V curves, using Hg as top electrode. To a first approximation tunneling does not depend on temperature. Therefore, the I-V plots in the tunneling-limited voltage regime should be temperature-independent, while in the semiconductor-limited regime currents

currents increase with temperature, as expected for a thermally activated process. Remarkably, we found for alkyls on Si that currents at high forward bias decrease with increasing temperature, providing clear evidence for the voltage where the dominant transport mechanism changes[20 21].

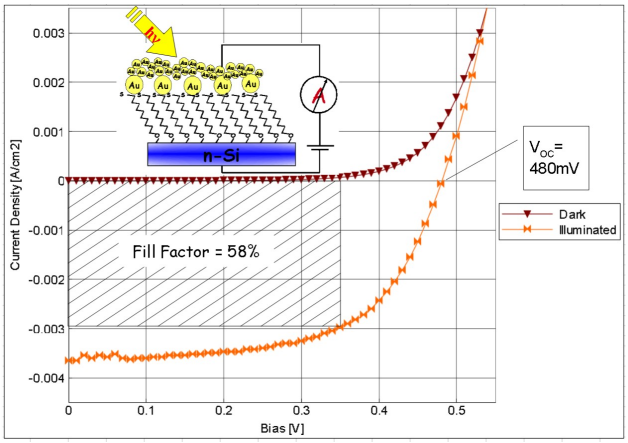

Fig. 3-1: Current-voltage characteristics of a 2x2mm n-Si-O-C_{11}-S-Au structure, fabricated by molecular self-assembly and electro-less Au plating, under ~25 mW/cm^2 (~0.25 AM1.5) illumination. The Au top contact is estimated to be 50-60% transparent for visible and near-IR radiation (300-1100 nm). Here and in all measurements bias is applied to the top contact while the substrate's back contact is grounded.

Fig. 3-2 presents temperature-dependent dark I-V measurements for an n-Si-O-C_{11}-S-Hg junction. Hg has a work function of 4.5 eV which is only slightly lower than the values 4.6 – 4.8 eV, measured for chemically-deposited Au, using Kelvin probe contact potential difference (CPD) measurements. The plots show the voltage where the temperature dependence changes from increasing to decreasing current with increasing temperature, with increasing forward bias, indicating that, indeed, around 470 mV the diode behavior becomes tunneling-limited, as expected from the photovoltaic measurements. The inversion voltage with the thiol-terminated alkoxy monolayer is in good agreement with our previous measurements of thiol-terminated alkyls, bound to n-Si through *Si-C,* instead of *Si-O-C* bonds, but is relatively low compared to the inversion voltage obtained with a methyl-terminated alkyl monolayer junction.[22] A likely reason is that the thiolated monolayer has a more positive dipole

than the methyl-terminated one. Our CPD measurements of *Si-C* bound monolayers gave a 0.4 V difference in Fermi level between the thiol- and the methyl-terminated monolayer.[22]

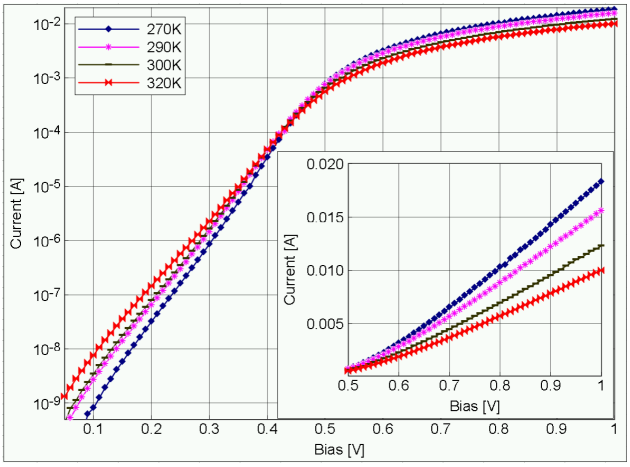

Fig. 3-2: Temperature-dependent dark I-V measurements on an n-Si-O-C_{11}-S-Hg, Si-monolayer-Hg junction. The bias at which the temperature dependence switches from increasing to decreasing current with increasing temperature can be clearly discerned, around 470 mV.

High density methyl-terminated SAM's are chemically non-reactive and very hydrophobic. Deposition of a *semi-transparent* solid state metallic electrode onto such a monolayer without penetrating it or creating pinholes is still a challenge. To be able, nevertheless, to test if changing the terminating group of the molecules will affect PV performance (by affecting the interface energetics) in the alkoxy systems, we used a methyl-terminated monolayer as an insulator in MOIS cells, but now with Hg as the top contact. PV measurements were done using a white light source, adjusted to yield roughly 100 mW/cm^2 with a 3300 K black body spectrum.

Naturally, with Hg as top electrode, the photocurrents, shown in Fig. 3-3, stem solely from light collected from the Hg electrode's periphery, making it not possible to normalize the current in terms of current density. However, because current is collected from the areas surrounding the electrode, it is likely to be more affected by surface recombination than in a usual solar cell or photodetector. Therefore, the V_{oc} and FF, measured on this structure present lower limits for a full PV device.

The junction in Fig. 3-3 showed an excellent, low, dark ideality factor (n=1.09) and, under illumination, 0.8 FF. The V_{OC} was 540 mV, respectable for n-Si based MIS cells of that resistivity.[23]

3.3 Summary

With the all-covalently-bound approach, the MOIS cell's open-circuit voltage may be increased by using amine-, rather than thiol-terminated alkoxies, to get a more negative dipole moment, while still allowing binding semi-transparent metal films. Alternatively, physisorbing suitable transparent conductors on top of methyl-terminated monolayers so as not to damage the layer, should allow significantly improved performance of these cells. Work in these and other related directions is being pursued in our laboratory.

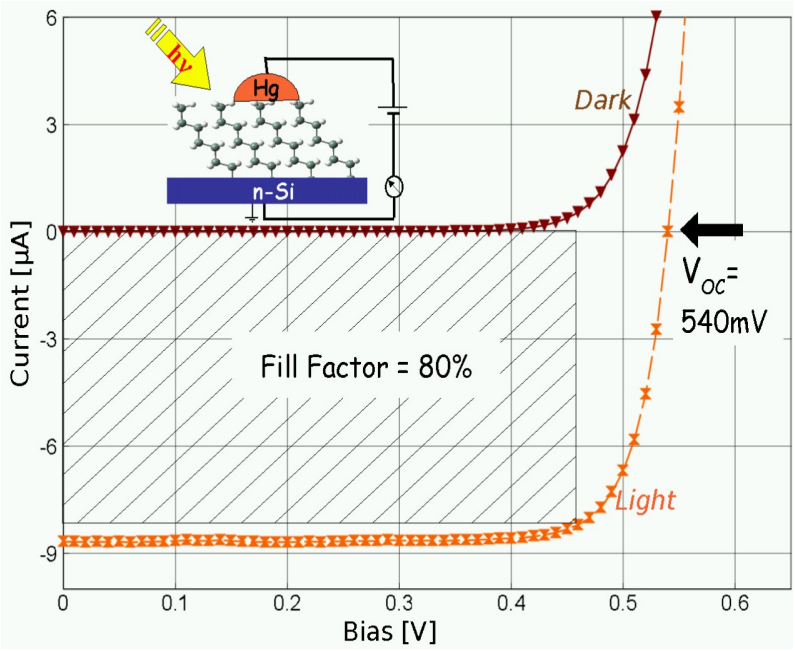

Fig. 3-3: Photovoltaic measurement on a junction, made by contacting an n-Si surface, to which a monolayer of $(CH2)_{11}CH_3$ molecules is bound via Si-O-C bonds, with Hg (n-Si-O-C_{11} / Hg). Illumination was with a Zeiss KL-2500 fiber light source adjusted to produce ~100 mW/cm^2 with a 3300K blackbody spectrum. The junction showed a low dark ideality factor n=1.09 and, under illumination, 80% fill factor and 540 mV open-circuit voltage. Geometric contact area: 0.2 mm^2.

3.4 References

1. Stirn, R.J. & Yeh, Y.C.M. A 15% efficient antireflection-coated metal-oxide-semiconductor solar cell. *Appl. Phys. Lett.* **27**, 95-98 (1975).
2. Ponpon, J.P. Open-circuit voltage of MIS silicon solar cells. *J. Appl. Phys.* **47**, 3248 (1976).
3. Metz, A. & Hezel, R. Record efficiencies above 21% for MIS-contacted diffused junctionsilicon solar cells. *, Proc. 26th photovoltaic Specialists Conference,*31-34, (IEEE, 1997).
4. Card, H.C. & Yang, E.S. MIS-Schottky theory under conditions of optical carrier generation in solar cells. *Appl. Phys. Lett.* **29**, 51 (1976).
5. Fonash, S.J. The role of the interfacial layer in metal−semiconductor solar cells. *J. Appl. Phys.* **46**, 1286 (1975).
6. Tarr, N.G., Pulfrey, D.L. & Camporese, D.S. An analytic model for the MIS tunnel junction. *Electron Devices, IEEE Transactions on* **30**, 1760-1770 (1983).
7. Shewchun, J., Singh, R. & Green, M.A. Theory of metal-insulator-semiconductor solar cells. *J. Appl. Phys.* **48**, 765 (1977).
8. El-Sayeda, M.A.-G. & Abdel-Rady, S. Effect of interface states on conversion efficiency of non-uniformly doped MIS solar cell. *Desalination* **209**, 15-22 (2007).
9. Green, M.A., King, F.D. & Shewchun, J. minority-carrier MIS tunnel-diodes and their application to electron-voltaic and photo-voltaic energy-conversion .1. Theory. *Sol Stat Elec* **17**, 551-561 (1974).
10. Salomon, A. et al. Comparison of electronic transport measurements on organic molecules. *Adv Mater Weinheim* **15**, 1881-1890 (2003).
11. Seitz, O., Böcking, T., Salomon, A., Gooding, J.J. & Cahen, D. Importance of Monolayer Quality

for Interpreting Current Transport through Organic Molecules: Alkyls on Oxide-Free Si. *Langmuir* **22**, 6915-6922 (2006).

12. Nesher, G. et al. Energy level and band alignment for GaAs-alkylthiol monolayer-Hg junctions from electrical transport and photoemission experiments. *J Phys Chem B Condens Matter Mater Surf Interfaces Biophys* **110**, 14363-71 (2006).
13. Haick, H. & Cahen, D. Contacting organic molecules by soft methods: towards molecule-based electronic devices. *Acc Chem Res* **41**, 359-66 (2008).
14. Glickman, E., Inberg, A., Fishelson, N. & Shaham-Diamand, Y. Electroless deposition and electrical resistivity of sub-100 nm Cu films on SAMs: State of the art. *Microelectronic Engineering* **84**, 2466-2470 (2007).
15. Boukherroub, R., Morin, S., Sharpe, P., Wayner, D.D.M. & Allongue, P. Insights into the Formation Mechanisms of Si−OR Monolayers from the Thermal Reactions of Alcohols and Aldehydes with Si(111)−H1. *Langmuir* **16**, 7429-7434 (2000).
16. Wanunu, M., Popovitz-Biro, R., Cohen, H., Vaskevich, A. & Rubinstein, I. Coordination-based gold nanoparticle layers. *J Am Chem Soc* **127**, 9207-9215 (2005).
17. Maldonado, S., Knapp, D. & Lewis, N.S. Near-Ideal Photodiodes from Sintered Gold Nanoparticle Films on Methyl-Terminated Si(111) Surfaces. *J. Am. Chem. Soc.* **130**, 3300-3301 (2008).
18. Jin, Y. et al. Controlled nucleation and growth of surface-confined gold nanoparticles on a (3-aminopropyl) trimethoxysilane-modified glass slide: a strategy for SPR substrates. *Anal. Chem* **73**, 2843–2849 (2001).
19. Pulfrey, D.L. MIS solar cells: A review. *IEEE T. Electron Dev.* **25**, 1308–1317 (1978).
20. We ascribed this phenomenon to un-tilting of the alkyl molecules with respect to the Si substrate, effectively increasing the width of the insulating molecular layer.
21. Salomon, A., Shpaisman, H., Seitz, O., Boecking, T. & Cahen, D. Temperature-Dependent

Electronic Transport through Alkyl Chain Monolayers: Evidence for a Molecular Signature. *J Phys Chem C* **112**, 3969-3974 (2008).

22. Böcking, T., Salomon, A., Cahen, D. & Gooding, J.J. Thiol-terminated monolayers on oxide-free Si: assembly of semiconductor-alkyl-S-metal junctions. *Langmuir* **23**, 3236-41 (2007).
23. Godfrey, R.B. & Green, M.A. 655 mV open-circuit voltage, 17.6% efficient silicon MIS solar cells. *Appl. Phys. Lett.* **34**, 790 (1979).

Chapter 4

Ambient organic molecular passivation of Si yields near-ideal, Schottky-Mott limited, junctions

Abstract. A short, *ambient atmosphere, at room temperature treatment* of oxide-free Si(100) in hydroquinone (HQ)/alkyl alcohol solutions, fully passivates its surface while allowing controlled change of the resulting surface potential. The junctions formed upon contacting such surfaces with Hg, a metal that does not chemically interact with Si, follow the Schottky-Mott metal-semiconductor model in a way that is closer to ideal than ever for Si-based junctions. Two cases of such ideal behavior are demonstrated:

a) Changing the alkyl chain length tunes the molecular surface dipole over 400 mV, with only negligible band bending. The excellent passivation results in junctions with Hg with barrier heights that follow the change in the Si effective electron affinity nearly ideally, highly unusual for a covalent, narrow bandgap semiconductor as Si.

b) For HQ/ methanol treatment, passivation is accompanied by large surface dipole, which suffices, as interface dipole, to drive the Si into strong inversion as we prove experimentally via its photovoltaic effect. *The near-perfect transfer of a surface effect to an interface effect* shows that even a ~0.3 nm interlayer suffices to prevent the metal-semiconductor interactions that are thought to be a cause for gap states at their interface.

This Chapter was submitted for publication:

4.1 Introduction

Metal / semiconductor junctions are basic building blocks of modern microelectronics, and ohmic metal / Si contacts or capacitive Metal-Oxide-Si junctions are widely used. Rectifying metal / Si junctions are used less, possibly because of our limited ability to tune their properties.

According to the Schottky-Mott model, if an n-type semiconductor with electron affinity X_{SC} and a metal with work function Φ_m are brought into intimate contact, they will, because of charge equilibration between the metal and the semiconductor, form an energy barrier for electron transport, with a Schottky Barrier Height (SBH) Φ_{Bn} :[1]

$$\Phi_{Bn} = \Phi_m - X_{SC} \qquad (1)$$

Quantitatively an empirical parameter, *S*, the index of interface behavior,

$$S = \frac{d\,\Phi_{Bn}}{d\,(\Phi_m - X_{SC})} \quad . \qquad (2)$$

was used to express how much the experimental system deviates from the Schottky-Mott model. Ionic semiconductors, such as ZnO and ZnS, were shown to approach the ideal Schottky-Mott limit, of S=1, in contrast to covalent materials such as Si, Ge, and GaAs, where $0.05<S<0.14$.[2]

This deviation from the Schottky-Mott model is commonly attributed, after Bardeen,[3] to surface states within the forbidden gap, which can be electrically (dis)charged, thus limiting the electron flow between the semiconductor and the metal, which is the origin of SBH formation upon metal/semiconductor contact. For a surface state density > 10^{13} cm^{-2} / eV the SBH will be independent of the Φ_m ,[3] a phenomenon known as Fermi level pinning.

The physical origins of the surface/interface gap states has been a subject of discussion for decades. Roughly, the explanations can be categorized into two groups:

1. Surface states that are an inherent property of the semiconductor and its surface, *prior to metal deposition.* The energy bands are a consequence of the lattice periodicity, and if this periodicity is abruptly discontinued, new states appear at energies that are, for bulk material, not allowed, i.e., in the semiconductor's forbidden bandgap.[4] Alternatively, atoms at the semiconductor surface are coordinatively unsaturated, and the resulting dangling bonds manifest themselves as energy states in the forbidden gap. Either argument leads to localized, rather than extended states, i.e., states where the electrons behave more as in simple molecules than as in extended solids.

2. Surface states that result from the *interaction between the semiconductor and the metal*. Such states can be induced by the exponential decay of the electron wavefunctions of the metal into the Si interface layer,[5] by defects at the interface that formed during metal deposition,[6] or by direct chemical semiconductor-metal interaction.[7] [8] Another view is that Fermi level pinning is caused by the polarizability of the chemical bond between metal and semiconductor rather than by surface states.[9]

The large *S* values (eq. 2) of ionic materials, compared to covalent ones, imply that surface / interface gap states are much more dominant for the latter materials. It was suggested that the effect of surface states is stronger for covalent semiconductors for which long-range interactions have a larger effect on the electronic potential of an atom, than for ionic ones in which the potentials are mainly governed by nearest-neighbor interactions.[4] An alternative explanation was that the more covalent the semiconductor is, the more chemically reactive it is towards most of the metals and, hence, their interaction is stronger and surface states formation is enhanced.[7]

According to what was stated above, Fermi level pinning can be avoided completely if:

1. the abruptness of the surface is mitigated by satisfying the dangling bonds, and

2. direct physical contact and chemical interactions between metal and semiconductor are prevented.

In the last decades it was shown that by adsorbing molecules, whose molecular dipole can be varied, on solids it is possible to tune the effective electron affinity of the resulting surface. However, in the case of semiconductors, due to surface states, systematic control over the surface potential (induced by the molecules) does not promise equal control over the semiconductor barrier for charge transport. In addition, it was shown by us as well as others, that a junction between Hg and an organic molecular monolayer on oxide-free on n-Si is not Fermi level pinned. We ascribe this to efficient passivation of the Si surface by the molecules and to the fact that Hg is one of the few metals that does not chemically interact with with Si (along with Pb, Bi, and Ti). In this study we use and adapt a room temperature, ambient atmosphere chemical modification procedure that allows both tuning the surface dipole and potential, as well as efficient passivation of the surface states *that is preserved upon junction formation*. This combination of effects enables us to make Si-based diodes that are closer than ever to ideal Schottky-Mott ones, i.e., with *S* approaching 1.

We modified the wet chemical hydroquinone-methanol (HQ-MeOH) passivation treatment for Si (100) that was reported to yield a primarily methoxy-terminated surface, with recombination velocities as low as 4.2 cm/s (measured for Float Zone, FZ, p-Si 150 Ω cm).[10] [11] This procedure has many advantages over other reported molecular modifications of Si that require either high temperatures,[12] UV activation, ultra-high vacuum conditions,[13] or use of a Grignard reagent,[14] all of which are more complicated and less practical. Furthermore, by using alkyl alcohols of different lengths as solvent rather than just methanol we tune the Si electron affinity and can measure the *S* parameter without changing the top metal electrode.[15]

The HQ treatment that exhibits the largest surface dipole is that with MeOH. We show that the junction of this surface with Hg is strongly type-inverted and current across it is dominated by minority carrier transport. Under illumination the junction acts as an ideal case of a Metal-Insulator-Semiconductor (MIS) photovoltaic device.

4.2 Results

4.2.1 Surface / interface dipole control over Si/Hg Schottky barrier height

Cz-grown, 0.1 Ω.cm P-doped n-Si (100) samples were degreased, etched and treated for 3 hrs with 0.01M HQ in 1-alcohol solutions in the dark and under ambient conditions. The molecule-induced surface dipole and the passivating effect of the HQ-alcohol treatment were studied by Contact Potential Difference (CPD) measurements of the surface, using a vibrating Kelvin probe. CPD in the dark provides a contact-less measurement of the surface work function (WF).[16] [17] Comparing n-Si CPD values before and after molecular modification shows the effect of the surface dipole, due to the molecular layer. Surface Photovoltage (SPV), which probes the band bending in the semiconductor, is measured in the same CPD setup by adding saturating supra-bandgap illumination. From the measured WF, Φ_{eff} , and band bending, Vbi, the effective electron affinity, X_{eff} , can be calculated through:

$$X_{eff} = \Phi_{eff} - \frac{E_C - E_{F,n}}{q} - V_{bi} \qquad (3)$$

where $E_C - E_{F,n}$ is the difference between bulk Fermi level and the bottom of the conduction band, which is calculated from the specified doping concentration and q is the electron charge.

By reacting the freshly etched, H-terminated, n-Si samples with different HQ-alcohol solutions, different surface dipoles are obtained, which correlate with the molecular length, decreasing with longer alcohols. For a 3h reaction in HQ solution in methanol (C1), 1-propanol (C3), 1-pentanol (C5),

1-heptanol (C7) and 1-decanol (C10), average X_{eff} values were 3.53 eV, 3.66 eV, 3.83 eV, 3.89 eV, and 3.92 eV, respectively, with <0.06 eV error. The likely cause of this variation is that fewer of the longer solvent molecules end up bound to the surface, either because of lower reactivity or due to larger steric hindrance between molecules. For both scenarios the surface dipole is reduced.[18]

SPV can, all other factors being equal, provide a qualitative indication for the quality of surface passivation. Measurements of molecularly modified n-Si show values < 80 meV, which is consistent with a very low density of surface states. This value can be compared to SPV≈30-40meV for H-terminated Si, consistent with a slight decrease in passivation quality upon HQ-alcohol treatment of the Si. That decrease might be due to the fact that alkoxy and HQ species are bulkier than H, which prevents them from binding to all the high coordination surface sites. The same measurement, done for methyl 10-undecenoate, attached to FZ p-Si(100), resulted in an SPV=130 meV,[12] significantly higher than found here.

The SPV remained <80meV for treated n-Si(100) exposed to air for 5 days, while for H-terminated Si(100) degradation starts within an hour. This stability agrees with microwave photoconductivity measurements, which show that the HQ-alcohol modification provides passivation, close to that provided by H-termination, but is much more stable in ambient.[10 19] The dipole values remain stable in ambient for several hours, after which they start to decrease slowly, decreasing by some 200 meV after 5 days in ambient atmosphere.

Fig. 4-1 shows characteristic I-V curves for Hg junctions of Si, treated with HQ solutions in different alcohols. Counter-intuitively, with *longer* alcohols at the interface, currents for both reverse and forward bias *increase*, a trend that is due to reduction of the SBH. For most metal-semiconductor junctions the dominant transport mechanism is thermionic emission of majority carriers over the barrier. In that case the SBH, Φ_{Bn}, can be extracted using the thermionic emission equation:

$$J_{TE} = A T^2 e^{\frac{-q\Phi_{bn}}{kT}} e^{\frac{-qV}{nkT}} \quad (4)$$

where A=110A/K^2 is the Richardson coefficient for electrons,[2] T=298K is the temperature, V is the applied bias, and n is the ideality factor. For junctions with SBH larger than the strong inversion threshold (which is 0.97 eV for the 0.1 Ω.cm n-Si samples that we use) this model no longer holds, because the current becomes minority carrier-dominated. This is the case for the HQ-MeOH treated samples, where the measured surface dipole exceeds 500 meV and fitting the thermionic emission model yields $\Phi_{Bn}^{Cl} = -1.03$. The next section will elaborate on that case of strong inversion, its manifestation in current-voltage measurements, and application as photovoltaic device.

In the top right of Fig. 4-1 we show the correlation between the electron affinity values, calculated from the CPD/SPV measurement of the free surface, immediately after molecular treatment, and the SBH extracted from the I-V measurements across the junctions, formed with Hg. The calculated Φ_{Bn} for the HQ-MeOH treated surface was added for the sake of comparison with previous reports. The extracted linear regression, S_{mod}, is the modified index of interface behavior:

$$S_{mod} = \frac{d\,\Phi_{Bn}}{d\,(\Phi_m - X_{eff})} \quad (5)$$

We use here S_{mod} instead of S, because electron affinity of the Si was modified (i.e., X becomes X_{eff}), rather than the metal (and its work function).[20 15] The present Si-molecules-Hg system appears unique in that it conforms to the Schottky-Mott model almost perfectly, with S_{mod}=0.89, whereas other Si systems, not only those prepared and measured under ambient conditions, fail to do so. If, as a more conservative assessment, we set the SBH of the HQ-MeOH to the strong inversion threshold $\Phi_{Bn}^{Cl} \equiv 0.97\text{eV}$, we get S_{mod}=0.76, while omitting that point from the linear regression, i.e., use only values for which the thermionic emission model, and, thus, eq. 4, holds, gives S_{mod}=0.99!

Past experiments to correlate the metal WF with the SBH, for metal / Si junctions, showed weak correlations, with a S=0.05-0.14.[2] Previous work of ours showed that molecular monolayer-modified n-GaAs, exhibits only a small correlation between measured electron affinity of the molecularly modified semiconductor surface and the junction barrier height with Au (S_{mod}=0.09), while similar experiments with ZnO yielded S_{mod}=0.55.[15] This was explained by the stronger tendency to Fermi level pinning of GaAs than of ZnO and other ionic semiconductors, either due to higher density of intrinsic surface states, or by a higher reactivity towards the contacting metal. Here we find that molecular monolayer modification that also electrically passivates the surface can yield near-ideal Schottky-Mott behavior for what is normally a Fermi level-pinned semiconductor.

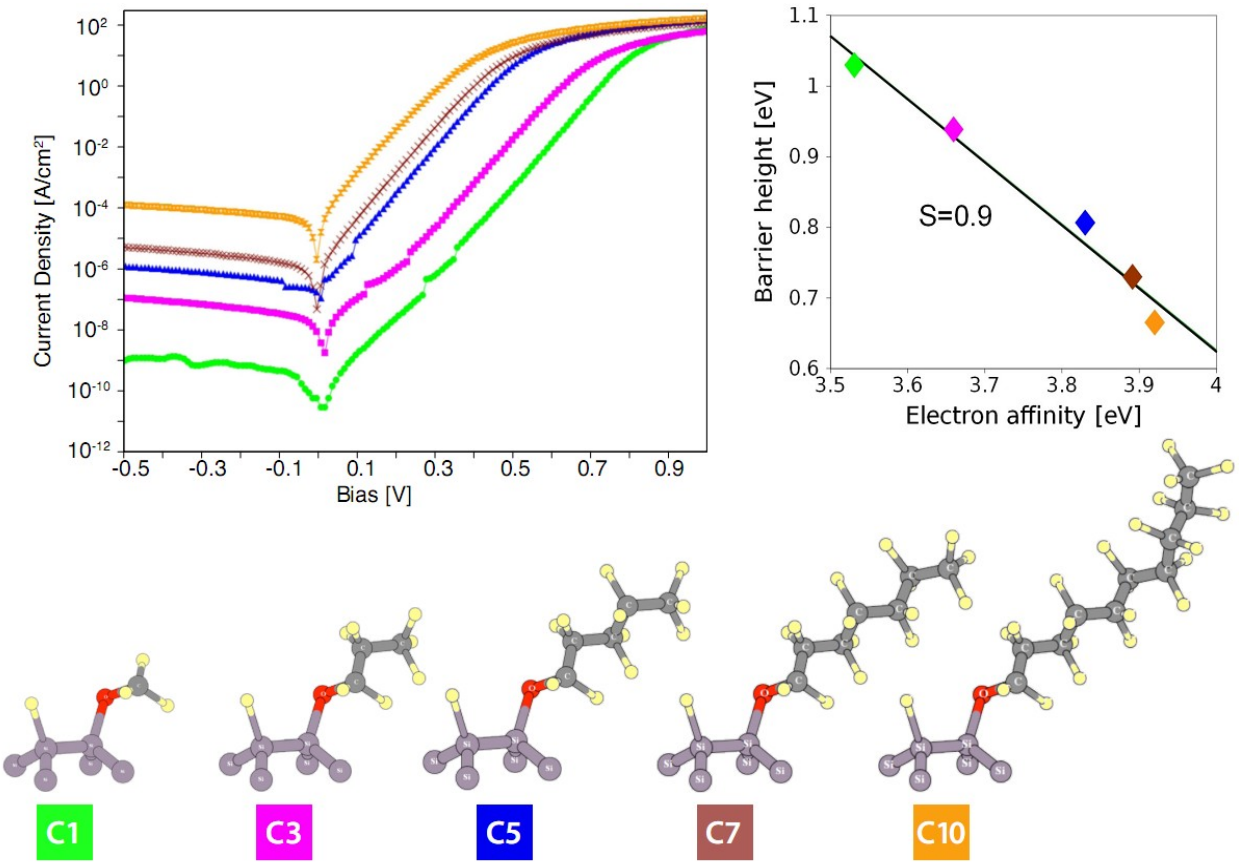

Fig. 4-1: Dark I-V curves of n-Si (100) 0.1 Ω.cm, treated with HQ solutions of different saturated alcohols and contacted with Hg. SBH is reduced with increasing length of the alcohol solvent. Inset: CPD vs. SBH plot, showing that This system follows the Schottky-Mott model almost exactly, with interface parameter S=0.9.

4.2.2 HQ-methanol treatment – the case of strong inversion

4.2.2.1 Surface dipole

The molecular monolayer introduced by the HQ-MeOH represent the extreme case among the HQ-alcohol treatments that we used. In terms of passivation, it was shown that lifetime values measured after HQ-methanol treatment surpass those obtained with ethanol, or after iodine-methanol passivation.[21] This treatment also yields the strongest surface dipole, according to Kelvin probe measurements, even though the length of the methoxy moiety and of the resulting molecular layer is only 3-4 Å.

The large surface dipole was further explored by independent X-ray photoelectron spectroscopy (XPS), which also served to estimate the molecular layer width, and by chemically resolved electrical measurements (CREM).[22] Comparison of H-terminated Si and a sample that was treated with HQ-MeOH shows that their Si2p binding energies differ by ≤ 40 meV, as shown in the supporting information. This result indicates that the band bending in both samples is identical within the instrument's resolution.

The CREM-based WF measurement[23] shows a 0.5 eV difference between H-terminated Si, 4.2 eV, and freshly treated surfaces, 3.7 eV. The latter value agrees well with the Kelvin probe WF data recorded under N_2 ambient, suggesting that this is an inherent surface property rather than the result of interaction with the ambient. This measured difference in WF, together with equal band bending, as probed (in situ) by XPS, again, reflects a dipole, restricted to the overlayer only. Furthermore, the XPS C1s line is, as shown in the supporting information, composed of C_{ox} and C_{HQ} peaks, both of which are shifted by ~500 mV relative to their literature values. These data further support the presence of a surface dipole and imply that most of this dipole is across the Si-O-C bond.

4.2.2.2 Current-voltage characteristics

Strong inversion is the situation where, due to full depletion of majority carriers from the space charge region, SCR, the minority carrier density exceeds the initial (majority carrier) doping level and dominates current flow through the junction. Strong inversion conditions are attractive for photovoltaic applications as will be explained below, but are commonly only created in MOSFET configurations under reverse bias. Strong inversion can also be thought of as a two-dimensional hole (electron) gas on top of an n- (p-)type substrate, and can serve as a test bed for phenomena related to it.

Experimentally, the transition between current dominated by majority carrier thermionic emission and minority carrier-dominated current is hard to distinguish. A unique characteristic of strong

inversion was shown by us earlier for Si/molecules/metal junctions by using molecular layers of different thickness.[24] The current-voltage plots overlap at reverse and low forward bias, regardless of molecular length, and only at high forward bias, where the junction is not anymore inverted, molecular length effects are seen. The strong rectification measured in the previous section for junctions of HQ-MeOH -treated Si with Hg is likely to be a case of such strong inversion, but here we cannot use length variation to verify this, because of the concomitant change in the surface dipole, shown in Fig. 1. Instead, we compared n-Si(100) of different doping levels to check if the HQ-MeOH treatment of Si indeed leads to strong inversion of Hg junctions with such substrate.

In strong inversion the reverse and forward bias current is dominated by generation and recombination, behavior that is described by:

$$J_{r-g} = \frac{q \cdot n_i \cdot W}{2\tau_r}\left(e^{\frac{-qV}{2kT}} - 1\right) \qquad (6)$$

where n_i is the intrinsic carrier density, W is the width of the SCR and τ_r is the bulk minority carrier recombination lifetime. The width of the SCR is related to the doping level (N_D) as

$W \propto \sqrt{\left(\frac{1}{N_D}\right)}$; τ_r was shown to be constant for doping concentrations of $N_D < 10^{16}$ and directly proportional to N_D with a < 0.5 power for $10^{16} < N_D < 10^{18}$.[25] So, if passivation is of high quality, so that the bulk lifetime properties are not screened by the surface ones, τ_r will be constant or increase weakly with N_D, while W decreases stronger, as $(N_D)^{-0.5}$. Thus, samples that are strongly inverted, but with different, moderate, doping levels, will differ in their reverse and low forward bias currents, with *higher* doped substrates yielding *lower* currents (eq.(6).

Current-voltage characteristics of junctions with n-Si(100) of three different resistivities are plotted in **Fig. 4-2**. Indeed for reverse and low forward bias, samples with *higher* doping yield *lower* currents, corresponding to the reduced SCR width. In the higher bias regime higher doping implies lower series resistance and, thus, higher currents. As far as we know, such behavior was only indirectly demonstrated once for high quality Si with ultra-thin thermally-grown oxide.[26] The reason is that the combination of excellent passivation with intimate metal-semiconductor contact is hard to meet. In comparison to the HQ-MeOH treatment, chemically-grown SiO_2 samples, results for which appear in Fig. 4-2 as dashed lines, exhibit minor rectification and for most of the voltage range scanned, lower resistivity samples imply higher currents - as expected for majority carrier-dominated current. The same substrates, when measured with Hg contacts, immediately after HF etching, i.e., as n-Si-H, demonstrate ohmic currents with the expected resistance.[27]

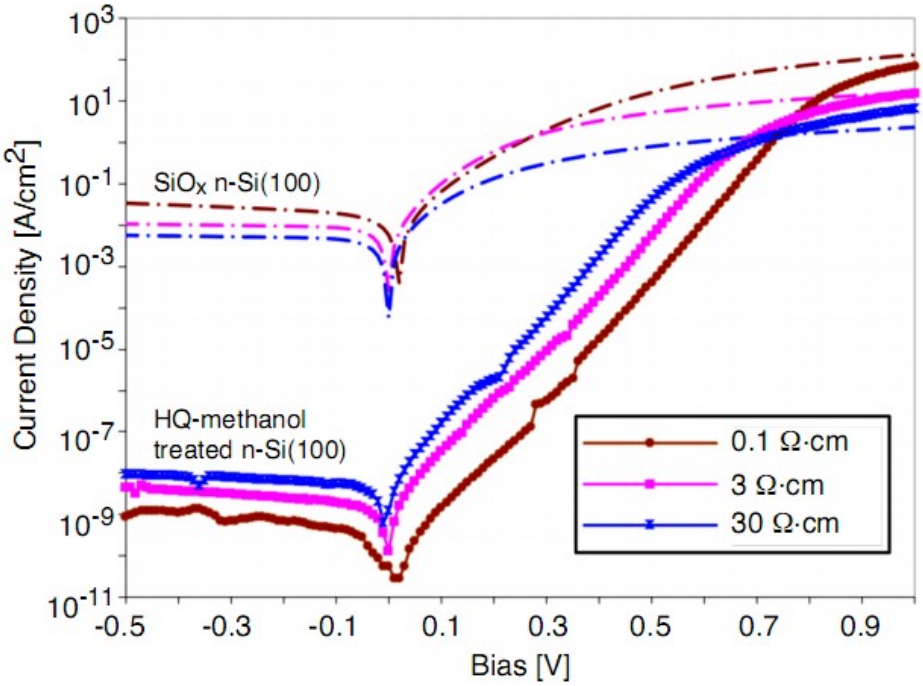

Fig. 4-2: Current-voltage measurements of n-Si (100) treated for 3h with 0.01M HQ-MeOH solution. As the Si is strongly inverted, transport is dominated by minority carrier generation-recombination currents that depend on initial doping density. This, rarely demonstrated, behavior for metal-semiconductor junctions is due to the effective molecular passivation of the Si surface. Dashed lines represent measurements on a substrate with thin SiO_2 , grown for 30 min in piranha solution.

4.2.2.3 PV measurement

A strongly inverted Si interface is very attractive for photovoltaic applications, because the inverted region can function as a *de facto* P+ emitter on top of the n-type base to separate photo-generated electron-hole pairs. This approach to photovoltaics,[28,29] that was popular several decades ago, has clear potential for cheaper and simpler solar cells, because the high-temperature diffusion processing, used to make conventional p-n junction solar cells, is avoided.

The photovoltaic current is ideally a linear combination of photo-generated current (J_{ph}) and the diode's measured dark current (cf. eq. (6) in the case of inversion). As was shown above, reduction of the dark current is possible in the case of strong inversion using a higher doped Si absorber. The photo-generated current, though, mainly depends on illumination intensity and on the absorber bandgap (neglecting the sheet resistance of the inversion layer), i.e., it is independent of doping. In **Fig. 4-3** we show the photovoltaic current for the n-Si / HQ-MeOH / Hg junctions, described above, illuminated with 590 nm laser light. The laser beam was directed to impinge on the sample under the Hg drop and its intensity was manually adjusted so that the junction gave J_{ph} = 10 mW/cm^2, to allow comparison between samples. Indeed, the open-circuit voltage, the voltage at which J_{ph} = -(dark current), and output power both are higher for samples of higher doping density. Earlier such a correlation between initial doping concentration and the photovoltaic V_{OC} of an MIS structure, was found for high purity FZ p-Si solar cells.[26] As can be seen from the high fill factor (FF), these PV measurements present a best case scenario. The current is being collected from a narrow inverted annulus in the Si, around the Hg drop, and suffers minimally from intrinsic resistance within the inversion layer.

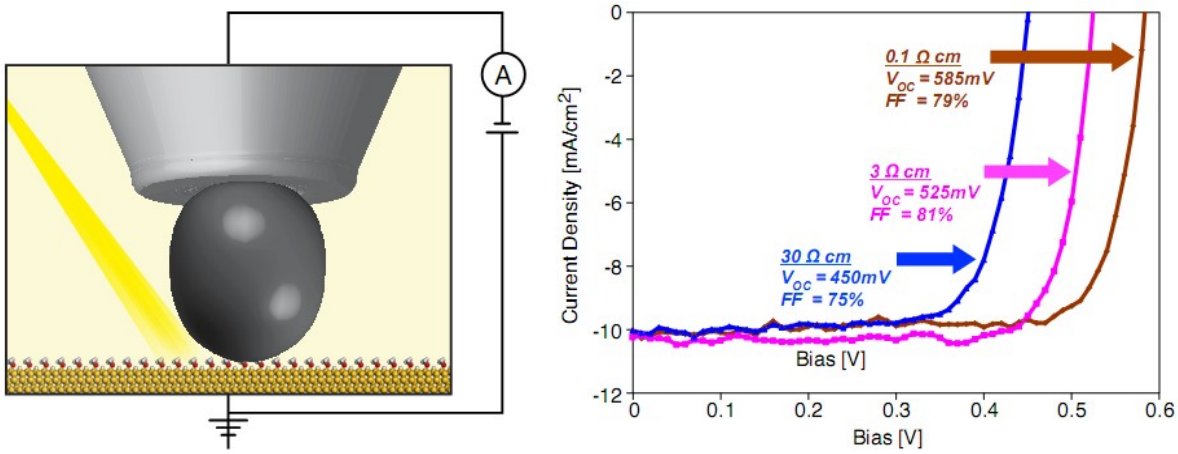

Fig. 4-3: Effect of doping density on PV characteristics for n-Si(100), treated with HQ-MeOH for 3h and contacted with Hg. The junctions were illuminated with 590 nm laser light, directed under the Hg drop and adjusted to produce J_{ph}=10 mW/cm^2.

We note that, from a practical point of view, there is a delicate trade-off between V_{OC} that increases with Si absorber doping, as demonstrated here, and sheet resistance of the inversion layer. In an MIS solar cell configuration, working with higher doping dramatically reduces the inversion layer thickness and, as a consequence, implies higher sheet resistance and lower FF.

4.3 Discussion

For decades the surface of Si, the most common and also most covalent semiconductor, was thought to be inherently Fermi level-pinned due to a high density of surface states. We studied the issue, using Hg as a contact to **n**-Si, to eliminate direct chemical interaction. While metal/**p**-Si diodes usually exhibit SBHs of less than half the bandgap, a p-Si-H/Hg diode with SBH of 0.9 eV was reported.[30] Such a large barrier height can in principle result from a high density of surface states located below the conduction band of the Si, rather than from ideal Schottky-Mott behavior. Because, unfortunately, H-termination is not stable and does not allow further variation of the surface properties, we showed here how an ultra-thin molecular layer can both mitigate the abrupt termination of the Si lattice periodicity and saturate the surface dangling bonds, similar to H-termination, but with much

improved stability. The molecular layer acts also to dampen the penetration of the electronic wave function of the metal into the semiconductor, thus minimizing this way to affect the Si.

Our results build on our recent work where we showed that a self-assembled molecular monolayer provides effective electronic passivation of the surface of oxide-free n-Si, while introducing a large surface dipole - effectively reducing the Si electron affinity. With a Hg contact on the surface of **n-**Si, modified with such monolayers, a junction with $\Phi_{Bn} > 0.9$ eV is formed and the Si space charge region (SCR) is driven into strong inversion.[24]

In the current work we were able, for the first time, to combine the unpinned Hg / molecule / Si junction with a variable dipole, and to demonstrate an index of interface behavior, *S*, approaching unity. Our work suggests that surface states are not an innate property of the semiconductor and can be manipulated via controlled contacting approaches.

Remarkably, the organic layer that we used here, which is composed of two molecular moieties, an alkoxy and a hydroquinone, can be discontinuous[31] and, thus, introduces only a minor, if any, tunneling barrier for transport across the junction. The junction energetics are affected by an average surface dipole rather than by the effect of individual molecules and transport likely does not occur across, but around the molecules, a process, previously described as the "Gate Keeper effect".[32]

In their quest for a Si Schottky barrier solar cell, Shewchun et al. could drive a Si substrate into strong inversion only in the presence of a thin oxide layer, that eventually unpinned the Fermi level of the Si and allowed them to utilize the large difference in WF between the p-Si and their upper metal contact.[33] It was thought that the insulating layer, introduced by the oxide, suppresses the majority carrier currents,[34] and that a metal / semiconductor junction cannot go into strong inversion with an interfacial layer thinner than 10-15 Å.29 [35]

We have shown here that n-Si can be driven into strong inversion with a molecular interfacial layer as thin as 3-4 Å and a Hg contact, and with a much milder chemical treatment than we used previously,[24] at room-temperature and in ambient, which is complete within a few hours.

The mechanism by which HQ-alcohol treatment passivates the surface of Si is not understood yet on an atomic scale. Chabra et al. suggested that it is the hydroquinone, which is a strong reducing agent, that reacts with H-terminated Si to form a Si-O-phenol-terminated surface.[36] Our XPS and ATR-FTIR measurements, however, show that immediately after the HQ-MeOH treatment the surface is mostly Si-methoxy (>95%), with only a minor fraction covered by Si-bound hydroquinone. We suggest that the hydroquinone acts as an initiator for nucleophilic substitution of Si-H with Si-alkoxy, as we also found a difference in reactivity between Si(100) and Si (111) towards this reaction. Alkoxy-terminated Si surface is more stable in ambient than its H-terminated analog and its eventual oxidation seems to be more controlled and to induce less surface states than that of H-terminated Si.

4.4 Summary

HQ-alcohol treatment of Si electrically passivates the surface and allows tuning the surface dipole over more than 400 mV. We demonstrated here for the first time a nearly unity index of interface behavior for the archetypical covalent semiconductor Si, which should be compared to S≈0.1 for Si diodes with metals of different work function.

The HQ treatment with MeOH as solvent provides superb surface passivation and introduces a large negative surface dipole, effectively decreasing the semiconductor electron affinity by 0.5 eV. This suffices, with a Hg contact, to drive n-Si into strong inversion, where current is limited by minority carrier (hole) generation and recombination within the bulk. Upon illumination the inversion layer acts as a *de facto* P+ region, and the junction performs as an ideal MIS photovoltaic device.

The convenient HQ-alcohol treatment and particularly HQ-MeOH passivation, produces an abrupt, yet surface state-free and relatively stable Si surface that should be of interest for basic science and devices.

4.5 Methods

Monocrystalline n-Si (100) (Phosphorus doped) samples with three different resistivities, 0.1 Ω.cm, 3 Ω.cm (both Cz from Virginia Semiconductors), and 30 Ω.cm (FZ from ITME), i.e., with N_D= 10^{14}, 10^{15}, and $7 \cdot 10^{16}$ cm^{-3}, respectively, were used. ~1cm x 1cm Si samples were rinsed with organic solvents (ethyl acetate, acetone, ethanol) and Doubly Distilled Water (DDW). They were thoroughly degreased using a Piranha solution (7:3 H_2SO_4:H_2O_2) for 30 min, followed by 1 min 2% HF solution oxide removal, another piranha cleaning and re-oxidation for 30 min (SiO_2 reference samples were dried and measured at that stage). After a final 1 min etch in 2% HF, samples were rinsed in DDW, dried vigorously in a N_2 stream and immersed for 3 hrs in 0.01M HQ-alcohol solution in the dark and under ambient conditions. After removing them from the reaction solution, the samples were sonicated for 3 min in ethyl acetate to remove access physisorbed organic species, followed by a dip in boiling dichloromethane, after which they were dried in a N_2 stream. Ohmic back contact was made with a GaIn eutectic.

CPD / SPV measurements were carried out in a N_2-filled glove box (1 atm.) at room-temperature. The CPD values were translated into WF ones by calibration with highly oriented freshly peeled pyrolytic graphite (HOPG), with a known WF of 4.6 eV.[37]

XPS and CREM analyses were performed on a slightly modified Kratos AXIS-HS setup, using a monochromatic Al Kα source and detection pass energies of 20-80 eV. The sample WF was measured *in situ*, applying a CREM-based technique.[23] This technique can be used in a mode where the fresh

area, that was not exposed to X-irradiation or flood-gun electrons, is inspected initially and, subsequently, re-measured to accurately follow the beam-induced changes in the surface potential.

4.6 References

1. Mott, N.F. & Gurney, R.W. *Electronic Processes in Ionic Crystals*. (Oxford University Press: 1948).
2. Sze, S.M. & Ng, K.K. *Physics of Semiconductor Devices*. (Wiley-Interscience: 2007).
3. Bardeen, J. Surface States and Rectification at a Metal Semi-Conductor Contact. *Phys. Rev.* **71**, 717 (1947).
4. Kurtin, S., McGill, T.C. & Mead, C.A. Fundamental Transition in the electronic Nature of Solids. *Phys. Rev. Lett.* **22**, 1433 (1969).
5. Heine, V. Theory of Surface States. *Phys. Rev.* **138**, A1689 (1965).
6. Spicer, W.E. Unified defect model and beyond. *J. Vac. Sci. Technol.* **17**, 1019 (1980).
7. Brillson, L.J. Transition in Schottky Barrier Formation with Chemical Reactivity. *Phys. Rev. Lett.* **40**, 260 (1978).
8. Freeouf, J.L. & Woodall, J.M. Schottky barriers: An effective work function model. (1981).
9. Tung, R.T. Chemical Bonding and Fermi Level Pinning at Metal-Semiconductor Interfaces. *Phys. Rev. Lett.* **84**, 6078 (2000).
10. Takato, H., Sakata, I. & Shimokawa, R. Quinhydrone/methanol treatment for the measurement of carrier lifetime in silicon substrates. *Jpn. J. Appl. Phys. 2* **41**, L870-L872 (2002).
11. The treatment was reported originally with quinhydrone (QH), a charge transfer complex of p-benzoquinone (p-BQ) and hydroquinone (HQ). In our hands, using p-BQ or HQ solution, instead of QH, produces the same results in terms of surface dipole and passivation, as will be discussed below. We ascribe this equivalence to cross contamination of p-BQ in the HQ and vice versa.

12. Sieval, A.B. et al. Silicon Surface Passivation by Organic Monolayers: Minority Charge Carrier Lifetime Measurements and Kelvin Probe Investigations. *J. Phys. Chem. B* **107**, 6846-6852 (2003).
13. Avasthi, S. et al. Silicon surface passivation by an organic overlayer of 9,10-phenanthrenequinone. *Appl. Phys. Lett.* **96**, 222109 (2010).
14. Nemanick, E.J., Hurley, P.T., Brunschwig, B.S. & Lewis, N.S. Chemical and Electrical Passivation of Silicon (111) Surfaces through Functionalization with Sterically Hindered Alkyl Groups. *J. Phys. Chem. B* **110**, 14800-14808 (2006).
15. Salomon, A., Berkovich, D. & Cahen, D. Molecular modification of an ionic semiconductor–metal interface: ZnO/molecule/Au diodes. *Appl. Phys. Lett.* **82**, 1051 (2003).
16. Kronik L. & Shapira Y. Surface photovoltage phenomena: theory, experiment, and applications. *Surf. Sci. rep.* **37**, 1-206 (1999).
17. To translate relative CPD values into WF the Kelvin probe reference electrode was calibrated against that of highly oriented freshly peeled pyrolytic graphite (HOPG), with a known WF of 4.6 eV.
18. Another possible explanation is that with longer alcohols as solvent the competition between hydroquinone and alkoxy species shifts towards the alkoxy, which has a lower dipole on Si than the quinone. This, though, is less likely, because even for methanol, HQ was found to bind only to a small fraction of the surface.
19. Chhabra, B., Suzer, S., Opila, R.L. & Honsberg, C.B. Electrical and chemical characterization of chemically passivated silicon surfaces. *Proc. 33rd photovoltaic Specialists Conference,* 1-4 (IEEE, 2008).
20. Ashkenasy, G., Cahen, D., Cohen, R., Shanzer, A. & Vilan, A. Molecular engineering of semiconductor surfaces and devices. *Acc Chem Res* **35**, 121-8 (2002).
21. Takato, H., Sakata, I. & Shimokawa, R. Surface passivation of silicon substrates using

quinhydrone/methanol treatment. *Proc. 3rd photovoltaic Energy Conversion,* **2**, 1108-1111 (IEEE, 2003).

22. Cohen, H. Chemically resolved electrical measurements using x-ray photoelectron spectroscopy. *Appl. Phys. Lett.* **85**, 1271 (2004).
23. Cohen, H., Nogues, C., Zon, I. & Lubomirsky, I. e-beam-referenced work-function evaluation in an x-ray photoelectron spectrometer. *J. Appl. Phys.* **97**, 113701 (2005).
24. Yaffe, O. et al. Molecular Electronics at Metal/Semiconductor Junctions. Si Inversion by Sub-Nanometer Molecular Films. *Nano Lett.* **9**, 2390-2394 (2009).
25. Schmidt, J. & Aberle, A.G. Accurate method for the determination of bulk minority-carrier lifetimes of mono- and multicrystalline silicon wafers. *J. Appl. Phys.* **81**, 6186 (1997).
26. Godfrey, R.B. & Green, M.A. 655 mV open-circuit voltage, 17.6% efficient silicon MIS solar cells. *Appl. Phys. Lett.* **34**, 790 (1979).
27. Yong-Jun Liu, H.-Z.Y. Alkyl Monolayer-Passivated Metal-Semiconductor Diodes: Molecular Tunability and Electron Transport. *ChemPhysChem* **3**, 799-802 (2002).
28. Stirn, R.J. & Yeh, Y.C.M. A 15% efficient antireflection-coated metal-oxide-semiconductor solar cell. *Appl. Phys. Lett.* **27**, 95-98 (1975).
29. Green, M.A., King, F.D. & Shewchun, J. minority-carrier MIS tunnel-diodes and their application to electron-voltaic and photo-voltaic energy-conversion .1. Theory. *Solid State Electron.* **17**, 551-561 (1974).
30. Wittmer, M. & Freeouf, J.L. Ideal Schottky diodes on passivated silicon. *Phys. Rev. Lett.* **69**, 2701 (1992).
31. Haick, H., Ambrico, M., Ligonzo, T. & Cahen, D. Discontinuous molecular films can control metal/semiconductor junctions. *Adv. Mater.* **16**, 2145–2151 (2004).
32. Haick, H., Ambrico, M., Ligonzo, T., Tung, R.T. & Cahen, D. Controlling Semiconductor/Metal

Junction Barriers by Incomplete, Nonideal Molecular Monolayers. *J. Am. Chem. Soc.* **128**, 6854-6869 (2006).

33. Shewchun, J., Green, M.A. & King, F.D. Minority-carrier MIS tunnel-diodes and their application to electron-voltaic and photo-voltaic energy-conversion .2. Experiment. *Solid State Electron.* **17**, 563-572 (1974).
34. Fonash, S.J. The role of the interfacial layer in metal−semiconductor solar cells. *J. Appl. Phys.* **46**, 1286 (1975).
35. Tarr, N.G., Pulfrey, D.L. & Camporese, D.S. An analytic model for the MIS tunnel junction. *IEEE T. Electron. Dev.* **30**, 1760-1770 (1983).
36. Chhabra, B., Bowden, S., Opila, R.L. & Honsberg, C.B. High effective minority carrier lifetime on silicon substrates using quinhydrone-methanol passivation. *Appl. Phys. Lett.* **96**, 063502 (2010).
37. Sommerhalter, C., Matthes, T.W., Glatzel, T., Jäger-Waldau, A. & Lux-Steiner, M.C. High-sensitivity quantitative Kelvin probe microscopy by noncontact ultra-high-vacuum atomic force microscopy. *Appl. Phys. Lett.* **75**, 286 (1999).

Chapter 5

Hydroquinone–methanol reaction with H-terminated Si surface bridging reaction mechanism and electrostatics

Abstract. The hydroquinone-methanol (HQ-MeOH) treatment was suggested for passivation of Si surfaces, mainly for bulk lifetime measurements. In chapter 4 we demonstrated the importance of that molecular treatment for semiconductor physics and molecular electronics research, and noted its potential use for photovoltaics and other semiconductor device applications. In this chapter we explore the molecular reaction with H-terminated Si(100) with common surface characterization techniques such as XPS and ATR-FTIR. We show that in contrast to some earlier publications the surface immediately after molecular treatment, is almost entirely one of Si-methoxy, with only a small fraction of Si-hydroquinone moieties. Using Kelvin probe CPD and SPV measurements we map the surface electrostatics, and its evolution with reaction parameters. We try to bridge those two "languages" and propose a mechanism for the HQ-MeOH reaction with Si surface and its known passivation abilities.

5.1 Introduction

The hydroquinone-methanol (HQ-MeOH) treatment was shown to be the best wet chemical passivation treatment of Si surfaces, to date, and can be used for measuring bulk properties such as minority carrier lifetime.[1] In chapter 4 we have shown that this treatment leaves a surface-state free

surface, with only a sub-nm thick molecular monolayer on it, which is important for basic semiconductor physics, and has potential in photovoltaic and other applications.

High quality monolayer of alkyl chains can be bound to an oxide-free silicon surface via Si-C and Si-O-C bonds. To prepare those monolayers mostly thermal alkylation or alkoxylation, with alkenes or alcohols, respectively, is required in an oxygen-free environment and at temperatures > 100°C. Reaction with both alkenes and alcohols can also be activated by UV radiation, again in an oxide-free environment. Another option is the two step chlorination-alkylation using hazardous chemicals. The proposed HQ-MeOH reaction is very different: it is done at room temperature and under ambient conditions. The original work was even done with normal rather than anhydrous solvents.

Focusing on passivation characteristics of the hydroquinone-methanol treatment, the initial work by Takato *et* al.[1] did not detail the chemical surface reaction with Si-H. Since then a few works used XPS, ATR-FTIR and TOF-SIMS to characterize the surface of Si wafers after the treatment.[2] [3] [4] All of these found evidence for the presence of both methoxy and quinone groups on the surface (and to some extent oxidized Si), but the chemistry remained unsolved. Figuring out the grafting mechanism along with eventual surface composition might shed light on the reason for the superb electrical passivation obtained with the treatment. It should also allow future works to exploit that mechanism to further increase the *molecular* toolbox for Si surfaces.

The treatment was reported originally with quinhydrone (QH), a charge transfer complex of p-benzoquinone (p-BQ) and hydroquinone (HQ), seen in Fig. 5-1. In our hands, using p-BQ or HQ solution, instead of QH, produces the same results in terms of surface dipole and passivation, measured by CPD/SPV. We ascribe this equivalence to cross contamination of p-BQ in the HQ and *vice versa*. We have used hydroquinone for the treatment, as it is stable under atmospheric ambient.

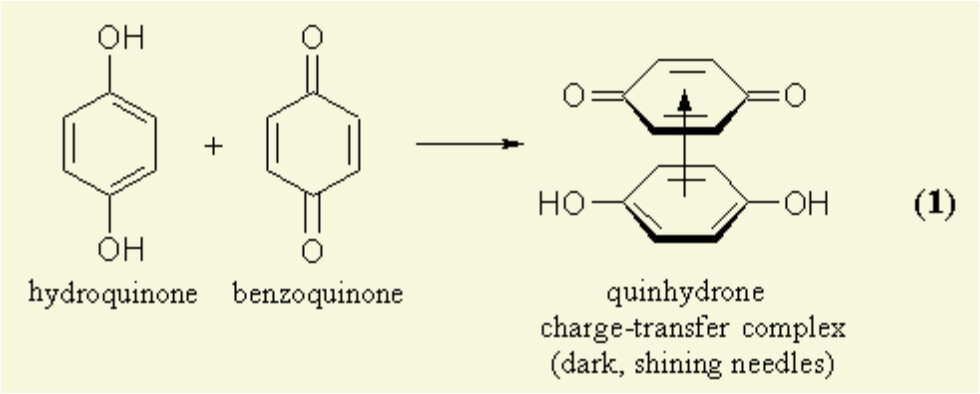

Fig. 5-1: Hydroquinone, benzoquinone and quinhydrone. Solutions of any of these in dry methanol produced comparable results in terms of passivation and surface dipole.

5.2 Surface characterization (XPS, ATR-FTIR)

Monocrystalline n-Si (100) (P-doped) 3 Ω.cm (CZ Virginia Semiconductors) ~1cm x 1cm samples were rinsed with organic solvents (ethyl acetate, acetone, ethanol) and Doubly Distilled Water (DDW). They were thoroughly degreased using a Piranha solution (7:3 H_2SO_4:H_2O_2) for 30 min, followed by 1 min 2% HF solution oxide removal, another piranha cleaning and re-oxidation for 30 min. After a final 1 min etch in 2% HF (H-terminated reference samples were dried and measured at that stage), samples were rinsed in DDW, dried vigorously in a N_2 stream and immersed for 3 hrs in 0.01M HQ-methanol solution in the dark and under ambient conditions.

The measurements described below were all performed on fresh samples, immediately after molecular grafting, whereas previous studies were carried out on samples that were kept first in the ambient for 12-24 hours.[2] [3] [4] After removal from the HQ-methanol solution the grafted samples were first sonicated for 3 min in ethyl acetate to remove physisorbed molecules, then immersed for 1 min in boiling di-chloromethane and blow-dried in N_2 to eliminate ethyl acetate and remaining traces of humidity.

XPS data were taken using a monochromatic AlKα source at 75 W and detection pass energies of 20-80 eV. In Fig. 5-2 we show the C1s region of HQ-MeOH treated n-Si(100). Most of the C1s peak is due to oxidized C (C_O) at a binding energy of 287.1 eV, while a much smaller signal of un-oxidized C (C_H) is detectable at BE 285.5 eV. The ratio between the C_O and C_H peaks was found to be 9.35:1. Taking into account that each methoxy group (from methanol that reacted with Si-H) has 1 C_O and each quinone group (from either hydro- or benzo-quinone that reacted with Si-H) has 4 C_H and 2 C_O, one can easily work out that quinones make up < 3% of the molecules on the surface, immediately after grafting.

The Si 2p region, shown in Fig. 5-3, shows extremely low quantities of oxidized Si around BE 103eV, that can be seen in the semi-logarithmic presentation (inset).

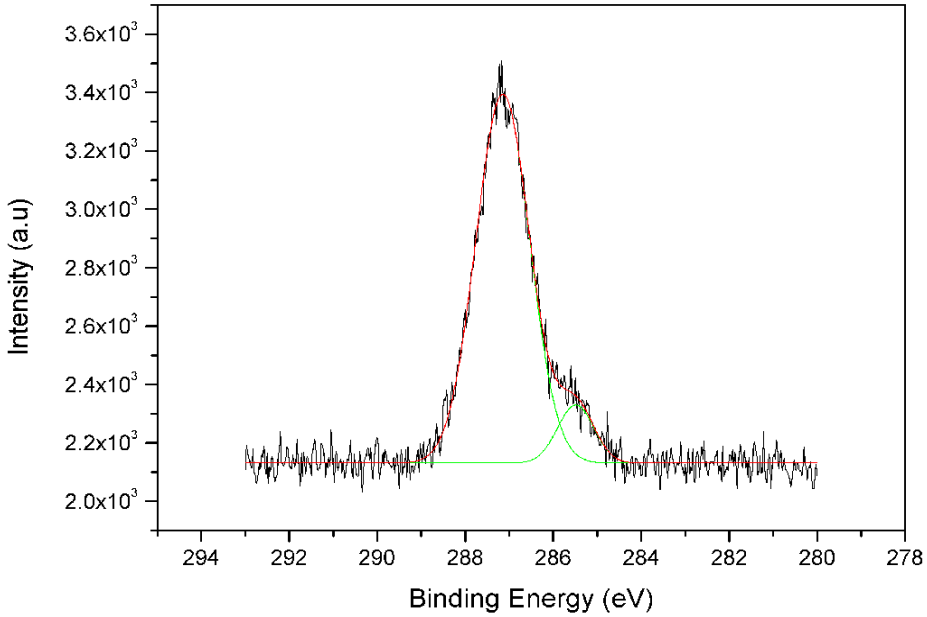

Fig. 5-2: XPS C1s region - ratio between oxidized C at BE 287.1eV to that of un-oxidized C at 285.5eV is 9.35:1 which indicates that the fraction of hydroquinone on the Si(100) surface is no more than 3% of the bound sites, while the rest is occupied by methoxy groups.

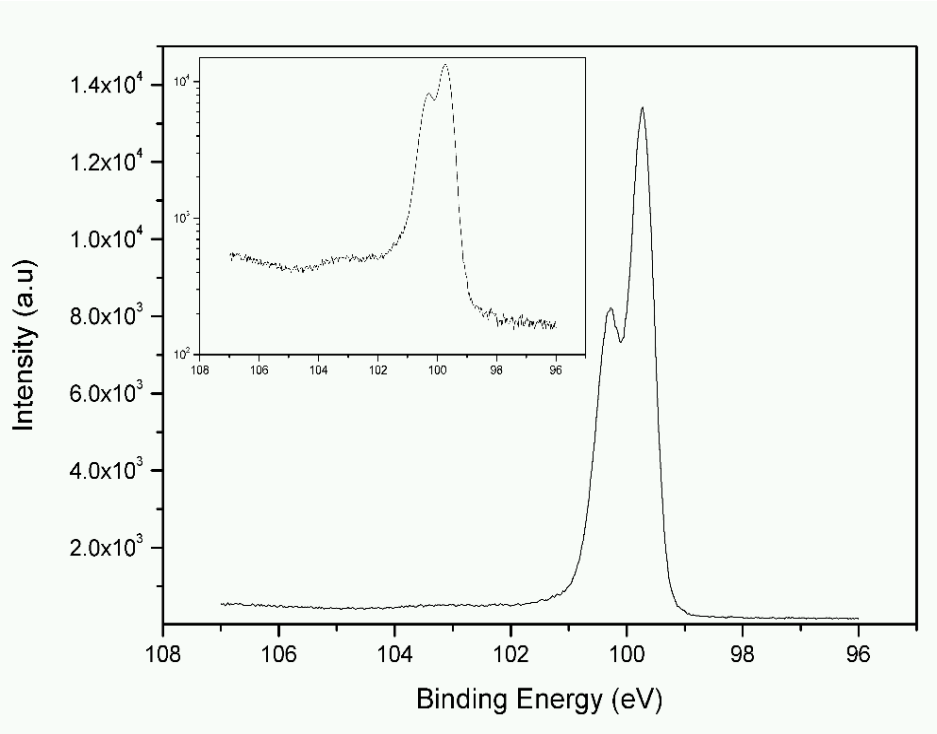

Fig. 5-3: XPS Si2p region measurement, immediately after molecular grafting. The very low Si-O signal at BE 103 eV can be seen on a semi-logarithmic plot (inset)

FTIR absorbance spectra taken in Attenuated Total Reflection (ATR) mode are shown in Fig. 5-4 for a freshly etched Si-H sample, after 1h, and after 3h in 0.01M HQ-methanol solution. Spectra are taken on the background of chemically grown SiOx. The Si-Hx symmetric stretch around 2100 cm^{-1} decays with the HQ-methanol treatment to 29% and 22% of the initial value after 1h and 3h, respectively. The 2800-3000 cm^{-1} spectra taken on the background of Si-H clearly show the CH_3 symmetric stretch at 2840 cm^{-1} and anti-symmetric stretches at 2940 cm^{-1} and 2975 cm^{-1} which are indicative for methoxy groups bound to the Si.[6]

FTIR spectra taken at the University of Texas, Dallas are shown in Fig. 5-5. The humidity-free dry box in which these transmission mode spectra were taken, enable us to see the quinone aromatic C-C stretch at 1500 cm^{-1} that were not detectable in the ATR-FTIR mode. One can also see that a larger initial concentration of HQ in the solution leads to an increase in the amount of quinones bound to the

surface. Both the broad phenol-hydroxyl stretch between 3200 cm^{-1} and 3550cm^{-1}, and the quinone carbonyl stretch at 1670 cm^{-1} cannot be seen in those measurements.

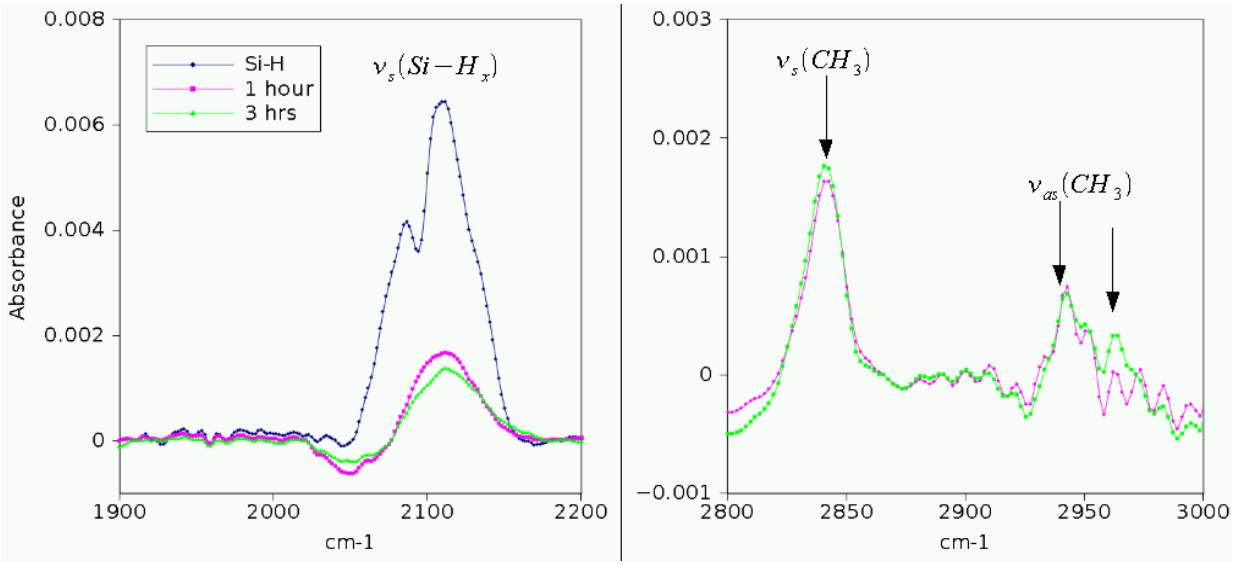

Fig. 5-4: ATR-FTIR absorbance spectra of freshly etched n-Si(100), after 1h and 3h treatment in 0.01M HQ-methanol solution. The symmetric stretches of Si-H_x seen in the etched Si samples, decay with treatment of HQ-methanol to 29% and 22% of their initial value after 1h and 3h respectively. 2800-3000 cm^{-1} spectra taken on the background of Si-H clearly show the CH_3 symmetric stretch at 2840 cm^{-1} and the anti-symmetric stretches at 2940 cm^{-1} and 2975 cm^{-1}. No evidence for hydroquinone presence on the surface was seen, using that method.

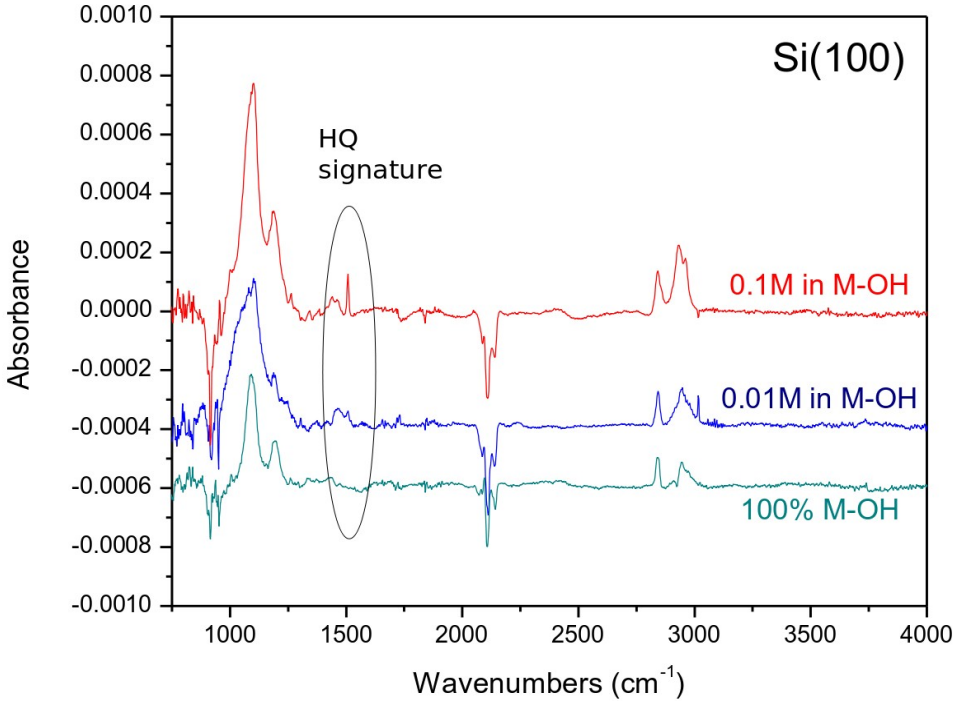

Fig. 5-5: FTIR measurement taken in transmission through the sample (rather than by way of the ATR mode) in a dry box at UT Dallas. Extremely low humidity conditions allow the tracing of the weak C-C aromatic stretch from the hydroquinone, around 1500 cm^{-1}.

To sum up our findings, XPS and FTIR surface characterization suggests that the HQ mainly acts as an initiator to assist the methanol reaction with the H-terminated Si. However, the HQ is not a catalyst *per se* because small quantities of that molecule end-up bound to the Si. The amount of HQ bound to the surface after 3h of reaction increases with increasing concentration in the reaction solution.

5.3 Evolution of the surface dipole using CPD-SPV measurements

The HQ-MeOH reaction is performed on freshly etched H-terminated Si(100) with minimal surface dipole, i.e., its electrostatic values such as work function and electron affinity reflect literature values almost perfectly. Replacing an H atom with either methoxy or HQ, both of them electron-withdrawing groups, should induce a negative surface dipole – effectively reducing the electrostatic values measured on the treated surface. From semi-empirical calculations the negative dipole of a

single HQ, bound to Si was shown to be almost twice that of methoxy-terminated Si (2.4D and 1.3D respectively) as illustrated in Fig. 5-6. This difference between surface dipole of H-, methoxy- , and HQ-terminated Si was taken advantage of as an indicator for surface molecular modification.

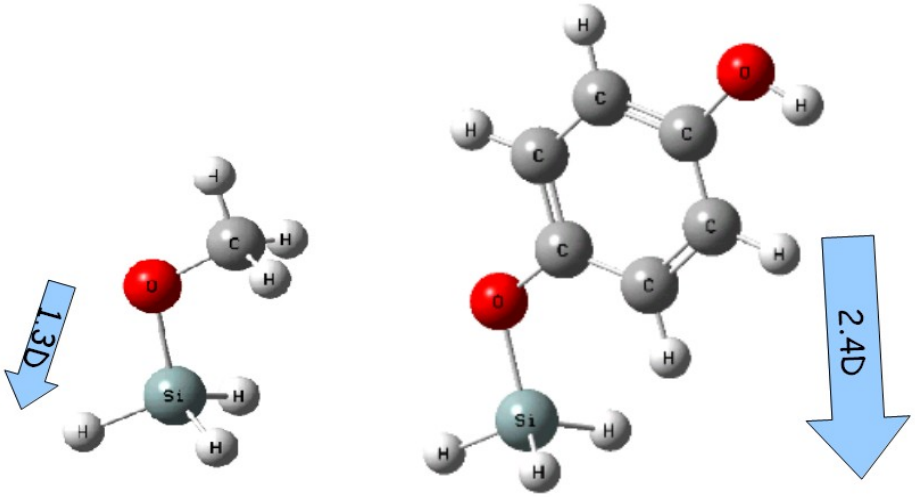

Fig. 5-6: Molecular dipole of H_3Si-methoxy, compared to H_3Si-HQ by semi-empirical calculation [AM1]

Contact potential difference (CPD) measurements, using a vibrating Kelvin probe, serve as a contact-less way to probe the (relative) surface work function6, which allows us to follow the effect of the surface dipole, added by the molecular layers as a function of the reaction parameters, such as reaction time, HQ concentration, and aging process in ambient atmosphere.

At the bare surface, band bending occurs due to surface states – either because of unsaturated dangling bonds, or surface morphological defects. Surface photovoltage (SPV) probes the band bending in the semiconductor and can thus provide an indication for the quality of surface passivation. SPV can be measured in the same CPD setup by adding supra-bandgap saturating illumination (SPV photosaturation).

CPD and SPV measurements of n-Si (100) 1-10 Ω.cm immeresed for 3hrs in methanol solution with different concentrations of HQ, are shown in Fig. 5-7. measurements are carried out ex-situ, the samples were taken out of the reaction solution cleaned and dried in the same manner described above. Initially passivation improves, and band bending decreases with increasing concentration of HQ in the solution – indicative for the significant role that the HQ plays in the Si surface modification process. Of course, the initial H-temination is a good passivation, but with low concentration of HQ in the solution the reaction is carried out slowly – allowing for O_2 and H_2O molecules from the ambient to attack the surface, and degrade the passivation. The decline in effective work function which accompanies that improvement in passivation is probably an outcome of the increase in number surface sites modified by the molecular treatment. Nevertheless, from an HQ concentration of 0.001 M onwards, the SPV does not decrease anymore (or even increases) while the dipole keeps growing stronger – indicating that with higher HQ concentration more quinones with their stronger negative dipole end up bound to the Si surface instead of methoxy groups, but the surface states that cause the band bending and can by this treatment, be passivated have all been passivated.

Fig. 5-8 shows CPD and SPV results for 0.01M HQ-MeOH treated Si surfaces for different reaction times. Interestingly, the surface passivation (within the resolution of the SPV measurement) seems to be constant from 30 min. on, while the surface dipole continues to grow, even after 3.5h. This phenomenon might indicate that after 30 min. of reaction most of the H-terminated reactive surface sites (preferred oxidation sites) were already modified by methoxy / HQ moieties, and that with increasing reaction times, methoxy groups are being substituted by HQ groups of stronger dipole. This notion is in agreement with ATR-FTIR measurements (Fig. 5-4) in which we found that 70% of the Si-H sites reacted during the first hour of reaction, and over the next couple of hours only 10% were added.

In contrast to the Si(100), reacting H-terminated Si (111) for 3 hours with 0.01M HQ-MeOH solution showed no detectable change in the surface dipole in CPD measurements.

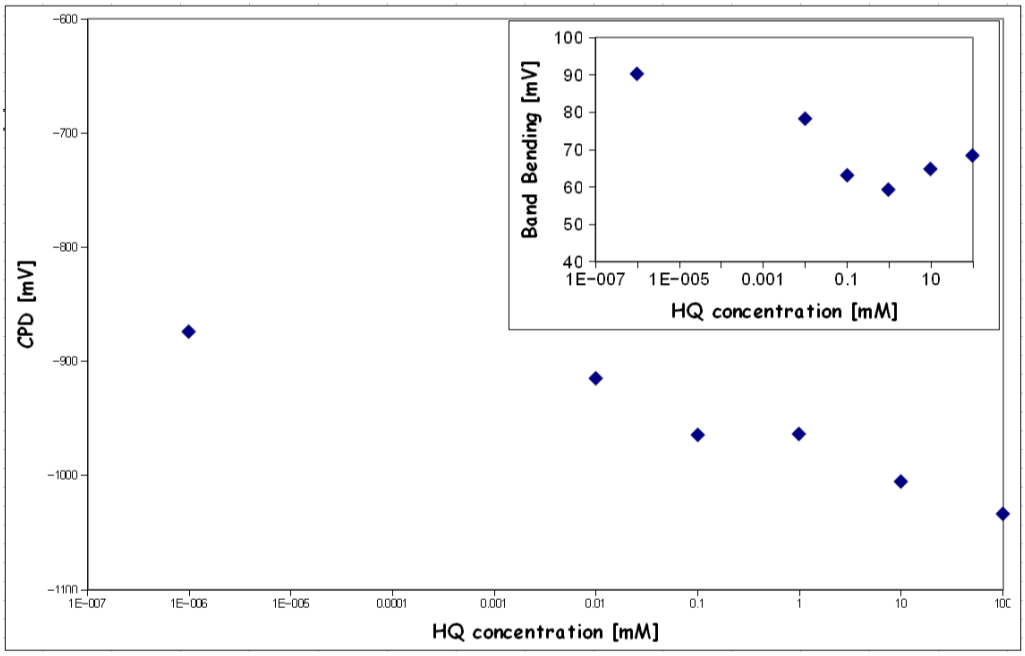

Fig. 5-7: CPD and SPV measurements vs. HQ concentration in methanol for n-Si(100) 1-10 Ω.cm, after 3h of measurement. A steady decline in effective work function with increasing HQ concentrations indicates that adsorbed quinone produces a stronger surface dipole than adsorbed methoxy, bound to Si. Lower initial concentration of HQ in the solution slow down the reaction and allow for O_2 and H_2O molecules from the ambient to attack the surface, which leads to worse passivation.

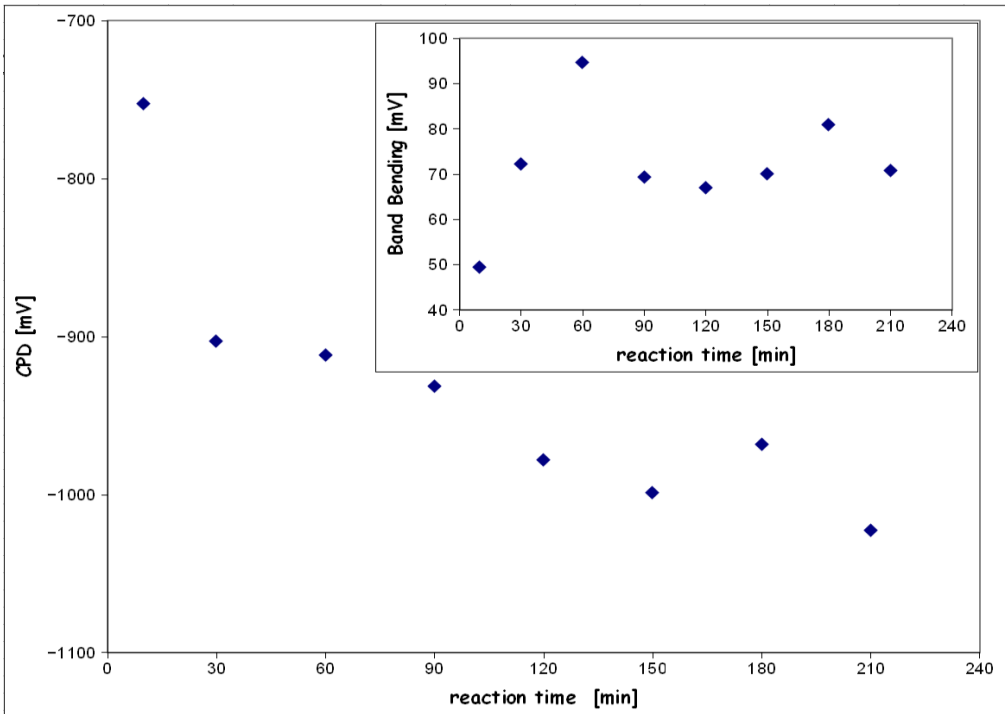

Fig. 5-8: CPD and SPV measurement vs. reaction time of n-Si(100) 1-10 Ω.cm, treated with 0.01M HQ-methanol solution. The reaction seems to continue even after 3.5h of reaction, introducing an ever stronger negative surface dipole, while the surface passivation seems to be constant after 30 min.,

Our CPD / SPV measurements of Si samples, treated with HQ-methanol and aged for 5 days in ambient atmosphere are shown in Fig. 5-9. During that period a dramatic drop in surface dipole of 150-200 mV was found, probably due to some slow, controlled surface oxidation or hydroxylation, that maintained or even improved the surface passivation reflected in SPV.

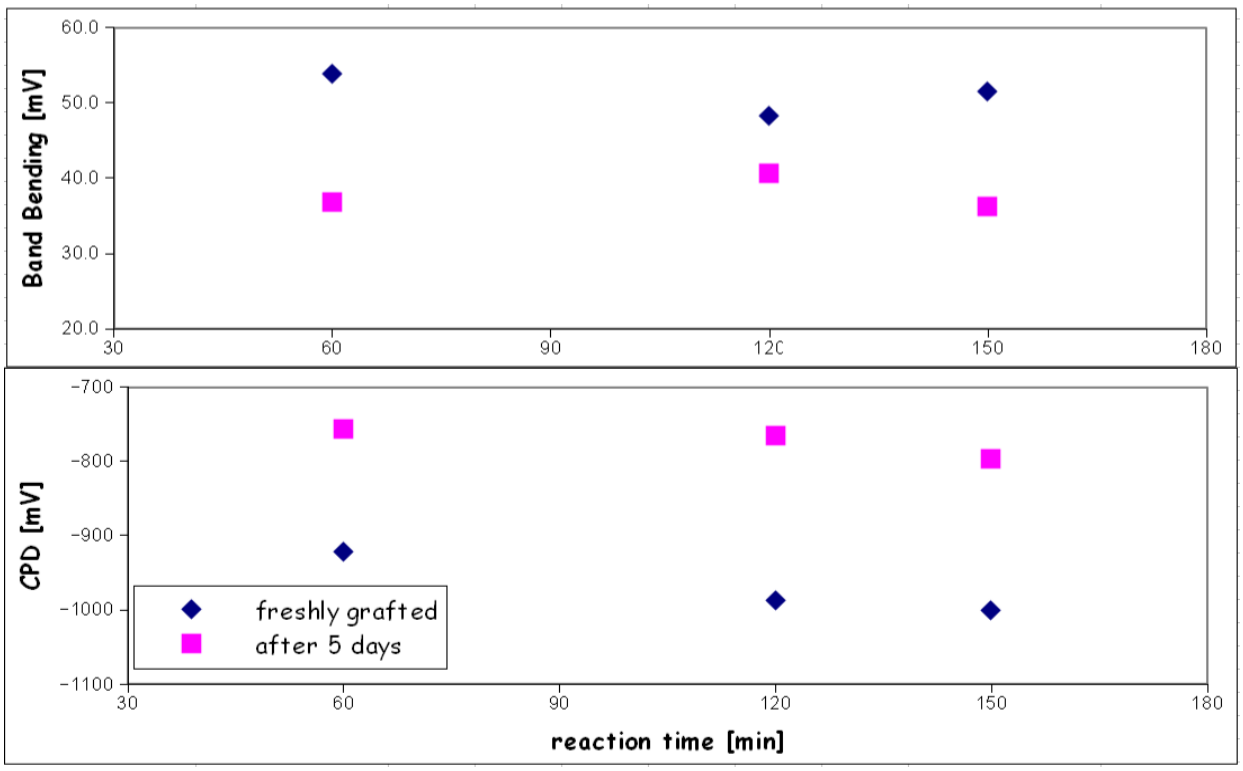

Fig. 5-9: CPD / SPV measurements of Si samples treated with HQ-methanol and aged for 5 days in ambient atmosphere. The 150-200 mV drop in surface dipole indicates oxidation or hydroxylation of Si-methoxy groups, while SPV, which is a measure of surface passivation indicates that the substitution was carried out controllably and no dangling bond were left behind.

5.4 Discussion

At room temperature pure methanol (and alcohols in general) do not bind spontaneously to H-terminated Si even though Si(100) was shown to be slightly more reactive than Si(111).[5] Usually in order to form a dense monolayers of alkoxy on oxide-free Si surface either elevated temperatures[7] or UV activation[8] are used, both of those in minimal O_2 and humidity environment. The HQ-MeOH reaction is, thus, very different since it is carried out fully at room temperature, and apparently the reaction is strong enough to compete with surface oxidation by environmental H_2O and oxygen.

Unlike self-assembly of alkenes on Si driven by a radical chain reaction, alcohols, if no UV light is illuminated, bind to Si through nucleophilic substitution – namely S_N2 – where the alkoxy group substitutes for the H and H_2 is generated.[9] It is because of that difference that alcohols in react

thermally differently with Si(100), which is known to be more reactive, than with Si (111),10 [11] whereas thermal alkylation with alkenes seems to be indifferent to the orientation of the substrate used. Extensive work of our group on this issue should be published soon, but is beyond of the scope of this dissertation.

The HQ is a strong reducing agent and is likely to react with H-terminated Si to form a Si-O-phenol-terminated surface, as was shown for porous-Si.[12] Indeed HQ fingerprints are found in the FTIR spectra, but our XPS measurements show that most of the surface ends up, grafted with methoxy, at least immediately after molecular treatment. The HQ, then somehow activates the surface – allowing for the MeOH to react more readily with the H-terminated surface to form Si-methoxy. Even though Harper and Sailor did not rule out the possibility of the BQ scavenging an H atom from the Si and leaving a Si radical behind,[12] the fact that in our hands Si(111) and Si(100) behave so differently implies that here, as well, the self-assembly isvia nuclephilic substitution.

We suggest that the first step of the reaction is HQ attacking a reactive surface site to form Si-HQ. The HQ group is strongly electron-withdrawing, leaving the HQ-bound Si atom positively charged. The neighboring Si sites, which now share this delocalized positive charge, become easier target for substitution by the methanol molecules that make up the vast majority of the solution. This suggested mechanism accounts for the critical role of the HQ in that reaction, and its larger presence on the surface with higher initial concentration in the solution. A minimal concentration of 0.001M is needed in order to efficiently modify the surface within 3 hours of reaction as seen in Fig. 5-7. With nucleophilic substitution rather than radical chain reaction, reactive surface sites (defects) are probably attacked first – a fact that can explain the high quality of passivation offered by that treatment, and its relatively high stability. It is also important to note that methoxy groups are compact and, thus, can

occupy more of the available surface sites than any other alkyl group, aprt from CH_3 as was shown by calculations.[13]

The second , slower step of the suggested mechanism is illustrated in Error: Reference source not found. With longer reaction times, Si-methoxy sites can be re-attacked and substituted by HQ molecules, a fact that will increase the resulting average surface dipole.

Previous work, aiming for chemical passivation, demonstrated that in the presence of a mild oxidant such as I_2, Br_2 or $FeBF_4$, the H-terminated Si surface is likely to react with methanol to form Si-O-CH_3.[11] In terms of passivation these surfaces were shown to be inferior to those treated with HQ-methanol solution, and kept degrading once introduced to ambient atmosphere,[2] probably because the tendency of Si-methoxy to oxidize. We believe that here as well, as shown by the surface dipole degradation with aging, methoxy groups tend to be oxidized in ambient, maybe a little slower and in more a controllable fashion than just H-terminated Si. The surface-bound quinones, which probably populate the more reactive, surface-state inducing sites are in comparison much more stable. This notion is further supported by comparing an XPS measurement conducted by Chhabra *et al.*[3] after 12h stay in the ambient, in which the quinone to methoxy ratio is much higher than calculated from Fig. 5-2.

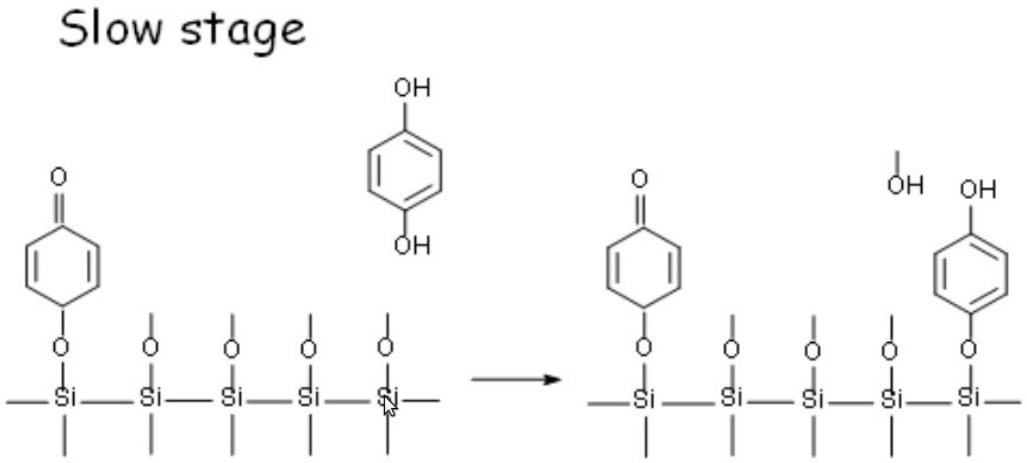

Fig. 5-10: Si-methoxy bonds, although kinetically favored, will slowly be replaced by Si-quinone ones, which are more stable thermodynamically. This explains the slow increase in surface dipole with reaction time.

5.5 Summary and further investigations.

The HQ-MeOH treatment for Si that was pointed-out as a measure of surface passivation, has many other applications in basic as well as applied research as was shown in the chapter 4. We used state of the art XPS and ATR-FTIR surface characterization techniques to show that most of the surface immediately after reaction is Si-methoxy rather than Si-HQ. With CPD/SPV we tracked the evolution of the surface dipole and surface passivation with reaction time, HQ concentration in the reaction solution, and aging in ambient atmosphere.

A surface reaction mechanism was suggested, in which HQ molecules first attack and substitute the more reactive sites of the surface, and this, in turn, activates the surface to allow broader reaction of the surface with MeOH to form Si-methoxy.

A more thorough XPS study is needed to probe the ratio of HQ and methoxy bound to the surface along the time of reaction, to further check the proposed hypothesis. Ageing and oxidation processes should be further explored as well due to their importance to the stability of the surface. the methoxy-

terminated Si surface can likely be activated by stronger nucleophiles such as OH^- or CN^- to allow for basic surface dipole research, as well as interesting surface chemistry.[14]

5.6 References

1. Takato, H., Sakata, I. & Shimokawa, R. Quinhydrone/methanol treatment for the measurement of carrier lifetime in silicon substrates. *Jpn. J. Appl. Phys. 2* **41**, L870-L872 (2002).
2. Chhabra, B., Suzer, S., Opila, R.L. & Honsberg, C.B. Electrical and chemical characterization of chemically passivated silicon surfaces. *Proc. 33rd photovoltaic Specialists Conference,* 1-4 (IEEE, 2008)
3. Chhabra, B., Bowden, S., Opila, R.L. & Honsberg, C.B. High effective minority carrier lifetime on silicon substrates using quinhydrone-methanol passivation. *Appl. Phys. Lett.* **96**, 063502 (2010).
4. Takato, H., Sakata, I. & Shimokawa, R. Modification of Surface Potential of Silicon by Organic Molecules. *Proc. 4th photovoltaic Energy Conversion world conference,* **1**, 249-252 (IEEE, 2006).
5. Michalak, D.J., Amy, S.R., Estève, A. & Chabal, Y.J. Investigation of the Chemical Purity of Silicon Surfaces Reacted with Liquid Methanol. J. Phys. Chem. *C* **112**, 11907-11919 (2008).
6. Kim, J.S. et al. Kelvin probe and ultraviolet photoemission measurements of indium tin oxide work function: a comparison. *Synthetic Metals* **111-112**, 311-314 (2000).
7. Boukherroub, R., Morin, S., Sharpe, P., Wayner, D.D.M. & Allongue, P. Insights into the Formation Mechanisms of Si−OR Monolayers from the Thermal Reactions of Alcohols and Aldehydes with Si(111)−H1. *Langmuir* **16**, 7429-7434 (2000).
8. Hacker, C.A., Anderson, K.A., Richter, L.J. & Richter, C.A. Comparison of Si−O−C Interfacial Bonding of Alcohols and Aldehydes on Si(111) Formed from Dilute Solution with Ultraviolet Irradiation. *Langmuir* **21**, 882-889 (2005).
9. Boukherroub, R., Morin, S., Sharpe, P., Wayner, D.D.M. & Allongue, P. Insights into the Formation

Mechanisms of Si−OR Monolayers from the Thermal Reactions of Alcohols and Aldehydes with Si(111)−H1. *Langmuir* **16**, 7429-7434 (2000).

10. Thieblemont, F. et al. Electronic Current Transport through Molecular Monolayers: Comparison between Hg/Alkoxy and Alkyl Monolayer/Si(100) Junctions. *Advanced Materials* **20**, 3931-3936 (2008).
11. Haber, J.A. & Lewis, N.S. Infrared and X-ray Photoelectron Spectroscopic Studies of the Reactions of Hydrogen-Terminated Crystalline Si(111) and Si(100) Surfaces with Br_2, I_2, and Ferrocenium in Alcohol Solvents. J. Phys. Chem. *B* **106**, 3639-3656 (2002).
12. Harper, T.F. & Sailor, M.J. Using Porous Silicon as a Hydrogenating Agent: Derivatization of the Surface of Luminescent Nanocrystalline Silicon with Benzoquinone. *J. Am. Chem. Soc.* **119**, 6943-6944 (1997).
13. Solares, S.D., Michalak, D.J., Goddard, W.A. & Lewis, N.S. Theoretical Investigation of the Structure and Coverage of the Si(111)−OCH3 Surface. J. Phys. Chem. *B* **110**, 8171-8175 (2006).
14. Michalak, D.J. et al. Nanopatterning Si(111) surfaces as a selective surface-chemistry route. *Nat Mater* **9**, 266-271 (2010).

Chapter 6

Hybrid, chemically passivated n-Si / PEDOT:PSS Semiconductor–Insulator-Semiconductor solar cell

Abstract. We describe a hybrid inorganic-organic solar cell, wherein the n-Si absorber interface is chemically passivated and electrically contacted by a conductive polymer, PEDOT:PSS. In this structure, which is completely fabricated from its components at room temperature, the Si is type-inverted at the hybrid interface with the polymer, thus effectively creating an SIS type solar cell without any significant insulating film. For moderately doped Si, the surface is strongly inverted and photo-generated current is being collected from the entire area of the solar cell. The good lateral conduction of minority carriers in the inversion layer helps to mitigate a major limitation of PEDOT:PSS, viz. its high sheet resistance.

This Chapter is published As:
'Hybrid Chemically Passivated n-Si / PEDOT:PSS Semiconductor-Insulator-Semiconductor Solar Cell' Har-Lavan, R.; Joshi, P.; Levine, I; Yaffe, O.; Cahen, D. proceeding of 37th IEEE photovoltaic Specialists Conference*, **2011***

6.1 Introduction

Inversion layer solar cells, also known as Schottky barrier or MIS solar cells, were introduced in the the 70's of the previous millennium to reduce (mainly Si) solar cell fabrication costs, without significant adverse effects on their efficiency.[1] [2] Ideally, if a metal makes electronic contact with a semiconductor, an energy barrier, , equal to the difference between the work function of the metal, , and the semiconductor's electron affinity, , (for n-type) forms within the semiconductor. Combining a high work function metal with n-Si, or a low work function metal with p-Si should, in principle, lead to type inversion in the space-charge region (SCR) of the Si. Such type conversion creates, *de facto*, an n-P+ junction (or p-N+, if p-Si is used), as shown in Fig. 6-1b, without the need for a high-temperature diffusion process step.

It was shown experimentally that if there is direct metal semiconductor contact, the open-circuit voltage (V_{OC}) does not meet the full potential difference between metal work function and semiconductor electron affinity, due to Fermi level pinning. Introduction of an ultra-thin insulating layer between the metal and the semiconductor, was demonstrated to unpin the Fermi level of the semiconductor – thus increasing the V_{OC} of MIS solar cell to values comparable with their p-n junction analogs.2 For decades it was believed that at least 10 Å of an insulation layer, usually a thermally grown oxide, is essential as tunneling barrier to diminish majority carrier transport and allow the device to be dominated by minority carrier currents.[3] Furthermore, thinner interfacial layer did not seem to prevent the direct metal-semiconductor reaction that is known to introduce surface states, and act to pin the semiconductor's Fermi level.[4]

Wittmer and Freeouf showed that with a non-interacting metal, such as Hg, as contact to H-terminated p-Si, the full difference between the semiconductor's ionization potential and the metal's work function is expressed in the resulting energy barrier height.[5] Lately we introduced a self-

assembled monolayer of organic molecules of different lengths as insulator in a Metal-Insulator-Semiconductor junction, and showed that the interfacial layer in such structures can be so thin (down to 2 Å), so as not to present a significant insulating barrier, while still leading to strong inversion of the Si.[6] Based on these findings, the requirements that an interfacial layer in an inversion layer solar cell ought to fulfill are:

1. prevent direct metal-semiconductor chemical interaction and formation of metal-induced gap states, MIGS (induced density of interface states, IDIS, in an SIS cell)
2. passivate the Si surface chemically to minimize dangling bonds, and electrically, to reduce the surface state density, and, specifically, to minimize potential mid-gap recombination-generation sites.
3. Optionally, the layer can introduce an interface dipole to alter the Si electron affinity to allow Si type inversion, if the initial potential difference is not sufficient.

The efficiency of SIS solar cells (P+-i-n or N+-i-p), where the metal is replaced by a degenerate wide bandgap semiconductor, should in principle exceed that of its parallel MIS since the absorber's majority carrier transport is suppressed by the forbidden gap of the window semiconductor.[7]

Here we present a Si inversion layer solar cell structure, where the monocrystalline n-Si absorber is chemically etched to produce an H-terminated surface, known for its superior passivation properties. The soft deposition of the PEDOT:PSS top electrode via spin-coating serves to preserve this passivation,[8] and protect the surface when a metallic grid current-collector is deposited by thermal evaporation.

Spin-coated PEDOT:PSS is > 90% transparent over the entire visible spectrum into the near-IR. This makes it a possible top contact, because in the MIS solar cell configuration incident light passes

through the metal contact to reach the Si absorber. The PEDOT:PSS work function (5.1-5.3 eV) should strongly invert the underlying n-Si surface, thus assuring sufficient lateral conduction of minority carriers within the SCR to compensate for the poor polymer conductivity. Thus, only a thin metal grid electrode on the PEDOT:PSS suffices to collect the photogenerated current. Fig. 6-1a shows a schematic cross-section of our inversion layer solar cell together with its idealized energy band diagram (Fig. 6-1b).

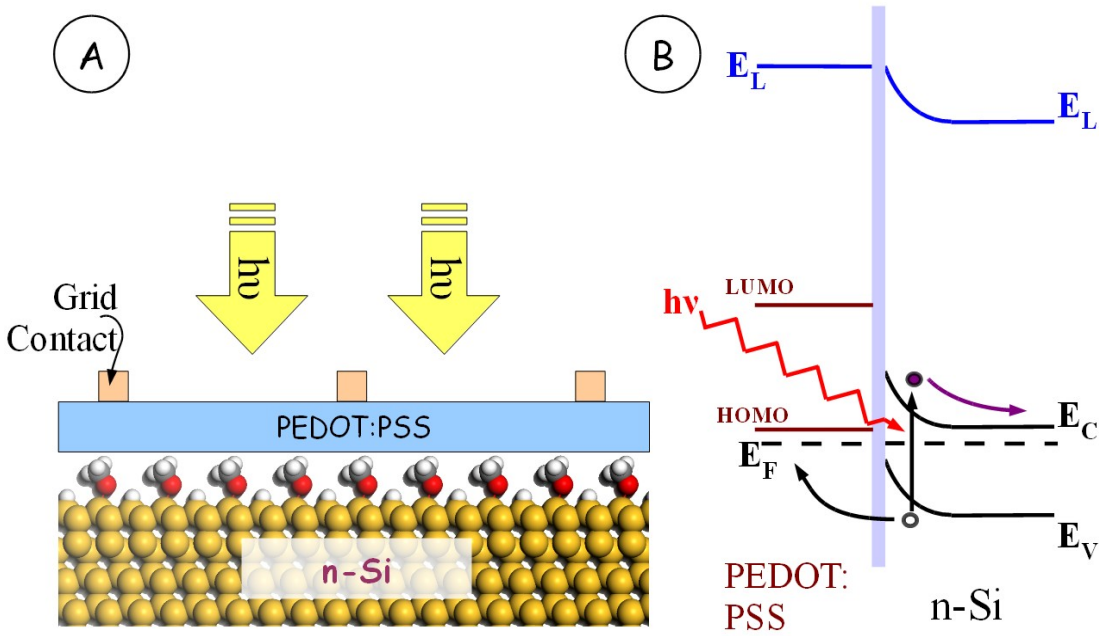

Fig. 6-1: a) Suggested structure for organic molecularly-passivated n-Si/PEDOT:PSS inversion layer solar cell. b) Energy band diagram of the solar cell, where EL is the local vacuum level, EL is the Fermi level, and EC and EV are conduction and valence band bottom and top, respectively.

6.2 Experimental

Monocrystalline Cz n-Si (100), 3 Ω cm and 0.1 Ω.cm, were purchased from Virginia Semiconductor. Resistivity was determined using a Tencor M-Gage 200. The Si was diced into 1 cm^2 squares and thoroughly de-greased in RCA1 solution (4:1:1 DI water:NH_3OH:H_2O_2) for 20 min. Then the oxide was stripped by 1 min immersion in 2% HF solution, followed by 20 min in RCA2 solution (4:1:1 DI water :HCl:H_2O_2). Surface passivation through H-termination was then realized through 1 min wet etching in 2% HF solution and a 15 sec rinse in DDW. Samples were then blown dry under N_2

flow and immediately transferred either to an N_2-filled glove box for CPD/SPV measurements, or to the spin-coater for PEDOT:PSS casting.

PEDOT:PSS aqueous dispersion (Clevios™ P) was purchased from H.C. Starck and mixed 4:1 with DMSO to increase its electrical conductance.[9] Following ref.[10] we added 0.07% wt Zonyl FSO-100 fluoro-surfactant to the PEDOT:PSS / DMSO solution to allow good adhesion to hydrophobic surfaces.

Spin-coating was performed at 1500 RPM for 7 sec for conformal coating, followed by 30 sec spinning at 4000 RPM to remove access water. The film was then dried in dry N_2 atmosphere till its optical interference pattern fully vanished. The thickness of the PEDOT:PSS film was determined, by a DekTak profilometer. For the solar cell's current collector, Au grid fingers 50 μm wide, with 0.5 mm spacing were evaporated on the PEDOT:PSS through a shadow mask, using e-beam evaporation under 10^{-6} torr. In the photovoltaic measurements a well-defined 0.8 cm^2 area of the 1 cm^2 total of the cell top surface was illuminated, by effective optical shielding of the non-illuminated remaining area.

We performed Contact Potential Difference (CPD) and Surface Photovoltage (SPV) measurements with a vibrating Kelvin probe, to probe the electrostatics of the solar cell, layer by layer. CPD measurements, relative to the Au reference electrode, serve as a contact-less way to probe the surface work function[11]. The WF of the reference electrode was calibrated against that of highly oriented freshly peeled pyrolytic graphite (HOPG), with a known, reproducible WF of 4.6 eV.[12] SPV probes the band bending in the semiconductor and can thus provide a qualitative indication of the extent of surface passivation. SPV can be measured in the same CPD setup by adding supra-bandgap saturating illumination (SPV photosaturation).[13] Specifically, SPV allows to probe the passivation of the H-terminated n-Si, and formation of/ change in a built-in potential after PEDOT:PSS deposition.

External quantum efficiency (EQE) measurements (without external bias) were conducted, using a regulated Xe lamp and Jobin Ivon 270M imaging monochromator. The incident photon flux was determined using an Ophir PD300-SH calibrated photodiode.

6.3 Results

Using SPV the band bending of H-terminated n-Si(100) was determined to be <40 meV for all resistivites used in that work, indicating for superb surface passivation. After spin-coating of PEDOT:PSS we find a polymer-induced band bending of 590 meV for moderately doped (3 Ω.cm) n-Si, very close to the 620 meV strong inversion threshold. For higher Si doping the higher absolute band bending (670 meV) is insufficient for strong inversion, which has a 820 meV onset.

Fig. 6-2 show a semi-log plot of dark current density-voltage (J-V) measurements for two typical solar cells, made from the above-mentioned Si samples. In agreement with the SPV results, the cell made with 3 Ω.cm Si shows strong rectification and a linear increase of the log(current) in the low forward bias range, characteristic for minority carrier-dominated devices (or devices with a high energy barrier for majority carrier transport; two cases that cannot be distinguished experimentally). The 0.1 Ω cm solar cell demonstrates 100x higher reverse bias currents and a smaller slope in the low-forward bias range. This behavior suggests that in this sample the Si is only weakly inverted and the current is mainly controlled by majority carrier thermionic emission. Currents in both types of cells become series resistance-limited around 0.6-0.7 V and, due to the higher substrate resistance of the low-doped sample, its absolute current density is slightly less.

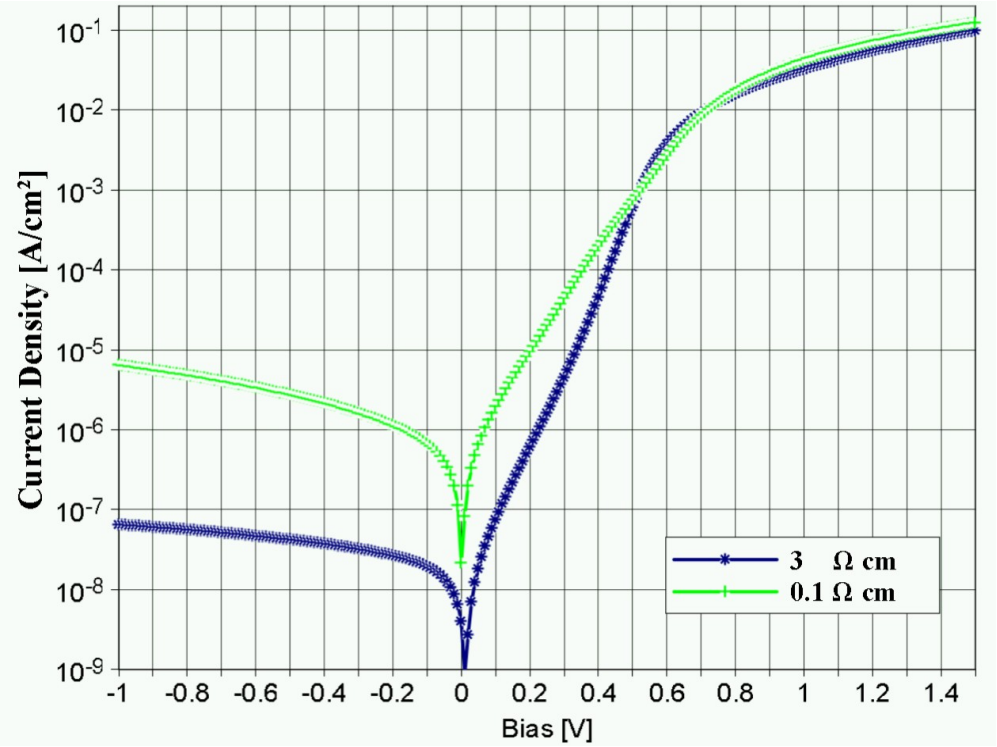

Fig. 6-2: Dark current density-voltage measurement of fully fabricated solar cells with 3 Ω.cm n-Si (blue diamonds) and 0.1 Ω.cm Si (purple squares). Both devices become series resistance-limited at ~0.6-0.7 V.

If the J-V characteristics were measured under 100 mW/cm^2 (wide spectrum halogen light; Fig. 6-3) the difference in the equilibrium state of the SCR between samples with different initial doping showed up in the results in three ways:

1. due to stronger Si inversion under the PEDOT:PSS layer, the electrical collection losses in the 3 Ω.cm solar cell are smaller, and, thus, J at short circuit is higher.

2. the 0.1 Ω cm solar cell has the higher V_{OC} by 35 mV; potentially it can be even higher as was shown experimentally[14] for Al/oxide/Si MIS cells, which makes this type of substrate a better candidate for future application than the more resistive one.

3. the series resistance current limitation dramatically degrades the fill factor of the moderately-doped solar cell, due to bulk Si resistance.

With weaker illumination, ~17 mW/cm^2 from an incandescent lamp (Fig. 6-3 inset), the series resistance effect on the cells' currents was weaker. Therefore, the 3 Ω.cm solar cell with the stronger inversion at equilibrium now performs better. The PV performances of both cells under both illumination conditions are summarized in the Table 1 below.

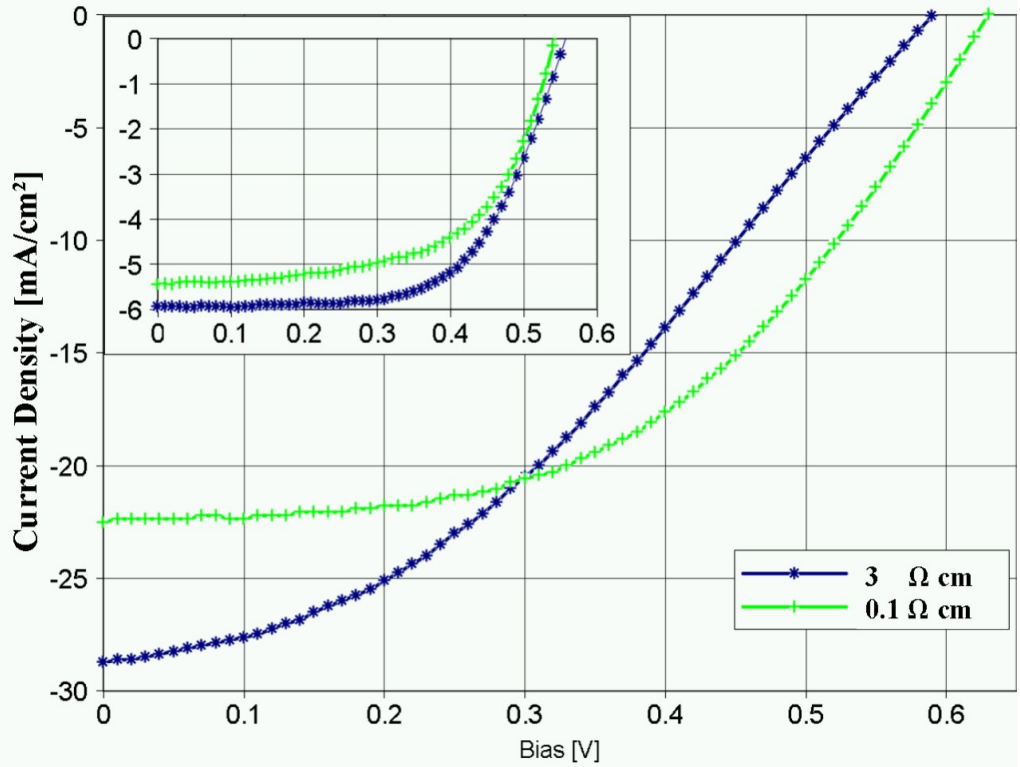

Fig. 6-3: Solar cell current density-voltage characteristics measured under 100 mW/cm2 wide spectrum halogen light and ~17 mW/cm2 yellow incandescent lamp light (inset). Blue diamonds: 3 Ω.cm solar cell; purple squares: 0.1 Ω.cm cell.

	100 mW/cm^2 wide spectrum halogen light			~17 mW/cm^2 yellow incandescent lamp light		
Si resistivity	J_{SC} [mA/cm^2]	V_{OC} [mV]	FF	J_{SC} [mA/cm^2]	V_{OC} [mV]	FF
3 Ω cm	25.5	585	0.4	-5.92	550	0.64
0.1 Ω cm	22.5	620	0.51	-5.45	540	0.51

Table 1: Photovoltaic performance of solar cells, made with 3 Ω.cm and 0.1 Ω.cm Si wafers. JSC is the short-circuit current, VOC is the open-circuit voltage and FF stands for the fill factor

Comparing short-circuit current values with those of high-end crystalline Si cells indicates that collection can be improved as well. To analyze that aspect of the solar cell performance low level external quantum efficiency (EQE) measurements (without external bias) were conducted (Fig. 6-4). One of the features of inversion MIS solar cells, the proximity of the junction to the optical entrance window, which makes for superior collection of the blue part of the visible spectrum, is seen in Fig. 6-4, where the EQE of both doping densities reaches 60% at 400 nm. However, the overall collection does not exceed 70%, a finding that we attribute mainly to the high reflectivity of the samples.

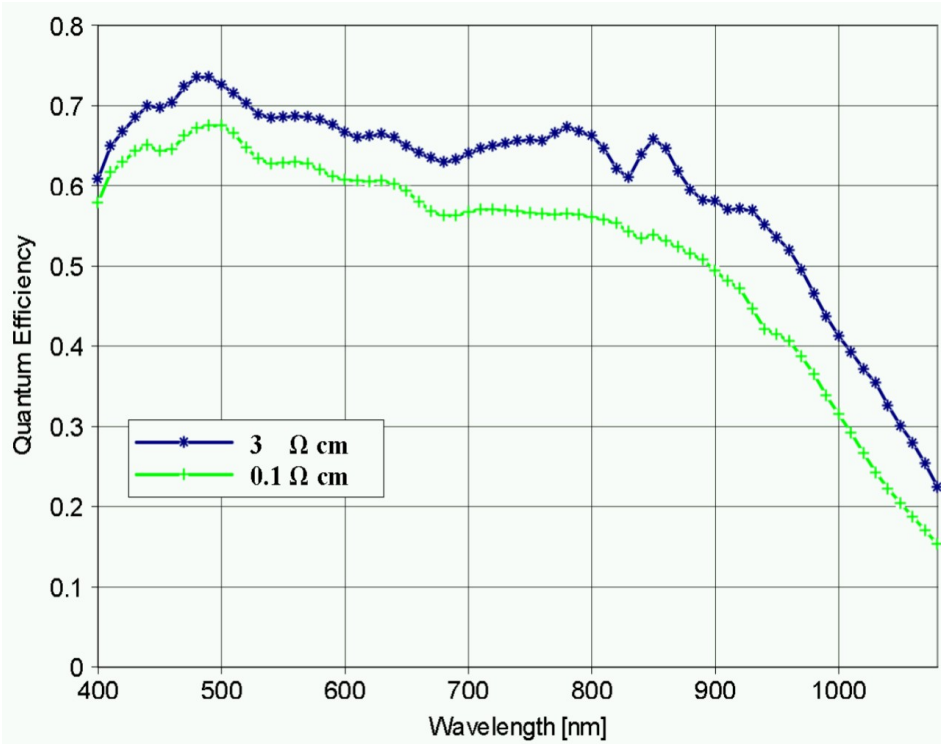

Fig. 6-4: Low level external quantum efficiency (EQE) measurements of hybrid n-Si / PEDOT:PSS inversion layer solar cells. 3 Ω.cm solar cell (purple) 0.1 Ω.cm (blue).

We also note that the PEDOT:PSS layer was rather thin (70 nm) and not optimized as anti-reflective coating. However, with a thicker PEDOT:PSS layer we have seen a space-charge limitation on the current extraction and the overall outcome was not be beneficial. Instead, we suggest that an

additional 80-100 nm thick dielectric layer on top of the metal grid will reduce reflectance and improve photon harvesting.

The solar cell with initial 3 Ω.cm resistivity, indeed presents improved collection efficiency, especially at longer wavelengths, as expected from its stronger inversion compared to its 0.1 Ω.cm counterpart. Stronger inversion means longer life time of minority carriers in the SCR, and, thus, higher probability to reach the Au grid.

6.4 Summary

We demonstrated for the first time a hybrid SIS solar with inverted n-Si as the absorber and PEDOT:PSS window layer. The whole fabrication is carried out, from the components, at room temperature and under ambient condition. Without optimization, these cells show > 7% conversion efficiency, and can, in principle, with polycrystalline Si, become efficient reduced cost alternatives to their p-n junction parallels.

The degenerate p-type PEDOT:PSS layer inverts the Si space charge region and allows minority carriers to diffuse within that layer to reach the Au grid current collector. A dielectric anti-reflective coating should improve the cell's photon harvesting and allow double-digit conversion efficiencies.

The concept should, in principle apply to all semiconductor absorbers, especially to other polycrystalline semiconductors , a direction that may lead to cost-effective hybrid solar cells.

6.5 References

1. Shewchun, J., Green, M.A. & King, F.D. Minority-carrier MIS tunnel-diodes and their application to electron-voltaic and photo-voltaic energy-conversion .2. Experiment. *Solid-State Electronics* **17**, 563-572 (1974).
2. Stirn, R.J. & Yeh, Y.C.M. A 15% efficient anti-reflection-coated metal-oxide-semiconductor solar cell. *Appl. Phys. Lett.* **27**, 95-98 (1975).
3. Fonash, S.J. The role of the interfacial layer in metal−semiconductor solar cells. *J. Appl. Phys.* **46**, 1286 (1975).
4. Green, M.A., King, F.D. & Shewchun, J. minority-carrier MIS tunnel-diodes and their application to electron-voltaic and photo-voltaic energy-conversion .1. Theory. *Sol Stat Elec* **17**, 551-561 (1974).
5. Wittmer, M. & Freeouf, J.L. Ideal Schottky diodes on passivated silicon. *Phys. Rev. Lett.* **69**, 2701 (1992).
6. Yaffe, O. et al. Molecular Electronics at Metal/Semiconductor Junctions. Si Inversion by Sub-Nanometer Molecular Films. *Nano Letters* **9**, 2390-2394 (2009).
7. Shewchun, J., Burk, D. & Spitzer, M.B. MIS and SIS solar cells. *IEEE T. Electron. Dev.* **27**, 705–716 (1980).
8. Akkerman, H.B., Blom, P.W.M., De Leeuw, D.M. & De Boer, B. Towards molecular electronics with large-area molecular junctions. *Nature* **441**, 69–72 (2006).
9. Kim, J.Y., Jung, J.H., Lee, D.E. & Joo, J. Enhancement of electrical conductivity of poly(3,4-ethylenedioxythiophene)/poly(4-styrenesulfonate) by a change of solvents. *Synthetic Metals* **126**, 311-316 (2002).
10. Akkerman, H.B. et al. Self-Assembled-Monolayer Formation of Long Alkanedithiols in Molecular

Junctions. *Small* **4**, 100-104 (2008).

11. Kim, J.S. et al. Kelvin probe and ultraviolet photoemission measurements of indium tin oxide work function: a comparison. *Synthetic Metals* **111-112**, 311-314 (2000).
12. Sommerhalter, C., Matthes, T.W., Glatzel, T., Jäger-Waldau, A. & Lux-Steiner, M.C. High-sensitivity quantitative Kelvin probe microscopy by noncontact ultra-high-vacuum atomic force microscopy. *Appl. Phys. Lett.* **75**, 286 (1999).
13. Kronik L. & Shapira Y. Surface photovoltage phenomena: theory, experiment, and applications. *Surface Science Reports* **37**, 1-206 (1999).
14. Godfrey, R.B. & Green, M.A. 655 mV open-circuit voltage, 17.6% efficient silicon MIS solar cells. *Appl. Phys. Lett.* **34**, 790 (1979).

Chapter 7

Inherent limitation of PEDOT:PSS as top contact in hybrid SIS solar cell

Abstract. We fabricated hybrid organic-inorganic n-Si / PEDOT:PSS inversion layer solar cells with and without molecular interfacial layer. Notwithstanding a large difference in the initial surface potential, both types perform almost identically immediately after preparation and aged in a comparable manner. Probing the Si band bending as a function of increasing PEDOT:PSS thickness, with surface photovoltage measurements, clearly shows that no Fermi level pinning occurs as a result of the deposition process. Surface hydroxylation is proposed as the mechanism by which the surface potential is changed during the interaction with the PEDOT:PSS solution, while, apparently, such hydroxylation preserves electrical passivaion, likely because all Si surface atoms are saturated, in terms of bonding. It is also suggested that in some cases, the PEDOT:PSS layer imposes an additional limitation on the cell's current extraction because of the ill-defined interfaces that are formed with the inorganic components , as was shown for other organic electronic materials.

7.1 Introduction

For H-terminated n-Si / PEDOT:PSS solar cells it was shown in chapter 6 that the device is under strong inversion when Si of moderate doping is used. Nevertheless, if, in order to gain higher V_{OC} values, Si of higher doping $N_D=7\cdot10^{16}\,cm^{-3}$ is used, only weak inversion is reached, which results in poorer current collection.

The surface, after HQ-MeOH treatment on n-Si(100), yields a high quality of passivation comparable to that of the H-terminated surface, as was shown in chapter 5, while resilience to oxidation in air was shown to be improved. In chapter 4 we have shown that the HQ-MeOH monolayer also induces a negative surface dipole, effectively reducing the Si electron affinity by up to 500 meV. With lower effective electron affinity one can ideally expect the eventual built-in potential to be higher after the deposition of top conducting polymer electrode.

7.2 Results

Samples of n-Si(100)/HQ-MeOH were fabricated by the procedure described in chapter 4. Taking them out of the reaction solution, the samples were sonicated in ethyl acetate for 3 min to remove physisorbed molecules, followed by 1 min in boiling dichloromethane,; they were blown dry under a N_2 stream. PEDOT:PSS was spin-coated onto the fresh, dry sample, as described in chapter 6, immediately afterwards.

Typical current-voltage results of hybrid n-Si/ PEDOT:PSS solar cells with the HQ-MeOH molecular interfacial layer under ~100 mW/cm^2 illumination are shown in Fig. 7-1, and compared to those obtained for an H-terminated sample under the same conditions. Surprisingly, even for the good cells with HQ-MeOH (on the average) neither the current nor the fill factor exceeded the result measured for the H-terminated samples. Moreover, the concave shape seen here (dashed line), that is

measured also for some cells made with H-terminated Si surfaces, appeared more often for cells with the molecular monolayer. the performance of a representative good cell with a convex-shaped photovoltaic measurement deteriorated after 1 day, and 5 days of aging in ambient atmosphere, with the fill factor decreasing from 47% to 44% and 34%, respectively. For the aging as well, no advantage was recorded for cells with a molecular monolayer instead of H-termination of the surface.

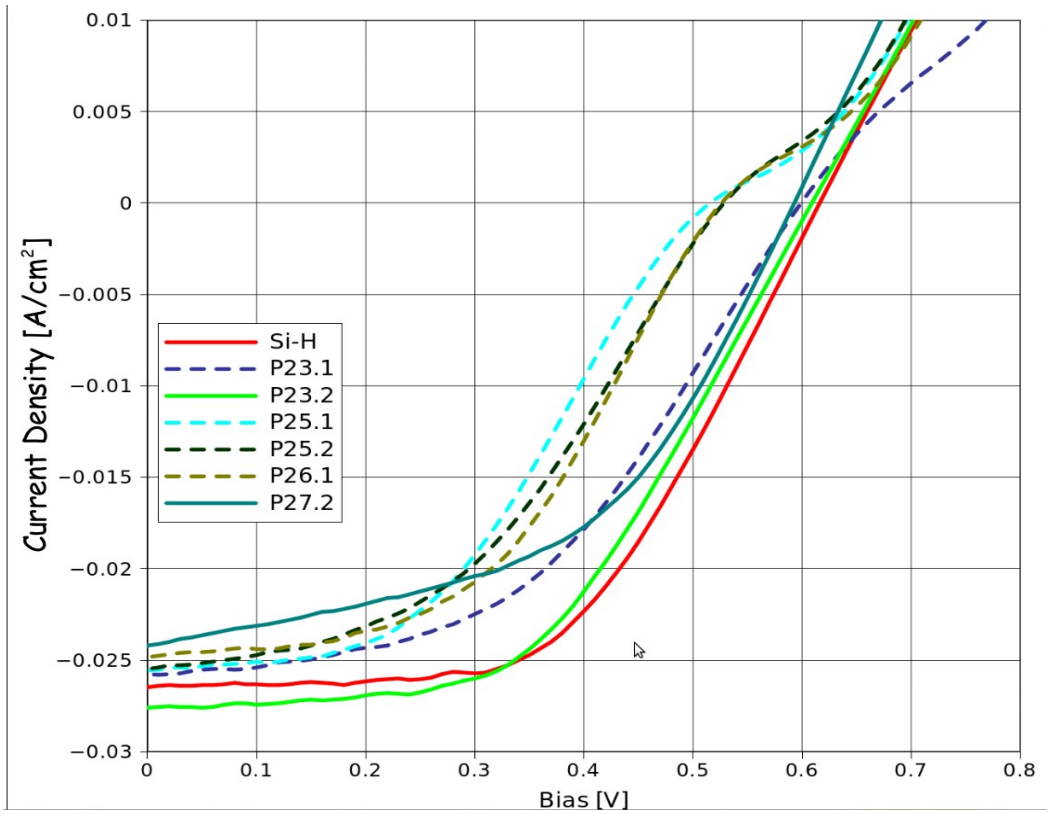

Fig. 7-1: n-Si(100) / PEDOT:PSS solar cells (labelled P) with HQ-MeOH molecular interfacial layer under ~100 mW/cm² illumination, compared to a cell made with an H-terminated surface. The concave shape seen here (dashed lines), appeared more often for cells with the molecular monolayer.

As was explained in chapter 2 every precaution was taken in order to avoid Fermi level pinning:

1. dangling bonds were saturated either by a molecular monolayer or by H
2. spin-coating was chosen as a gentle method to deposit the contact and the polymer was dried under a N_2 stream rather than annealed in order not to damage the surface termination.

3. A conducting polymer that should not react chemically with Si was used instead of a metal top electrode.

Nevertheless, if two very different semiconductor samples end-up to behave exactly the same in contact with a metal-like electrode, one should always suspect Fermi level pinning. Kelvin probe SPV is known to measure both the uppermost surface and the buried interfaces.[1] Here, we took advantage of this feature together with the transparency of PEDOT:PSS to monitor the band bending within the Si SCR through the polymer layer deposited on it.

Photo-saturation SPV results of the Si, measured through the top PEDOT:PSS layer, are presented in Table 2 for HQ-methanol-treated and H-terminated n-Si with 0.1 Ω.cm and 3 Ω.cm resistivites. Indeed it seems that some inherent limitation blocks the band from being bent as in the model, and prevents the large surface dipole of the HQ-methanol layer from being manifested as a large barrier height as was shown with the Hg drop electrode. An alternative explanation is that the known limitation of the photo- saturation technique to fully estimate the band bending[2] comes into play here, when large bending is measured.

	3 Ω.cm		0.1 Ω.cm	
	H-terminated	HQ-methanol	H-terminated	HQ-methanol
Φ_{PEDOT} to χ_{eff} difference	830	1370	770 mV	1200 mV
SPV	580 mV	590 mV	680 mV	720 mV
Strong inversion band bending	630 mV		820 mV	
Fermi level from E_V	290 mV	280 mV	280 mV	240 mV

Table 2: SPV measurement of PEDOT:PSS covered n-Si(100) 0.1 Ω.cm and 3 Ω.cm either directly after HF etching (H-terminated) or after 3h HQ-methanol treatment. With PEDOT-PSS the HQ-methanol treated samples do not show the SPV that is expected from the large difference between the PEDOT:PSS work function and the effective Si (surface) electron affinity as band bending (in the Si, after contact with PEDOT-PSS), in contrast to the Si/molecules/Hg drop systems.

According to the photosaturation SPV, eventually the Fermi level position of both the 0.1 Ω .cm and and 3 Ω cm Si samples is 240-290 meV from the valence band after contact with PEDOT:PSS. The

measurement presented in Fig. 7-2 below was made to examine if the Fermi level is pinned in those junctions.

PEDOT:PSS Clevios™ P dispersion was diluted with double-distilled water to yield 25%, 33%, 50%, 75%, 100% solutions, and 0.08% wt of Zonyl FSO-100 fluoro-surfactant was added to each. The different solutions were spin-coated on HQ-methanol treated and H-terminated n-Si (100) 0.1 Ω .cm samples, and blown dry in N_2 stream. The thickness of the polymer was assessed using ellipsometry (Cauchy model).

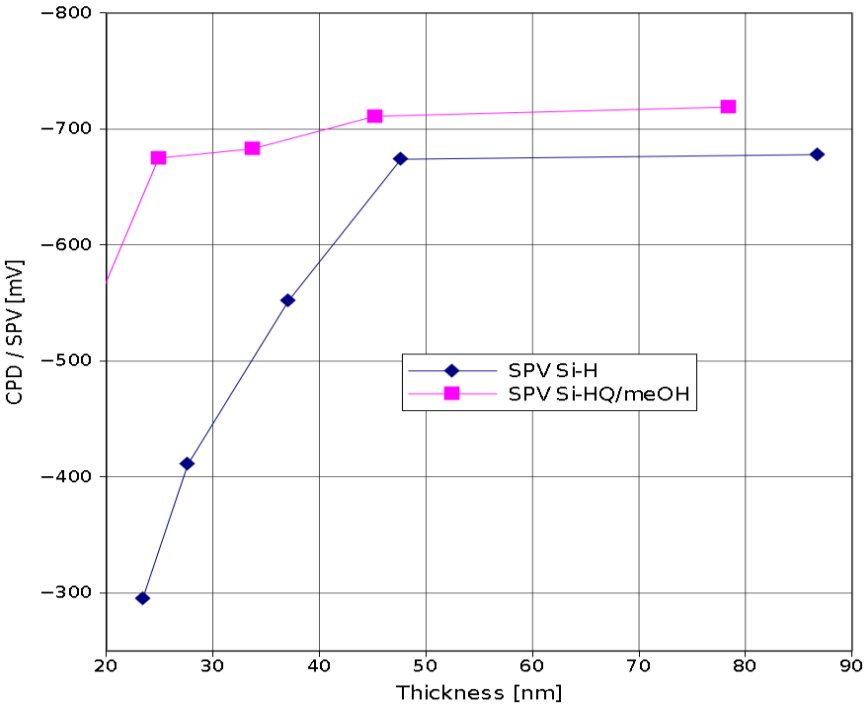

Fig. 7-2: Si surface photovoltage evolution with PEDOT:PSS overlayer thickness as measured by spinning PEDOT-PSS layers of different thickness and monitoring each of the resulting junctions, individually. The driving force for band bending is larger in the presence of the molecular dipole, due to the HQ-MeOH treatment and, thus, the SPV builds up faster than for Si-H. Nevertheless, the final SPV values are almost identical, which indicates that there is a limitation for this value to be further increased. If either chemical interaction between PEDOT:PSS and the Si surface or MIGS formation are considered, one would expect an abrupt effect within the first 10 nm of polymer rather than a gradual built-up.

The surface photovoltage of the underlying Si was measured for the different PEDOT:PSS widths and was found to grow gradually with the polymer's thickness, then saturating to a value, lower than that needed for strong inversion, from 50 nm onwards. If indeed chemical interaction was changing the nature of the Si-molecules-polymer interface – one would expect this phenomenon to be abrupt, within the first few nm of the deposited polymer. The fact that for the treated Si band bending evolves faster than for H-terminated Si shows that the molecules still have an effect on the junction electrostatics.

7.3 Discussion

Two different observables have to be considered when evaluating n-Si/HQ-MeOH/PEDOT:PSS solar cells in comparison to their H-terminated parallels:

1. On the average , a good solar cell with molecular monolayer is not superior to its H parallel either in J_{SC} or in fill factor, and does not seem to be more resilient to ambient atmosphere degradation. As expected, for exclusive minority carrier-dominated SIS junctions, V_{OC} reaches its maximum with both types of surface terminations. Cells with molecular monolayer are more likely to develop a concave shape current-voltage behavior than those made with H-terminated Si; such shape is typical for a structure with two diodes in series.
2. The band bending within the SCR of the Si evolves with the growing thickness of the PEDOT:PSS window. With an HQ-MeOH interfacial layer the band bending evolves faster, probably due to a stronger driving force than with only H-termination. The eventual SPV measured for the 2 samples differs in only a few tens of meV – much smaller than their initial potential difference.

The concave current-voltage characteristic was reported for other organic and polymeric solar cells though it does not seem to be cell-to-cell reproducible. [34] Gupta et al. attributed this behavior to

non-ideal polymer-metal contact that produces charge accumulation in the contact, and, thus, limits the current extraction from the cell. In our case, one should recall that in order to maintain high quality surface passivation, PEDOT:PSS was not annealed >100°C as is usually done for this polymer, but rather dried under N_2 stream till the optical diffraction pattern completely vanished. Kim et al. found almost no correlation between the annealing temperature of the PEDOT:PSS anode and the performance of a PCBM/P3HT bulk heterojunction solar cell.[5] It is reasonable to expect, though, that in their case the ITO/PEDOT:PSS interface was not the current limiting factor. If we assume that the method of drying that we used is insufficient, or that the polymer solidified in a way is morphologically different from that of the annealed PEDOT:PSS that might explain the non-ideality and the current limitation. The fact that with HQ-MeOH monolayer there is a stronger tendency to develop such non-ideal interface might suggest that, in our case, the semiconductor-polymer interface is also involved.

As for the photo-saturation SPV results, one might suggest that inherently charges within the PEDOT:PSS are fully delocalized as in a metal or inorganic semiconductor. In that case, electrons that had to migrate from the Si in order to equalize the initial differences in surface potential, create now a space charge on the polymer side of the interface. Upon polymer-Si contact the amount of electrons that will flow in that direction will be limited by the steady-state electron capacity of the polymer, and the rest of the potential difference will be translated to the interface dipole.

This hypothesis does not hold though, recalling that e lower resistivity sample exhibited the higher SPV values. Solving the full depletion approximation for a known charge, Q, yields:

$\Phi_{bi} = \frac{Q^2}{2\epsilon_s q N_D}$, which means that the band bending (or built-in potential), Φ_{bi} , inversely depends on the initial doping concentration, N_D. Thus, if indeed PEDOT:PSS can only accommodate a certain

concentration of charge, Si of higher doping should yield smaller absolute band bending, and *vice versa*.

An alternative explanation that can account for the eventual band bending limitation along with the gradual change in SPV of the n-Si/PEDOT:PSS structure has to do with surface hydroxylation. It is not unthinkable that both Si-H and Si-methoxy surfaces in aqueous solution, will undergo a surface substitution of H or methoxy with a hydroxide that will leave no dangling bonds. Our experiments showed that such hydroxylation of Si-methoxy surface does not happen readily in distilled water at room-temperature, but the other ingredients as well as the different pH in the PEDOT:PSS solution might initiate such reaction. Si-hydroxyl should have higher electron affinity than both Si-H and especially Si-methoxy, and its junction with PEDOT:PSS should thus result in lower barrier height and smaller band bending. This explanation is consistent with the similar performances recorded under illumination for Si-H and Si-methoxy -based junctions. The small fraction of the surface bound to HQ, in the case of HQ-MeOH monolayer can explain, then, the small difference in SPV between the two cases. If this is the case, changing the methoxy to HQ ratio on the surface, prior to PEDOT:PSS deposition could, of course, change the extent of eventual band bending.

Recently Avasthi et al. fabricated a hybrid n-Si/P3HT/PEDOT:PSS solar cell using methods very similar to ours on H-terminated Si.[6] Changing the thickness of the P3HT layer, they reported that best performance for the thinnest, 10 nm thick, P3HT layer. Especially for an organic semiconductor, a 10 nm thick layer cannot be regarded as capable of forming a full forms p-n junction with n-Si. Instead, if the junction is proven to perform better with a thin P3HT layer than without P3HT at all, a comparison that, unfortunately, the authors did not conduct, the P3HT could be thought of as buffer layer that electrically mitigates the PEDOT:PSS effect on the Si, but prevents the direct interaction of the Si with the polymer and its solution. It is important to note in that context, that P3HT, in contrast to

PEDOT:PSS, is spin-coated from organic solvents, such as dichlorobenzene, and requires no surfactant to wet hydrophobic surfaces. Such buffer layer can, in principle, protect the Si surface from hydroxylation, if indeed protection is needed.

7.4 References

1. Kronik L. & Shapira Y. Surface photovoltage phenomena: theory, experiment, and applications. *Surf. Sci. rep.* **37**, 1-206 (1999).
2. Aphek O.B., Kronik L.[1], Leibovitch M. & Shapira Y. Quantitative assessment of the photosaturation technique. *Surface Science* **409**, 485-500 (1998).
3. Chan, C.K., Zhao, W., Kahn, A. & Hill, I.G. Influence of chemical doping on the performance of organic photovoltaic cells. *Appl. Phys. Lett.* **94**, 203306 (2009).
4. Gupta, D., Mukhopadhyay, S. & Narayan, K.S. Fill factor in organic solar cells. *Solar Energy Materials and Solar Cells* **94**, 1309-1313 (2010).
5. Kim, Y., Ballantyne, A.M., Nelson, J. & Bradley, D.D.C. Effects of thickness and thermal annealing of the PEDOT:PSS layer on the performance of polymer solar cells. *Organic Electronics* **10**, 205-209 (2009).
6. Avasthi, S. & Sturm, J.C. Charge Separation And Minority Carrier Injection In P3HT-Silicon Heterojunction Solar Cells. *Proc. 37th Photovoltaic Specialists Conference,* TBP. (IEEE, 2011)

Chapter 8

General Discussion and Future Prospects

8.1 Surface control by SAMs on oxide-free semiconductor

At the heart of the issues of surface states and Fermi level pinning lie the surface atoms of the semiconductor with their unsaturated chemical bonds. Morphological defects and irregularities can also contribute to this deviation from ideal, model behavior of semiconductors. Depends on their binding, molecular monolayers self-assembled on an oxide-free surface of a (non-oxide) semiconductor can provide one with an abrupt, defect-free, passivated surface that is very difficult to get by any other means. In other words, with the toolbox of molecular monolayers one can re-gain full **surface control** with ultra-thin layers of thickness < 2 nm. In chapter 4 I have shown that specifically with the mixed HQ-alcohol layer it is possible to manipulate the surface potential over a respectable range, while retaining high quality passivation.

Over the years, different technological approaches were developed, especially for Si, to overcome the normally poor control over especially Si surfaces . The Si-based microelectronics industry, that has achieved the most impressive accomplishments in this respect, can probably get along without relying on SAMs. Other fields of research, though, may well be able to benefit a lot from the latest results of molecular electronics.

Generally speaking, semiconductors other than Si, such as the III-V and II-VI families can benefit more from the surface control gained by molecular monolayers as in this way their preferred properties, e.g. optical properties, can be brought out with minimal interference and readily utilized. I chose to use crystalline Si, though, as a model system due to its known and controlled bulk properties on the one hand, and its versatile chemical toolbox on the other, which enabled me to explore new frontiers of both molecular electronics and semiconductor physics.

8.2 An experimental window to fundamental semiconductor physics

The fact that semiconductors and materials in general are accessed through their non-ideal surfaces have made some basic elements of semiconductor physics very hard to reach for experimentalists. By stabilizing the surface, SAMs directly bound to the semiconductor can open up a rare window to the bulk properties of the material, for example minority carrier life-time,[1] and can unveil hidden or forgotten elements of semiconductos physics. This important aspect of SAM research has just started to gain attention, here and by others,[2] but may well play a big role in the embedding of SAMs in modern electronics. With HQ-alcohol treatment and Hg I demonstrated for the first time ideal Schottky-Mott behavior for Si, the most studied electronic material, that was considered to be nearly intrinsically Fermi-level pinned, especially under ambient conditions.

Realizing strong inversion conditions in t Si in equilibrium can serve as a test bed for 2D electron/hole gas phenomena and devices based on it. Usually a 2D gas is explored in epitaxially grown buried interfaces or under external bias conditions. As was emphasized in chapter 2, direct metal-semiconductor chemical interaction is detrimental for surface passivation and should thus be avoided. Apart from polymers and poly-Si, other metals that can be used as contacts to maintain the preferred surface properties achieved by using molecular monolayer are Pb and Bi which are immiscible with Si.

8.3 The HQ-MeOH surface reaction with Si(100)

The HQ-MeOH surface reaction is rather unique as it is carried out from mixed solution and both reactants bind to the surface.[3] The reaction mechanism which allows binding of those molecules to Si(100) at room-temperature and under ambient atmosphere, remained vague till now.

Using XPS, FTIR and kelvin probe CPD/SPV measurements, I could propose in chapter 5 a nucleophilic substitution mechanism that can account for the extensive set of observables as well as for the results reported by others.[4] [5] The surface resulting after this treatment is largely methoxy-terminated

with a small fraction of Si-HQ moieties. I suggest that the ratio between those two moieties on the surface is tunable, using solutions of different concentrations and different reaction times. With aging in ambient air, methoxy-terminated sites tend to oxidize[6] and loose their dipolar effect. It seems, though, that this oxidation or hydroxylation is done through nucleophilic substitution in a manner that leaves no dangling bonds and, thus, preserves the high quality of surface passivation.

For this proposed mechanism and aging to be well accepted among surface scientist further experiment have to be done. Especially, the measurements carried out by CPD / SPV should be further backed using XPS, which is a well established surface characterization tool.

8.4 Inversion layer solar cells

Inversion layer solar cells that were considered in the 1970s and 1980s to be a cheap, yet efficient alternative to the p-n junction solar cell, were left aside with the improvement Si technologies. In terms of conversion efficiency, one crystalline Si p-n junction solar cell was demonstrated to yield 25%,[7] while an MIS-IL cell was shown to produce 18.5%.[8] To properly compare these data we need to realize the minimal capital and research efforts invested in inversion layer solar cells, compared to those spent on conventional p-n junction solar cells. Unfortunately, the dense grid current collector, required in order to overcome the sheet resistance of the inversion layer, is too fine to be screen printed. The additional photolithography process step required to fabricate the grid of MIS and MIS-IL solar cells partially negates the advantage that these cells have in that they can be made without the need for a high energy diffusion process step. Among different configurations reviewed in chapter 2, it seems that MIS-IL with Al_2O_3, deposited by plasma assisted ALD, on n-Si is the best candidate for rather efficient cell fabrication with current screen printing technology. Recently a method was suggested by which the inversion layer will lie at the bottom of the solar cell to decrease the shadowing of the dense metal grid, and laser etching will be used rather than photolithography to fabricate the fine finger structure.[9] As far

as I know this concept was not yet realized.

In principle, among the family of inversion layer solar cells, the SIS structure is the most viable as a low cost solution. In SIS the upper window is a degenerate wide bandgap semiconductor, rather than a semi-transparent metal or a dielectric. Separated minority carriers can travel in the SIS structure in the window layer and thus need not to suffer from the high sheet resistance within the inversion layer. In a sense, in the SIS structure, the roles are separated – the inversion layer repels majority carriers from the interface and decreases surface recombination, while conduction is mainly in the upper window semiconductor. If the window semiconductor is selected to be of opposite type to that of the base material (P+ on n-type and N+ on p-type), the V_{OC} should approach its maximum, because majority carriers are not allowed into the window's bandgap and the current is forced to rely on minority carriers alone.[10] ITO which is the current best transparent conductive oxide and is a degenerate n-type semiconductor, is not ideal to couple with a p-type absorber due to its high work function, but was shown to invert n-Si in an N+-n SIS structure.[11]

The inversion layer solar cell as a concept aimed to be cheap but efficient alternative to p-n junction solar cells. As such, it should be realized on a cheap polycrystalline absorber, and better yet, on a thin-film polycrystalline semiconductor. For chalcogenides, for example, or chalcopyrites which are hard to dope by diffusion, the SIS structure might be a route for the next generation of thin film photovoltaics.

8.5 SAMs in inversion layer solar cells

The superb passivation and surface control achieved by molecular monolayers on oxide-free Si seems to perfectly fit the application of the inversion layer solar cell. The concept of solution-based self-assembly and the mild requirements that go with it match well with the idea of inexpensive processing that was the benchmark of those cells to start with. Molecular monolayers do, however,

impose some limitations on the next processing step that has to be mild, and their long-term stability has yet to be explored.

Different candidates for a window layer to be deposited on a molecular monolayer are conducting polymers, as demonstrated in chapter 6, 7 and wide band gap semiconductors such as NiO_2, MoO_3 and ZnO deposited by ALD. As was the case for PEDOT:PSS and HQ-MeOH, the upper material and the deposition procedure might alter the monolayer, change its properties or completely obliterate it. Therefore, the combination and the fine details of the process need to be optimized carefully.

8.6 Hybrid n-Si / PEDOT:PSS inversion layer solar cell

PEDOT:PSS is the most widely used conducting polymer and it is commercially available. On paper, its low work function, its soft deposition via spin coating, and its transparency throughout the visible range matches well with HQ-MeOH modified n-Si. The relatively high sheet resistance of PEDOT:PSS – usually measured 5-10 kΩ/□ can be partially relieved if the SCR is strongly inverted and the two work as parallel conduction channels for minority carriers to the metal grid.

In practice, though, strong inversion conditions were only demonstrated for n-Si of moderate doping $N_D=1\cdot.10^{15}$ cm^{-3}. For higher doping the SCR was only weakly inverted, as shown in chapter 6, affecting the current collection from areas far from the metal fingers. I hypothesized that for both Si-H and Si-methoxy the PEDOT:PSS solution induces rapid hydrxylation of the surface that dramatically changes the potential differences between the Si and the polymer and the eventual built-in potential with it. In order to explore if indeed such hydroxylation happens, an ATR-FTIR configuration might be used, to measure for Si-H, Si-methoxy, and Si-OH vibrations, all of which are observable using this technique. Using P3HT, spin-coated from organic solution as a buffer layer between molecules and PEDOT:PSS[12] might also be considered as a way around hydroxylation.

Fill factor issues for the hybrid n-Si/PEDOT:PSS were also discussed in chapter 7. With PEDOT:PSS the J-V characteristics of some of the cells under illumination demonstrated a concave-shaped curve in the fourth quadrant, with fill factor <25%. This phenomenon was not cell-to-cell reproducible, but appeared more frequently in cells with an HQ-MeOH molecular interfacial layer than for Si-H cells. This issue might stem from a non-ideal PEDOT:PSS interface with the metal grid, or with the Si,[13] and might be improved on by a different annealing scheme.

8.7 References

1. Takato, H., Sakata, I. & Shimokawa, R. Quinhydrone/methanol treatment for the measurement of carrier lifetime in silicon substrates. *Jpn. J. Appl. Phys. 2* **41**, L870-L872 (2002).
2. Yaffe, O. et al. Molecular Electronics at Metal/Semiconductor Junctions. Si Inversion by Sub-Nanometer Molecular Films. *Nano Lett.* **9**, 2390-2394 (2009).
3. Takato, H. & Shimokawa, R. Modification of Surface Potential of Silicon by Organic Molecules. *Proc.* 4th *Photovoltaic Energy Conversion* **1**, 249–252 (2006).
4. Chhabra, B., Bowden, S., Opila, R.L. & Honsberg, C.B. High effective minority carrier lifetime on silicon substrates using quinhydrone-methanol passivation. *Appl. Phys. Lett.* **96**, 063502 (2010).
5. Takato, H., Sakata, I. & Shimokawa, R. Surface passivation of silicon substrates using quinhydrone/methanol treatment. *Proc. Photovoltaic Energy Conversion,* **2**, 1108-1111 (IEEE, 2003).
6. Haber, J.A. & Lewis, N.S. Infrared and X-ray Photoelectron Spectroscopic Studies of the Reactions of Hydrogen-Terminated Crystalline Si(111) and Si(100) Surfaces with Br2, I2, and Ferrocenium in Alcohol Solvents. *The Journal of Physical Chemistry B* **106**, 3639-3656 (2002).
7. Green, M.A., Emery, K., Hishikawa, Y. & Warta, W. Solar cell efficiency tables (version 37). *Progress in Photovoltaics: Research and Applications* **19**, 84-92 (2011).

8. Metz, A., Meyer, R., Kuhlmann, B., Grauvogl, M. & Hezel, R. 18.5% efficient first-generation MIS inversion-layer silicon solar cells. *Proc. 26th IEEE Photovoltaic Specialists Conference* 31-34 (IEEE, 1997)
9. Martín García, I., Lövblom, R., Alcubilla González, R. & others High-efficiency solar cells based on inversion layer emitters. (2009).
10. Shewchun, J., Bürk, D. & Spitzer, M.B. MIS and SIS solar cells. *Trans. Electron Devices,* **27**, 705-716 (IEEE, 1980).
11. Malik, O., De la Hidalga-W, F.J., Zúñiga-I, C. & Ruiz-T, G. Efficient ITO-Si solar cells and power modules fabricated with a low temperature technology: Results and perspectives. *Journal of Non-Crystalline Solids* **354**, 2472-2477 (2008).
12. Avasthi, S. & Sturm, J.C. Charge Separation And Minority Carrier Injection In P3HT-Silicon Heterojunction Solar Cells. *Proc. 37th Photovoltaic Specialists Conference,* TBP. (IEEE, 2011)
13. Gupta, D., Mukhopadhyay, S. & Narayan, K.S. Fill factor in organic solar cells. *Solar Energy Materials and Solar Cells* **94,** 1309-1313 (2010).